NASA/CR—2015–219075

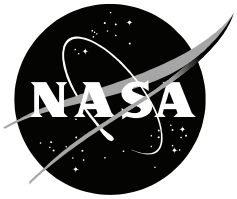

SMART Rotor Wind Tunnel Test Report

Friedrich Straub, Vaidyanathan Anand, and Terry Birchette
The Boeing Company, Mesa, Arizona
Ames Research Center, Moffett Field, California

July 2015

NASA STI Program ... in Profile

Since its founding, NASA has been dedicated to the advancement of aeronautics and space science. The NASA scientific and technical information (STI) program plays a key part in helping NASA maintain this important role.

The NASA STI program operates under the auspices of the Agency Chief Information Officer. It collects, organizes, provides for archiving, and disseminates NASA's STI. The NASA STI program provides access to the NTRS Registered and its public interface, the NASA Technical Reports Server, thus providing one of the largest collections of aeronautical and space science STI in the world. Results are published in both non-NASA channels and by NASA in the NASA STI Report Series, which includes the following report types:

- TECHNICAL PUBLICATION. Reports of completed research or a major significant phase of research that present the results of NASA Programs and include extensive data or theoretical analysis. Includes compilations of significant scientific and technical data and information deemed to be of continuing reference value. NASA counterpart of peer-reviewed formal professional papers but has less stringent limitations on manuscript length and extent of graphic presentations.

- TECHNICAL MEMORANDUM. Scientific and technical findings that are preliminary or of specialized interest, e.g., quick release reports, working papers, and bibliographies that contain minimal annotation. Does not contain extensive analysis.

- CONTRACTOR REPORT. Scientific and technical findings by NASA-sponsored contractors and grantees.

- CONFERENCE PUBLICATION. Collected papers from scientific and technical conferences, symposia, seminars, or other meetings sponsored or co-sponsored by NASA.

- SPECIAL PUBLICATION. Scientific, technical, or historical information from NASA programs, projects, and missions, often concerned with subjects having substantial public interest.

- TECHNICAL TRANSLATION. English-language translations of foreign scientific and technical material pertinent to NASA's mission.

Specialized services also include organizing and publishing research results, distributing specialized research announcements and feeds, providing information desk and personal search support, and enabling data exchange services.

For more information about the NASA STI program, see the following:

- Access the NASA STI program home page at http://www.sti.nasa.gov

- E-mail your question to help@sti.nasa.gov

- Phone the NASA STI Information Desk at 757-864-9658

- Write to:
  NASA STI Information Desk
  Mail Stop 148
  NASA Langley Research Center
  Hampton, VA 23681-2199

NASA/CR—2015–219075

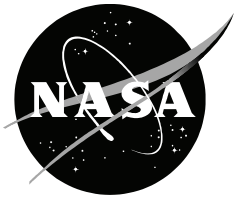

SMART Rotor Wind Tunnel Test Report

Friedrich Straub, Vaidyanathan Anand, and Terry Birchette
The Boeing Company, Mesa, Arizona
Ames Research Center, Moffett Field, California

National Aeronautics and
Space Administration

Ames Research Center
Moffett Field, CA 94035-1000

July 2015

ACKNOWLEDGMENTS

Funding for the wind tunnel test was provided by DARPA as part of the Helicopter Quieting program and by the NASA Subsonic Rotary Wing program. The valuable contributions of the many dedicated staff members at Boeing, NASA, Army, DARPA, Air Force, MIT, UCLA, and the University of Maryland are gratefully acknowledged. In particular, the authors would like to thank Mr. Daniel Newman, Dr. William Warmbrodt, and Dr. Ram JanakiRam for their support and many helpful discussions. Special thanks go to the authors of the companion papers, Drs. Ben Sim, Ram JanakiRam, and Steven Hall for sharing their material. Thanks also go to the following individuals: Mr. Roger Smith for his evaluation and assessment of SMART rotor performance; Mr. Dave Mittleider for his evaluation of rotor dynamics data; Ms. Beatrice Roget (NIA) and Inderjit Chopra (UMd) for development of the IBC controller; and Greg Carman (UCLA) and his students for their work in testing piezoelectric stacks and materials.

Available from:

NASA STI Support Services
Mail Stop 148
NASA Langley Research Center
Hampton, VA 23681-2199
757-864-9658

National Technical Information Service
5301 Shawnee Road
Alexandria, VA 22312
webmail@ntis.gov
703-605-6000

This report is also available in electronic form at

http://ntrs.nasa.gov

TABLE OF CONTENTS

List of Figures iv
List of Tables v
Nomenclature vi
Summary 1
1 .0 Introduction 1
2 .0 Test Objectives 2
3 .0 Test Article 4
4 .0 Test Equipment 6
5.0 Instrumentation 7
6.0 Test Setup, Checkout, and Procedures 8
7.0 Test Personnel 12
8.0 Calibration Data 12
9 .0 Data Acquisition and Flap Control Software 13
10.0 Data Acquisition and Reduction 13
11.0 Specific Test Conditions 15
12.0 Test Results 17
13.0 Conclusions 17
14.0 Additional Information 18
15.0 References 19

Appendices
A SMART Rotor Test Runs, Wind Tunnel and Whirl Tower 39
B SMART Rotor 40x80 Test—Tare Data Curve Fits, 2008 41
C Checklist 43
D Baseline and Performance Test Conditions, Active Flap Test Conditions 45
E Photographs 53

LIST OF FIGURES

Figure 1a: Test stand, rotor, elevator setup (for LHX test). 23
Figure 1b: System integration test at whirl tower showing LRTS test stand and SMART rotor setup (2008). 23
Figure 1c: SMART rotor at whirl tower (2003). 24
Figure 1d: MDART rotor in NFAC 40- by 80-foot wind tunnel (looking downstream (1992)). 24
Figure 1e: SMART rotor in the NFAC 40- by 80-foot wind tunnel (looking upstream). 25
Figure 1f: Close-up view of the SMART rotor, blade, and flap in the tunnel. 25
Figure 2a: Schematic of SMART rotor and test stand components. 26
Figure 2b: Health monitoring system parameters. 27
Figure 3: Hub-mounted data/power transfer system (note: in wind tunnel the slip ring and encoder are mounted below the transmission). 28
Figure 4: Slip ring for data (14 ch) and power (28V—4 ch, 1500V—8 ch). 28
Figure 5: MD900 hub and blade root attachment structure. 29
Figure 6: SMART rotor blade, trailing-edge flap, and actuator installation. 29
Figure 7a: Active flap components. 30
Figure 7b: Active flap rotor blade cross section. 30
Figure 8: 2X-frame actuator, including piezoelectric stack columns. 31
Figure 9: Blade, flap, and actuator close-up. 31
Figure 10: SMART rotor blade (bottom view). 32
Figure 11: SMART rotor data/control system. 33
Figure 12: Data acquisition and active flap control system. 34
Figure 13: Blade planform, airfoil distribution, and position of strain gauges on flexbeam, pitchcase, and blade of arm 1. 34
Figure 14a: SMART rotor in 40- by 80-foot anechoic test section and microphone configuration (looking downstream). 35
Figure 14b: SMART rotor disk and microphone layout for acoustic test setup (top view). 35
Figure 15: Tare Conditions. Configuration “hub” is with blades off (i.e., includes hub, PCM, flexbeam, pitchcase, spacers, and blade bolts). 36
Figure 16: MDART full-scale rotor whirl tower test frequency run chart. 36
Figure 17: Control room layout and station assignments in wind tunnel. 37
Figure 18: Test points and conditions for validation database. 38

LIST OF TABLES

Table 1a: SMART Rotor Characteristics 5
Table 1b: MD900/SMART Blade Mass Properties 5
Table 2: Flap Characteristics 6
Table 3: 2X-Frame Actuator Characteristics 6
Table 4: Blade Instrumentation 7
Table 5: Microphone Position Relative to Hub Center (alfa_su = 0) 8
Table 6: Rap Test of SMART Rotor Hub on LRTS at Whirl Tower 9
Table 7: Rap Test of SMART Rotor Hub on LRTS in Wind Tunnel 9
Table 8: Test Data Directory Structure 14
Table 9: Active Flap Test Conditions 16

NOMENCLATURE

α	shaft angle
CT	thrust coefficient, also C_T
μ	advance ratio
σ	solidity

AFC	active flap controller; also active flap computer
ASAP	access, select, analyze, present
AVA	advanced vibration analyzer
BDM	blade displacement measurement
BVI	blade vortex interaction
BVISPL	BVI sound pressure level (8–60th blade passage harmonics)
CIFER™	comprehensive identification from frequency responses
CTHHC	continuous time higher harmonic control, also CTC
DARPA	defense advanced research project agency
EOP	emergency operating procedures
HHC	higher harmonic control
HMS	health monitoring system
HQP	Helicopter Quieting Program
HV	high voltage
IBC	individual blade control
L/D	lift-to-drag ratio
LFSPL	low-frequency sound pressure level (first six-blade passage harmonics)
LRTS	large rotor test stand
MDART	McDonnell Douglas advanced rotor technology
NFAC	national full-scale aerodynamics complex
OAT	operating ambient temperature
PCM	pulse code modulation
RAP	response analysis pulse
RCC	rotor control console
RH	relative humidity
RTF	remote test facility
RTM	real-time monitoring
SMART	smart material actuated rotor technology

SMART ROTOR WIND TUNNEL TEST REPORT

Friedrich Straub,[1] Vaidyanathan Anand,[1] Terry Birchette[1]

Ames Research Center

SUMMARY

The Boeing Company, Mesa Arizona, has been developing smart material actuated rotor technology (SMART) under in-house, DARPA, NASA, and Army funding. A whirl tower test of the SMART active flap rotor system was successfully conducted at the remote test facility (RTF) in Mesa, Arizona, in 2003. Under DARPA and NASA funding, the SMART rotor system was tested in the NASA Ames National Full-Scale Aerodynamics Complex (NFAC) 40- by 80-Foot Wind Tunnel in 2008. The objectives of the DARPA program were to demonstrate the active flap impact on rotor acoustics in forward flight and establish a validation database for noise prediction tools. Under NASA funding, additional wind tunnel tests were conducted with the objective to demonstrate and quantify vibration, noise, and performance improvements.

Wind tunnel testing was successfully and safely concluded, meeting all high-priority objectives. The authority, effectiveness, and reliability of the flap actuation system were demonstrated in 65 hours of testing at up to 155 knots and 7,700 pound thrust. Validation data was successfully acquired for four test conditions; blade loads were too high for the high-speed condition. The effectiveness of the flap for noise and vibration control was demonstrated conclusively, with results showing significant reductions in blade vortex interaction (BVI) and in-plane noise as well as vibratory hub loads. The impact of the flap on control power and rotor smoothing was also demonstrated. Data evaluating any benefits in aerodynamic performance and impact on flight controls were acquired but will need more detailed evaluation. Both open-loop control and closed-loop feedback control, using continuous time and higher harmonic controllers, were applied.

The purpose of the this report is to provide a comprehensive document that describes the preparation for and conduct of the wind tunnel test, and summarizes the processing and evaluation of wind tunnel test data for the DARPA and the NASA portion of the test. Reference 1 provides an overview of the wind tunnel test and results. Details on the testing and results for BVI noise, in-plane noise, and vibrations are provided in references 2–4, respectively. These references are four papers that were presented at the American Helicopter Society Annual Forum in 2009. A brief description of the delivered electronic data is provided in reference 5.

1.0 INTRODUCTION

The Boeing Company, Mesa Arizona, has been developing smart material actuated rotor technology (SMART) under the DARPA smart materials and structures demonstrations program. The objectives of this program were to demonstrate smart materials for active control on a helicopter rotor, and quantify performance and cost benefits. Piezoelectric actuators, driving trailing-edge flaps on a modified MD900 rotor, are used to reduce vibrations and noise, improve aerodynamic performance, and perform other active control functions. Development of the actuation and rotor system, as well as full-scale rotor whirl tower tests, were supported by DARPA. Fabrication of the rotor blades was supported by NASA/Army.

[1] The Boeing Company, 5000 E. McDowell Road, Mesa, AZ 85215.

Under this previous program, Boeing developed the technology and demonstrated that smart material actuated flaps are feasible and practical for high bandwidth, limited authority active control of a helicopter main rotor. The MD900 Explorer twin engine, light utility helicopter was selected as the demonstration vehicle. Its state-of-the-art five-bladed, composite, bearingless main rotor system was modified to include on-blade piezoelectric actuators and trailing-edge flaps. A whirl tower test of the SMART active flap rotor system was conducted in 2003 at the remote test facility (RTF) in Mesa, Arizona. The purpose of the whirl tower test was to perform system integration, and conduct rotor and active flap control system testing to demonstrate safety and performance. Whirl tower testing was conducted with full rotor instrumentation and a five-component rotor balance. The rotor was tested for 13 hours under a range of conditions, including 7 hours of flap operation. Flap inputs included open-loop static and dynamic commands. The flaps showed excellent authority with oscillatory thrust greater than 10 percent of the steady baseline thrust. Various flap actuation frequency sweeps were run to investigate the dynamics of the rotor and the flap system. Limited closed-loop tests used hub accelerations and hub loads for feedback.

The DARPA Tactical Technology Office initiated the Helicopter Quieting Program (HQP) in 2004. The HQP in Phase I developed state-of-the-art noise prediction tools for use in designing next-generation advanced rotorcraft with reduced acoustic perceptibility. These tools were validated for conventional rotors currently in the field, and demonstrated improved accuracy and correlation versus classical, comprehensive rotor computational tools. The HQP Phase Ib was initiated in 2007 to demonstrate and validate these new HQP design tools against measurements for unconventional rotor designs. The next generation of rotorcraft may include high-bandwidth on-blade controls, which pose unique modeling challenges for the noise prediction tools. Therefore, DARPA selected the Boeing SMART active flap rotor for a 7-week wind tunnel test to provide the test data needed to fulfill the validation requirements.

The overall objectives of the DARPA program were to demonstrate the active flap impact on rotor acoustics in forward flight and establish a validation database for the HQP Phase I tool set. The preparation and wind tunnel test effort included the following:

1. New actuator access covers were fabricated and blades were modified, based on results from the previously completed blade mid-section fatigue test. A fatigue test of the piezoelectric actuator was conducted, and the actuator was qualified for large motions (see ref. 6).
2. The SMART rotor system components and test stand were adapted and prepared for installation in the NASA Ames National Full Scale Aerodynamics Complex (NFAC) 40- by 80-Foot Wind Tunnel test section. All components were refurbished as required. The data system and power amplifiers were refurbished and upgraded, and algorithms for flap position control were developed. Mechanical and electrical interfaces and data processing software integration with NFAC systems were established and implemented.
3. The buildup, checkout, and integration of the test stand, drive system, rotor control console, health monitoring system (HMS), rotor, data/power transfer, smart material actuators, amplifiers, flap control system, and data system were conducted at the RTF to ensure readiness for the wind tunnel test. Whirl tower testing in early 2008 verified all upgrades and demonstrated full system functionality.
4. The buildup and checkout of the system at the NFAC was started in February 2008. A full set of data was obtained at three test conditions for the baseline configuration, i.e. no flap deflections, and for three conditions with the active flap following specific deflection schedules, using closed-loop position control. Data included trim, performance, loads, and BVI, as well as in-plane acoustics, establishing an aeromechanics database for validation of the HQP aeroacoustic prediction tools.

The DARPA-funded SMART rotor wind tunnel test presented NASA with a unique opportunity to extend the testing to gather data to demonstrate the effects of on-blade control on rotor aeromechanics. Therefore, NASA funded a 4-week extension of the wind tunnel test. The overall objectives of the NASA program were to gather data to demonstrate and quantify the effects of on-blade control on rotor aeromechanics, including performance, vibration, loads, and acoustics. In addition, NASA funded the development and implementation of closed-loop test capability for aeromechanics research. Three controllers were developed and implemented: higher harmonic control (HHC), continuous time higher harmonic control (CTHHC), and individual blade control (IBC). NASA also funded piezoelectric material and stack actuator testing to expand actuator authority for the wind tunnel test program. Results of these two efforts are reported in reference 7.

SMART rotor wind tunnel test planning and preparations were conducted in accordance with references 8 and 9. The McDonnell Douglas Advanced Rotor Technology (MDART) rotor, a prototype of the MD900 rotor, was tested in the NFAC 40- by 80-foot wind tunnel in 1992, using Boeing's Large Rotor Test Stand (LRTS). The SMART rotor design, analysis, and wind tunnel test planning made extensive use of the available MDART information (refs. 10–22). Detailed documentation of the SMART rotor wind tunnel test preparations and planning are provided in references 23–30.

The wind tunnel test was conducted in the NFAC 40- by 80-foot test section during an 11-week period from February 13 through May 2, 2008. A detailed schedule of daily activities and summary of the setup and test runs, including objectives, comments, control algorithms used, and run times, are provided in Appendix A.

2.0 TEST OBJECTIVES

The overall goal of the DARPA wind tunnel test was to establish an aeromechanics database for validation of new aeroacoustic prediction tools. Validation of these tools was needed to use them in the design of next-generation advanced rotorcraft with significantly reduced noise signature. The specific objectives, in order of priority, were:

1. Verify system functionality and safe operation of the active flap rotor system throughout the intended test envelope.
2. Acquire rotor trim, performance, loads, and acoustic data for a few select test conditions where the active flap significantly impacts the rotor acoustics in forward flight. These conditions were defined using comprehensive analysis codes. Test data was to be acquired for the baseline case, i.e., without flap deflection, and with the flap operating in closed-loop position control mode.
3. Acquire data for some test conditions from the 1992 MDART entry in the 40- by 80-foot wind tunnel.

The overall goal of the NASA wind tunnel test was to gather data to demonstrate and quantify the effects of on-blade control on rotor aeromechanics, including performance, vibration, loads, and acoustics. Specific objectives accomplished were:

1. Noise reduction. In-plane noise as well as BVI noise were reduced. A traversing microphone array was used to map out BVI noise contours in detail. Open-loop flap 2–6/rev harmonic inputs were used, with phase and amplitude sweeps to determine inputs for best noise reduction. Flap motion for the baseline and harmonic input cases was precisely controlled using closed-loop feedback of flap position. Both the HHC and CTHHC controllers were used for closed-loop flap position control.

2. Vibration reduction. Vibratory rotor balance loads were reduced. Open-loop flap 4, 5, and 6/rev inputs with phase sweeps were used to establish the effectiveness of the flap in reducing vibratory hub loads. The flaps were driven using open-loop voltage commands without position feedback control. Vibration reduction with closed-loop feedback of vibratory hub loads was demonstrated using the CTHHC controller.
3. Flight controls and rotor dynamics. Flap input frequency sweeps from 0.2 to 9 Hz were conducted to determine rotor system dynamics including regressive lag mode frequency and damping. Frequency sweeps from 0 to 80 Hz characterized rotor dynamics, and sweeps from 0 to 200 Hz characterized flap actuator dynamics.
4. Control Power. Steady-state collective and cyclic flap inputs quantified the effect of the flap on rotor thrust and hub moments.
5. Rotor smoothing. Steady-state open-loop inputs to individual blades demonstrated the effectiveness of the flap for rotor smoothing (blade tracking).
6. Performance. The impact of the flap on rotor performance was demonstrated using 2/rev open-loop inputs.
7. Blade displacement measurements (BDMs). NASA's stereo photogrammetry system was set up and successfully measured rigid body and elastic blade deflections in forward flight.

3.0 TEST ARTICLE

The test article consists of the full-scale SMART active flap rotor and Large Rotor Test Stand (LRTS). The SMART rotor design, analysis, and 2003 whirl tower test are described in detail in references 31–40. Detailed descriptions of the SMART and MDART rotor geometry and properties (see ref. 41) were provided for SMART pretest predictions and correlation with earlier MDART test data, using the newly developed HQP tools.

Figure 1a shows the test stand mounted on the elevator in the whirl cage at the RTF. Figure 1b shows the SMART rotor mounted on the LRTS at the RTF for system integration testing before the wind tunnel test. A close-up of the flap and data system during the 2003 whirl test is shown in Figure 1c. Rotor loads are measured by a five-component balance. The upgraded AD-10 transmission (6.135 gear ratio) is used. The rotor is driven by a 1500-hp motor (2405 RPM) mounted on the test stand sled. At the whirl tower, the test stand sled is attached to the whirl cage elevator by an adapter structure. The elevator is not raised, and no fuselage structure is used.

Figure 1d shows the MDART rotor in the 40- by 80-foot test section during the 1992 entry. The SMART rotor on the LRTS in the 40- by 80-foot test section is shown in Figure 1e. In the wind tunnel, two 9-foot 1-inch front struts with 6.187-inch tips and an extendable tail strut are used. The LRTS is mounted on this three-strut support system placing the rotor hub 23.7 feet above the tunnel floor at 0-degree shaft tilt. Aerodynamic fairings are used for the struts, sled, standpipe, and rotor balance. A close-up of the flap, rotor balance fairing, and data system during the wind tunnel test is shown in Figure 1f. A schematic of the rotor and test stand components is shown in Figure 2a. Rotor collective and cyclic pitch control is provided by the Rotor Control Console (RCC). Basic test stand parameters are monitored with a health monitoring system (HMS) (see Fig. 2b).

The hub-mounted data and power system, Figure 3, contains the Metraplex system for multiplexing of all rotor data. For whirl tower and wind tunnel tests, the slip ring, Figure 4, and encoder are mounted beneath the transmission. The arrangement of the MD900 hub, flexbeam, and pitchcase in relationship to the blade

and their attachments are shown in Figure 5. For the wind tunnel entry, the refurbished MDART hub, remanufactured pitch links, standard pitchcases, snubber/dampers, and the latest flexbeams (configuration -115) are used. The installation of the piezoelectric actuator, flap, and related components in the blade is shown in Figures 6–7. The piezoelectric actuator consists of two x-frame mechanisms and four piezoelectric stack columns (Fig. 8). A close-up of the actuator installation in the blade and the inboard flap section is shown in Figure 9. The SMART rotor blade assembly is shown in Figure 10.

The two x-frames are mechanically in parallel, in a push-pull configuration, thus forces add up and displacements are constrained to be identical. The stack columns in each x-frame are mechanically and electrically preloaded to always be in compression. Applying a positive voltage to the two stack columns extends their length, thus reducing the enclosed angle and closing the x-frame mechanism.

Flap motion control typically is achieved by supplying a bias (0 to 10 VDC) and dynamic (0 to ±10 VAC) voltage command to the amplifier. The amplifier gain is fixed at 75 and drive voltages for the two channels, i.e. inboard and outboard x-frame actuator, are set 180 degrees out of phase.

$$\text{Inboard:} \quad V1 = Vbias + Vdyn \sin n\omega t$$
$$\text{Outboard:} \quad V2 = Vbias - Vdyn \sin n\omega t$$

The bias voltage contributes to the actuator preload but ideally produces no flap deflection. The flap deflection is proportional to the dynamic voltage. A positive Vdyn results in a positive, flap down deflection (TE down). The sign for the dynamic voltage is set by a switch for each channel on the amplifier (normal for +, invert for –). Assuming identical but phase shifted inputs to each blade, one bias and five dynamic commands are required. The voltages for the kth blade are

$$V_k 1,2 = Vbias \pm Vdyn \sin (n \psi_k + \varphi), \; n = 0 \ldots 11$$

where $\psi_k = \psi_1 - (k-1)2\pi/5$. Simple harmonic excitation is assumed. Other possible inputs are described in reference 7.

Basic rotor, flap, and actuator characteristics are presented in Tables 1–3.

Table 1a: SMART Rotor Characteristics

Rotor blade	modified MD900
Hub type	bearingless (MD900)
No. of blades	5
Rotor diameter	33.85 ft (R = 203.1 in.)
Rotor speed	392 RPM
Tip speed	695 ft/s
Chord	10 in.
Airfoils	HH-10, t/c = 12%, to 0.74R HH-06, t/c = 9.5%, from 0.84R
Tip sweep	parabolic LE, from 0.93R; 22 deg at tip
Tip taper	2:1, straight trailing edge
Twist	–10 deg
Torsion frequency	5.8/rev

Table 1b: MD900 / SMART Blade Mass Properties

	MD900	SMART
Weight (lb)	39.16	44.22
Span moment (in.-lb)	4550	5244
CG chordwise	27.3%	26.7%

Table 2: Flap Characteristics	
Radial station	150–186 in.
Span length	36 in.
Chord length	3.5 in. ($c_f + c_o$)
Hinge location	75% of blade chord
Flap twist axis	1.0 in. aft of flap LE
Control horn length	0.75 in.
Max flap angle	±6 deg
Flap weight	1.26 lb

Table 3: 2X-Frame Actuator Characteristics	
Blocked force	113 lb
Free stroke	0.081 in.
Maximum work	2.28 in.-lb
Voltage, max (nom)	475 ±725V (400 ±500V)
Weight	2.16 lb
Specific work	1.1 in.-lb/lb

4.0 TEST EQUIPMENT

The Model Rotor Control Console (RCC) provides the necessary capabilities to control the swashplate collective and cyclic trim inputs and provide system excitation for stability determination. A complete description of the RCC is given in reference 15. The Model Rotor Control Panel has a number of built-in self checks and monitoring systems for the rotor control panel and includes the rotor test stand health monitoring panel.

A special system is used for data acquisition and flap actuator control. The overall arrangement and components of the data/control system are shown in Figures 11 and 12. A hub-mounted Metraplex Mini 770 system is used for signal conditioning, A/D conversion, and pulse code modulation (PCM) multiplexing of rotor, flap, and actuator data (rotating system). A second Metraplex system is used for the test stand data, flap actuator control data (fixed system), and wind tunnel data. Both PCM data streams are continuously recorded on a digital tape recorder (Heim D12).

A CyberResearch PC (active flap computer (AFC)) with two Lumistar Decom boards and two Lumistar DAC boards is used to acquire both PCM data streams and feed a PC-based data system and various analog input devices. The AFC also provides continuous incident recording, mass storage (160 GB hard drive), and data archiving (DVD). Details on the AFC are provided in reference 7. Two desktop PCs with Lumistar LDPS software are used to feed four LCD displays for real-time monitoring (RTM). All three PCs communicate via a local network. Additional equipment includes up to two Dash-18 strip chart recorders (18 channels each) and a 4-channel Siglab signal analyzer.

The 2x-frame actuator is powered by a two-channel switching power amplifier. Five amplifiers and three 28V power supplies are required to drive the actuators in five blades. Actuator control is provided via the AFC using a dSpace controller board and software, and special purpose software.

5.0 INSTRUMENTATION

There are a total of 27 rotor measurements, 18 actuator and flap measurements (rotating system), 26 actuator control measurements (fixed system), 34 test stand measurements, and 27 health monitoring system measurements. During the wind tunnel test 14 additional parameters, including 9 tunnel operational measurements and acoustic data from 4 microphones, were also acquired.

Strain gauges are mounted at different stations on the main rotor blade, pitchcase, and two flexbeams to measure the flap bending, chord bending, and torsion moments (see Fig. 13). The type and location (blade station in inches) of these gauges is shown in Table 4. Additional rotor measurements are pitch link load (2) and drive shaft torsion (2).

Each active flap actuator is instrumented to measure force and displacement output. In addition, flap actuator frame forces (4), stack temperatures (2), and flap hinge support forces (2) are measured. Actuator control measurements include the two voltages and currents per actuator, the amplifier input voltage and total current, the amplifier input current for one flap actuator, the amplifier heat sink temperature, and humidity.

For acoustic measurement, 14 microphones were strategically placed around the model to capture rotor noise sources of interest (see Fig. 14a). These microphones were grouped into: a) out-of-plane fixed microphones (M1 and M4) to correlate to microphones used previously in the MDART test (ref. 20); b) traverse microphones (M5 through M12) that can be moved along guided rails for blade-vortex interaction noise mapping; c) in-plane microphones (M13, M14, and M15) for low-frequency, in-plane rotor noise measurement; and d) fixed microphone (M16) on the rotor balance fairing. Microphones M13, M14, and M15 were mounted on tower struts to be near in-plane of the rotor (approximately 10 degrees below wind tunnel horizon). With the exception of M14, all microphones are located within the acoustically treated portion of the 40- by 80-foot test section. The microphone traverse travel ranges from 200 inches upstream of the center of the rotor hub to 200 inches downstream with traverse stopping at every 40 inches. The plane of traverse microphone positions is located 89.4 percent radius below the rotor hub center, and extends from 41 percent to 141 percent radius across the test section on the advancing side, and from 98.5 percent radius upstream to 98.5 percent downstream. A top view of the microphone layout is shown in Figure 14b. The microphone positions relative to the hub center are listed in Table 5. Data from microphones 1, 4, 13, and 16 were acquired by the Boeing data system.

Table 4: Blade Instrumentation

Blade 1	Flap:		42.75	70	87	120	164	180
	Chord:		42.75	70		120	164	
	Torsion:		51	71		130	165	
Flexbeam 1, 2:	Flap	9	Chord	26.5	Torsion	26.5		
Pitchcase 1:	Flap	33.25	Chord	33.25	Torsion	25.5		

Table 5: Microphone Position Relative to Hub Center (alfa_su = 0)

Mic. No.	x_h, ft	y_h, ft	z_h, ft	r_h, ft	r_h / R	ψ_h, deg	θ_h, deg	Notes
M1	–29.67	10.27	–17.94	36.16	2.14	160.9	–29.7	Fixed
M4	–27.92	15.59	–17.87	36.63	2.16	150.8	–29.2	Fixed
M5	16.73	6.97	–15.13	23.61	1.39	157.4	–39.9	Traverse
M6	–16.73	9.79	–15.13	24.59	1.45	149.7	–38.0	Traverse
M7	16.73	12.02	–15.13	25.56	1.51	144.3	–36.3	Traverse
M8	–16.73	14.17	–15.13	26.64	1.57	139.7	–34.6	Traverse
M9	–16.73	16.42	–15.13	27.90	1.65	135.5	–32.8	Traverse
M10	–16.73	18.67	–15.13	29.28	1.73	131.9	–31.1	Traverse
M11	–16.73	20.90	–15.13	30.75	1.82	128.7	–29.5	Traverse
M12	–16.73	23.92	–15.13	32.88	1.94	125.0	–27.4	Traverse
M13	–29.67	10.27	–5.34	31.85	1.88	160.9	–9.7	In-plane
M15	–38.77	8.73	–7.13	40.38	2.39	167.3	–10.2	In-plane
M14	–80.38	–0.33	–14.84	81.72	4.83	180.2	–10.5	In-plane

The data system components and functions included the following:

- Continuous recording of 115 channels of data (incident recording).
- Continuous monitoring of all critical system safety measurements.
- Maximum, minimum, cyclic, and limit checking on all channels.
- Engineering units conversion.
- Four color video monitors (19-inch LCDs) for alphanumeric and graphics displays.
- Two Dash-18 digital data loggers (strip charts) with 18 channels each.
- Derived parameter calculations (rotor thrust coefficient, L/D, figure of merit, resultant measurements, etc.).
- 2048 point FFT in 20 msec per channel.
- Moving block analysis and Randomdec.

6.0 TEST SETUP, CHECKOUT, AND PROCEDURES

WHIRL TOWER TEST

In preparation for the wind tunnel entry, a brief whirl tower test was conducted (see Fig. 1b). This system integration test verified operation of the SMART rotor, large rotor test stand (LRTS), rotor control console (RCC), test stand health monitoring system (HMS), flap actuator power amplifier and control system, and data acquisition, processing, and display systems.

As part of the whirl tower test, a response analysis pulse (RAP) test of the test stand was performed. Results shown in Table 6 confirmed the test stand modes (elevator unlocked) to be similar to those obtained in 1991 during the shake test conducted in preparation for MDART testing (ref. 12). All whirl tower testing was performed with the elevator unlocked. Rotor collective pitch was limited to 8 degrees maximum, because of the 150-cycle motor generator set limitations. Ground resonance testing was performed using the RCC dynamic console to perform a cyclic control stick stir with regressing lag mode damping obtained through a moving block analysis. Adequate damping up to 107 percent nominal rotor speed (N_R) was confirmed.

Table 6: Rap Test of SMART Rotor Hub on LRTS at Whirl Tower

	SMART—2007				MDART—1991	
	Elevator unlocked		Elevator locked			
Test Stand Modes	Hz	%	Hz	%	Hz	% critical
1st lateral	2.7	3.1	3.0	1.2	2.2	7.7
1st longitudinal	4.2	0.7	4.2	0.7	4.0	1.7
2nd lateral	6.9	0.4	6.9	0.4	6.9	1.2

WIND TUNNEL

The wind tunnel test was conducted in the NFAC 40- by 80-foot test section during an 11-week period from February 13 through May 2, 2008. Setup and checkout were performed in accordance with references 23–29. The setup used 9-foot 1-inch front struts with 6.187-inch tips, and the wind tunnel scale damper-on, snubbers-off configuration. After installation of the test stand, a checkout of the motor, motor control, transmission, control console, and test stand instrumentation and health monitoring system (HMS) was performed. The full-scale SMART rotor hub, flexbeams, snubber/dampers, pitchcases, drive shaft, Metraplex, and slip ring were installed and hub runs were conducted. After installation of the blades, a complete instrumentation, data, and flap actuator power system verification/checkout was conducted. Various numerical and graphical displays were set up and checked out to ensure safe operation of the test. Details of the major steps in the setup and checkout are provided below.

The LRTS, rotor balance, and mast were lifted into the test section as an assembly. Lift-in was performed in accordance with reference 29. The LRTS was installed on two 9-foot 1-inch front struts with 6.187-inch tips and an extendable tail strut stand. The 1500-hp motor, swashplate, and hub assembly including hub, flexbeams, snubber/dampers, and pitchcases were lifted separately. Power, lubrication, instrumentation, and cooling lines were installed and secured. The test stand buildup and checkout proceeded to the point of installation of the control system. The motor polarity was verified, and the motor and transmission were run (Run 1) and operation of the HMS was verified. The test stand angle-of-attack calibration was completed.

The fairings and shake test plate were installed, and the tunnel scale system was in the damper-on, snubbers-off configuration. A rap test was performed to compare with data from the earlier MDART shake test (see ref. 22). In the MDART test the upper drive shaft was connected to the transmission. Data were obtained using a hydraulic shaker in two sets of bandwidths (64 Hz and 16 Hz). The SMART hub could rotate freely because the upper drive shaft was not connected to the transmission. SMART test stand modes were excited with a large instrumented hammer. The hammer could not excite the low frequency of the wind tunnel scale below 3 Hz.

The location of the hub accelerometer could not capture the longitudinal modes between 6 and 8 Hz. Table 7 lists the approximated frequencies (from the imaginary part of the response) for the SMART data compared with MDART data for the damper-on, snubbers-off configuration. Results confirmed that the SMART modal frequencies are similar to those obtained for MDART.

Table 7: Rap Test of SMART Rotor Hub on LRTS in Wind Tunnel

Test Stand Modes	SMART—2008, Hz		MDART—1992, Hz			
Longitudinal	4.38		4.26	6.57	7.78	
Lateral, yaw	6.88	12.5	2.94	4.64	6.72 (yaw)	12.27

Checkout of the rotor control console, the instrumentation and dynamic control console, and the test stand instrumentation were completed. The hydraulic system for swashplate control was installed and checked out. One pitch link was installed and rotor rigging, blade pitch calibration, and checkout of control system clearance were completed. Several tests were run to improve the hydraulic system configuration and verify adequate performance of the hydraulic accumulators (5 and 10 gallons) in case of pressure drop (Runs 2, 4).

The hub-mounted Metraplex system and slip ring were installed. Checkout and calibration of rotating system instrumentation (except blades) was started. Sufficient clearance of the Metraplex to pitchcase was verified. The hub (without blades, Run 3) was run up to 110 percent N_R (431 RPM) and dynamically balanced using the advanced vibration analyzer (AVA). The hub assembly was balanced to 0.17 ips lateral and 0.05 ips longitudinal at 100 percent N_R, 0.09 lateral and 0.02 longitudinal at 110 percent N_R. The motor drive control up to 110 percent N_R was verified, and the control system was exercised through 100 percent of its collective and cyclic pitch range (collective 0 to 15, longitudinal –7 to 10, lateral –7 to 4 degrees).

Check-loading of the rotor balance and static mast measurements was completed (Run 5). Hub weight tares (nonrotating, vary shaft angle, zero speed, Run 6) and rotation tares (rotating, vary shaft angle, zero speed, Run 8) were completed. Aero tares (rotating hub only, vary shaft angle and tunnel speed, Run 9) were completed next. Test conditions for the tare runs are shown in Figure 15. Reduction of the tare data was provided by NASA. The tare data used for data processing are shown in Appendix B.

Rotor blades were installed and checks of the calibrations on the blade, control system, flexbeam, drive system, and rotor balance measurements were performed. Static check loads were applied to blades 1 and 2 (Runs 10, 18). Blade weight tares (nonrotating, vary shaft angle, zero speed), rotor track and balance, and stability testing up to 105 percent N_R (412 RPM) in hover were completed (Runs 11–13). MDART shake test data and SMART rap test data provided information on stand resonances to avoid during rotor run-up (see Fig. 16). Ground resonance testing was performed using the RCC dynamic console to perform a cyclic control stick stir with regressing lag mode damping obtained through a moving block analysis. Adequate damping up to 105 percent N_R was confirmed. The control system was exercised with up to 10 degrees collective control and small excursions in cyclic control.

Rotor track was accomplished by adjusting pitch links. No trim tab adjustments were used for tracking. The blades were tracked within ±0.25 inch during hover and checked during forward flight runs. The AVA tracking feature used in combination with the NFAC tunnel lighting was unable to provide track data. The NFAC tracking strobe system was used in place of the AVA system camera to provide visual track data. Rotor balance was accomplished by harmonically analyzing the AVA accelerometers and adding weight as required to the pitchcase attach bolts. The rotor was balanced to 0.30 ips lateral and 0.05 ips longitudinal at 100 percent N_R during hover at 4 degrees collective and $\leq$ 0.13 ips lateral and $\leq$ 0.12 ips longitudinal in forward flight at 62 knots, $\alpha = -5$ degrees, and $C_T/\sigma = 0.075$.

Imbalance was checked at 124 knots, $\alpha = -9.1$ degrees, and $C_T/\sigma = 0.04$ resulting in 0.15 ips lateral and 0.12 ips longitudinal at 100 percent N_R. A total balance weight of 1030.5 grams was added to the rotor for wind tunnel testing.

Forward flight checkout of all systems (except active flap control) at speeds up to 124 knots was completed with Runs 14 and 15. These runs revealed high flexbeam loads. Subsequent adjustment of the flexbeam limits, taking the special properties of the –115 flexbeam configuration into account, and performing additional flexbeam inspections allowed continuation of the test through the planned test envelope. Results of flexbeam stiffness tests and analyses conducted in 2009 showed that the external wraps on the –115 flexbeam configuration contribute significantly to the flexbeam stiffness (see ref. 42).

The high-voltage (HV) amplifier system and wiring was installed, and the amplifier instrumentation was calibrated. Checkout of the active flap controller (AFC) and HV system to the slip ring was completed. Actuator and flap instrumentation was calibrated. The controller, HV system, actuators and flaps were checked out using open-loop voltage control and closed-loop control of the actuator stroke. Performance and safety of the system was established without rotation (Runs 16, 19) and in hover and forward flight (Runs 17, 20). Adjustment of flap linkages was not required.

During open-loop testing the actuator was cycled at 0 through 6/rev using operator selected amplitudes and phasing. During closed-loop testing the optimal controller (HHC or CTHHC) determined the amplitudes and phasing at the rotor speed multiples to be controlled. Frequency sweeps were conducted at up to 200 Hz and 200V. Initial setup and checkout of the actuators was performed with limited voltages and frequencies. The actuator voltage was generally limited to 400 ±500V, unless vibration or noise reduction was the test objective.

OPERATIONAL ENVELOPE

The rotor speed was limited to 107 percent N_R (419 RPM). Main rotor pitch control was limited to 14 degrees collective and cyclic as required for level flight trimmed to zero flapping. Alternate rotor trim to target hub loads was not used. Forward flight speed was limited to 155 knots.

During the test, no peak loads were allowed to exceed 80 percent of the defined limit load. In addition, the oscillatory loads were not allowed to exceed the endurance limit established for each measurement location. Under the cyclic excitations, the oscillatory loads were not allowed to exceed 10-hour limits.

Flap actuator operations were limited to a dynamic voltage of 400 ±500V with relative humidity (RH) less than 55 percent, and 400 ±600V with RH less than 45 percent.

CHECKLISTS

An Inspection Checklist was used for a daily check on rotor, data acquisition, and monitoring systems. This checklist helped to identify any changes in rotor characteristics due to wear, damage, or other causes. The Inspection Checklist for the wind tunnel test is provided in reference 28.

A Pre- and Post-run Checklist was used for each test run during the wind tunnel entry. This checklist was used to confirm completion of inspections, track model and software changes, and guide the startup and shutdown of the model and control room systems. This checklist is provided in Appendix C.

EMERGENCY OPERATING PROCEDURES

Emergency Operating Procedures (EOP) were established so that recovery from an unsafe condition can be accomplished without adversely affecting the rotor and support structure. The emergency procedures are invoked for a critical test condition, model failure, or actuator failure. Reference 27 contains a description of possible emergencies.

A concise summary chart of emergency procedures was developed in conjunction with NFAC personnel during the model setup period. This effort also included refining procedures and agreeing on commands that team members from different organizations could readily understand and follow. Lastly, several practice sessions were held to exercise standard and emergency operating procedures, and form a cohesive team.

OPERATIONAL SAFETY REQUIREMENTS

Operational Safety Requirements included facility operations and controls that may affect safety. The following items were established and required for safe operation of the test being conducted.

- Facility fail-safe controls required for power, hydraulics, and mechanical systems.
- Crew training in use of facility systems and vehicles.
- Availability of medical facility or emergency response.
- Automatic lockout of personnel in lieu of warning devices.

Operational safety required the use of fall protection, protection from electrical and hydraulic energy sources, and fail-safe controls, etc. Proper training and equipment and standard lockout/tag-out procedures were used to mitigate such hazards.

During test preparations all personnel working on the test stand were notified before hydraulics or HV power was enabled. All unnecessary personnel were removed from the test stand. Two-way radio communication was used between the control room and test stand. In addition, warning signs and lights were displayed in the test section and/or control room as required.

7.0 TEST PERSONNEL

A list of Boeing personnel functions and responsibilities, as well as duties and specific assignments for the SMART rotor test, are provided in reference 23. The control room layout and station assignments for the wind tunnel test are shown in Figure 17. Boeing personnel stations and equipment are indicated in red. Maximum crew size was 12, including the test team lead. A minimum crew of eight was required to run the test. However, because of the reliability of the HV flap amplifiers, a separate operator for the amplifiers was not used during most of the testing.

8.0 CALIBRATION DATA

All measurements, including strain gauges, displacement transducers, accelerometers, voltage and current sensors, etc., were calibrated during test preparations or test setup. The calibration data is provided as part of the electronic data set. Reference 30 describes the calibration procedures and associated calibration data and results for components of the active flap double-X frame actuator: individual X frames, actuator stiffness, Hall Effect sensors, actuator frequency sweeps, piezoelectric stack column/segment stroke tests, and actuator load links. In addition, rotor system, test stand components, and wind tunnel parameters are included: rotor blade, flexbeam, pitchcase, pitch link, drive shaft, mast, stationary swashplate, rotor balance, LVDTs, test stand accelerometers, rotor speed, rotor azimuth angle, data alignment signal, and NFAC wind tunnel parameters.

9.0 DATA ACQUISITION AND FLAP CONTROL SOFTWARE

The software used for the SMART rotor data acquisition and postprocessing, and flap actuator control is briefly described below. Details are provided in references 25 and 7.

Data. Lumistar LDPS-8x Professional is used for acquiring, processing, displaying, and archiving the fixed and rotating PCM data streams. Some custom data processing routines were added to the built-in data processing and conversion library to enable data display as required for the test. All of the data relevant to acquiring and processing the PCM data streams is contained in the runtime data base for the SMART Rotor project, which is located inside the Lumistar directory tree on the AFC. Post test, the main data processing program, *smartdata*, reads the raw end-to-end data archive files created by the Lumistar LDPS data acquisition system, along with various input files. It generates the discrete event data files in the formats specified by NASA and required by Boeing's access, select, analyze, present (ASAP) program, as well as various statistical data files and resampled time history files. The program is written in C and compiled into a Windows executable along with various supporting code files.

Flap Actuator Control. SMART rotor flap actuator control is performed using a custom control program written as a Simulink model that is converted by dSpace-provided utilities to an executable that runs on the DS1103 controller board. Flap actuator control modes included open loop, using voltage commands, or closed loop, using flap position or vibratory hub loads for feedback.

10.0 DATA ACQUISITION AND REDUCTION

All acquired measurements were recorded on tape in raw PCM format. The output of all measurements and the derived parameters were recorded in the PC-based data acquisition system. The recorded data was processed in the format required by NASA and for access using Boeing's ASAP program. Details of the data acquisition and reduction are provided in the Software Plan (ref. 25).

The electronic data is delivered on an external PC hard drive. The size of all files is about 650 GB. All the data acquired by Boeing during the wind tunnel test, as well as all the data derived from the measured parameters, are included. Raw time histories, time slices, and statistical data for a total of 39 runs and 2,675 points are provided. Boeing run numbers are used in naming the data files. A summary of the test runs including objectives, comments, controller used, and run times is provided in Appendix A. The current data set represents the most accurate depiction of the data Boeing acquired during the wind tunnel test.

Raw time history data is provided in binary format with two files per run, one for the rotating and one for the nonrotating PCM data stream. For each test point in a run, time history data for each measured parameter (raw and converted) and derived parameter are included in binary file format, one file per point and parameter. Typically, time slice length is 12 seconds (about 78 rotor revolutions) for steady-state conditions and 45 seconds for frequency sweeps. For a few baseline steady-state cases, the time slice length is 42 seconds.

For steady-state cases, statistical data and harmonic data (up to 20/rev) are included in csv file format, one file per run and measured or derived parameter. Following Boeing flight test convention, the average, cyclic, and harmonic values are taken from the rotor revolution where the cyclic value is a maximum. Similarly, steady-state values of select rotor performance parameters are included in csv file format, one file per run.

Table 8: Test Data Directory Structure

\SMART\Processed\NFAC			event slice data processed into NASA formats
	\nnnnn		data for run nnnnn
		\ppppp\binary\mmmmm.dat	time histories, full fidelity (binary)
		\stats\mmmmm.csv	statistical data, all points average, cyclic, harmonics from rotor revolution with largest cyclic value (points, statistical data)
		perf.csv	performance data, all points (points, average of performance parameters)
	\NFAC_AvgRev		data averaged on a per revolution basis
		\statsnnn	data for run nnn
		mmmmm_rev.csv	time histories, 1 rotor revolution, all points, 256 values per revolution (values, points), 1st column is azimuth data
		mmmmm.csv	statistical data, all points
		perf.csv	performance data, all points
	\NFAC_MaxCycRev		data from rotor revolution with the maximum cyclic value
		\statsnnn	data for run nnn
		mmmmm_rev.csv	time histories, 1 rotor revolution, all points, 256 values per revolution
		mmmmm.csv	statistical data, all points
		perf.csv	performance data, all points

n - run number, 1 - 47 (Boeing values) p - point number, 1 - ….
m - measurement number, 1001 - 21005; including derived parameters

In addition, the time history data is averaged on a per revolution basis over all available rotor revolutions. This averaged time history and the time history for the rotor revolution with the maximum cyclic value are resampled with 256 samples for the rotor revolution. Statistical data, including harmonic data, and performance data are computed for both the averaged and maximum cyclic time histories.

An initial data set was provided at the conclusion of the wind tunnel test. The data was reviewed and completely reprocessed in late 2008 and again in late 2009. This most recent data set includes a complete set of test runs, is based on gap-free data reacquired from tape (except runs 16, 31, 32, 44, and 46) and uses updated slicing times. Starting value offsets for flap link loads, rotor balance loads, and drive shaft torques were updated. Some errors in processing the azimuth data and aero tares were corrected. Test cards were updated to clarify test conditions, improve test point labels, add individual points for repeat frequency sweeps, and add cards that had not been formalized before.

The hard drive main folder (SMART) includes four folders. “Acquisition From Tape” contains Lumistar LDPS raw data reacquired from tape to eliminate gaps in the data. “Recovered Data” contains original LDPS raw data for those tests that are not on tape (Runs 16, 31, 32, 44, and 46). “Processed” contains folders and files used in processing the raw data and the folder “NFAC” for the processed data. The folder “src” contains the source code for the processing programs. Additional details are provided in references 5 and 25. The structure and content of the processed data in the “NFAC” folder are shown in Table 8.

In addition to the full length and resampled time history slices, “NFAC” contains two types of files.

mmmmm.csv: A “stats” CSV file provides statistical and harmonic data for the parameter for each point in this run. It contains as many rows as the number of points for this run, with each row containing the following fields: test number, point number, point description, minimum value, maximum value, average value, cyclic value (half peak-to-peak), mean value, rms value, and sine and cosine coefficients for the first 20 harmonics. The average, cyclic (max–min)/2, and harmonic coefficient values are taken from the rotor cycle where the cyclic value is a maximum.

perf.csv: A "performance" CSV file provides a summary of performance-related parameters for each point in this run. It contains as many rows as the number of points for this run, with each row containing the following fields: test number, point number, point description, VKTS, TSR, VSOUND, RHO, RPM, OMEGR, MTIP, MAT, VOR, ALFSU, COLL, LONG, LAT, ALFSC, HFOR, YFOR, THRUST, RFOR, RMOM, ANGX/L, HP, HP2, HPQW, HP2QW, CXR/S, CP/S, CYR/S, CLR/S, CMX/S, CMY/S, CMZ/S, CQ/S, FE, L/D, FMERIT, CT, CT/S, CP, FBM1FB91S, and FBM1FB91C. The last two parameters are the first harmonic coefficients for the flexbeam flap bending at station 9; these are used as an indication of rotor trim. The performance parameters are calculated based on the average values as written to the stats folder.

11.0 SPECIFIC TEST CONDITIONS

Hover test conditions for the baseline rotor (no active flap inputs) consisted of track and balance runs, ground resonance stability runs, and swashplate controls checkout. Active flap frequency sweeps were performed to investigate rotor and active flap dynamics. In general, hover cases were run with a –10 degree shaft tilt and 4 degrees of collective, to reduce recirculation and provide for a smooth environment.

Forward flight testing included speeds from 42 to 155 knots. The primary thrust setting was $C_T/\sigma = 0.075$, corresponding to 5811 pounds thrust at sea level standard day. Shaft angles were representative of level forward flight or landing approach. In general, the rotor was trimmed to zero flapping, or the control settings were left unchanged during a sweep of active flap input parameters such as phase or frequency.

Specific test points for the HQP validation database are shown in Figure 18. These included three flight conditions (83, 123, and 155 knots) and four active flap schedules. Limited forward flight testing was conducted for baseline cases to check out swashplate controls, establish rotor performance for a range of shaft angles and thrust values, and conduct shaft angle sweeps to determine conditions for maximum BVI noise. In addition, rotor performance was evaluated for flap inputs of 0 degree and 1.5 degrees at 2/rev. These conditions are summarized in Appendix D.

Extensive forward flight testing was conducted to evaluate the effects of the active flap on BVI and in-plane noise, vibrations, control power, rotor smoothing, and performance. Table 9 provides a summary of these active flap test conditions. Numerous active flap frequency sweeps were conducted to obtain data required for the flight controls objective and for determining the parameters for the closed-loop CTHHC vibration controllers. All active flap test conditions are summarized in Appendix D in chronological order and sorted by test objective. In addition, test cases for specific active flap objectives are listed in the appendix in test card format (event times not updated).

A complete set of test cards was prepared and served as test log including the chronology of events. The test cards include a description of test objectives, the test configuration, test date, and atmospheric conditions at the beginning of the test run (barometric pressure, operating ambient temperature (OAT), and relative humidity). Unique assigned test point numbers and event times, specific test conditions, controllers used, comments, anomalies, and concise test point labels are provided.

In addition, the progress reports prepared during the wind tunnel entry and photographs taken during the test preparations, whirl tower test, and wind tunnel test are provided in Appendix E.

Table 9: Active Flap Test Conditions

Objective	Condition	Velocity* V, kt	Advance Ratio*, μ	Tip Mach # MT	Adv Tip Mach # MAT	Shaft Angle uncorrected α, deg	Blade Loading C_T/σ	Active Flap Control: Harmonic Number, n	Active Flap Control: Amplitude A, deg [V]	Active Flap Control: Phase φ, deg
Validation	1	123	0.3		0.805	–9.4	0.08	5	0, 2	90
	2	123	0.3		0.805	–9.4	0.08	3	0, 2	60
	3	155	0.375		0.852	–9.3	.07, (.075)	5	0, (1)	180
	4	83	0.2		0.746	0.9	0.075	2 & 5	0, 2 & 1	240 & 330
BVI Noise	1	62	0.15	0.623		4	0.075	2,3,4,5	1 - 2	sweep
(RPM = 392)	2	68	0.165	0.617		1.8	"	3,4	1 - 2	"
	3	82	0.2	0.623		2	"	2,3,4,5	1 - 2.5	"
In-plane Noise	1	124	0.3	0.623	0.809	–9.1	0.075	2,3,4,5	1 - 2	"
Vibration	1	82	0.2	0.623		2	0.075	2,3,4,5,6	250V	sweep
	2	"	"	"		"	"	Closed Loop: NF 5,1,1-5P; RM 5,1,1-5P		
	3	124	0.3	"		–9.1	"	2,3,4,5,6	250V	sweep
	4	"	"	"		"	"	Closed Loop: 1-5P, 10P; PM 1-5P		
Control Power	1	82	0.2	0.623		–5.5	0.075	0,1	–3 to 3	0,90
	2	"	"	"		2	"	"	"	"
	3	124	0.3	"		–9.1	"	"	"	"
Rotor Smoothing	1	0	0	0.623		–10	0.028	0	A1 = –3 to +3	
	2	82	0.2	"		2	0.075	"	"	
	3	124	0.3	"		–9.1	"	"	"	
	4	"	"	"		"	"	"	A2 = –3 to +3	
Performance	1	82	0.2	0.623		2	0.075	n/a	0V, 0	
	2	124	0.3	"		–9.1	0.075	"	0V, 0	
	3	"	"	"		"	0.075	2	0, 1.5	sweep
	4	"	"	"		"	0.09	"	"	"

NF - normal force, RM - roll moment, PM - pitch moment, [alternate units], (target condition, not achieved)
* Condition is set to value shown in large type font.

12.0 TEST RESULTS

An overview of the entire test effort and a sample of test results covering all the objectives is presented in reference 1. Detailed results for BVI noise, in-plane noise, vibration reduction, and flap position control are shown in the companion papers (refs. 2,3,4).

SMART rotor performance data was obtained for several values of advance ratio, rotor shaft angle, and thrust. The data was measured by the rotor balance, rotor shaft instrumentation, and the wind tunnel air data system. Test data repeatability was found to be typical of rotor performance wind tunnel testing. SMART rotor baseline performance data with no command (zero voltage) versus zero position commanded showed very similar results. Agreement of baseline SMART and MDART performance is poor, possibly because of differences in hub aerodynamics, trim condition, or differences in the primary and secondary shaft torque gauge. The effect of active flap inputs (1.5 deg at 2/rev) on rotor performance was found to be negligible or within the data scatter.

An analysis of frequency response data to identify blade and actuator modes was conducted using comprehensive identification from frequency responses (CIFER^{TM}). The basic input/output relationships between the command voltage to the active flap and variables directly associated with flap motion had reasonable data quality. However, even the most direct and simple relationships such as actuator voltage to actuator motion were severely corrupted around 1P because of aerodynamic influences disturbing the blade flap motion.

13.0 CONCLUSIONS

A wind tunnel test of the SMART active flap rotor was conducted in the anechoic test section of the NFAC 40- by 80-Foot Wind Tunnel at NASA Ames Research Center. Loads, performance, and acoustic data were acquired in support of validating high-fidelity physics-based CFD-CSD rotor-noise prediction tools. The effectiveness of the active flap control on noise and vibration was conclusively demonstrated. Results show reductions in blade vortex interaction (BVI) and in-plane noise as well as vibratory hub loads. Noise reductions up to 6 dB, as well as vibratory hub load reductions of about 80 percent, were measured. Trailing-edge flap deflections were controlled with less than 0.2 degree rms error for commanded harmonic profiles of up to 3 degrees amplitude. The impact of the active flap on control power, rotor smoothing, and aerodynamic performance was also demonstrated. Finally, the reliability of the flap actuation system was successfully proven in more than 60 hours of wind tunnel testing. Specific conclusions are as follows:

1. Both CTHHC and HHC were effective in controlling active flap position, using position feedback and applying individual control to each flap. When commanding zero deflection, flap deflections were within 0.12 degree for all speeds tested. When commanding harmonic deflection profiles, the rms error was less than 0.2 degree.
2. Data for the validation of physics-based aeroacoustic prediction codes was successfully acquired at three test points. For the high-speed condition at 155 knots, blade loads were too high to exercise the specified flap deflection schedule, however baseline data (with 0-degree flap deflection) was acquired.
3. Reductions in BVI noise in simulated descending flight and in-plane noise in level flight were demonstrated using active flap position control with single harmonic inputs. The best flap deflection profiles were determined through systematic variation of input phase, frequency, and amplitude. Both BVI and in-plane noise reduction incurred higher vibratory hub loads.

4. BVI sound pressure level (BVISPL) reductions at the baseline rotor BVI hot spot varied between 3.5–6 dB at $\mu = 0.15$, and 3–5 dB at $\mu = 0.165$. At $\mu = 0.2$ smaller reductions of up to 3 dB were measured under the rotor disk. In all three cases, 1.5 degree flap amplitude gave the best reductions.
5. In-plane noise reductions of up to 6 dB low-frequency sound pressure level (LFSPL) were measured at $\mu = 0.3$, with a best active flap command of 1.3 degrees/4P/180 degrees.
6. Vibratory hub load reduction was demonstrated using the CTHHC algorithm for feedback control of one hub load at a time. Control of vibratory normal force was very effective, reducing harmonics 1–5P by 95 percent for both the level flight and descent conditions. Control of vibratory roll moment in descent and pitch moment in level flight was shown to be slightly less effective, reducing harmonics 1–5P by 68 percent and 73 percent, respectively.
7. Steady-state flap inputs resulted in thrust and hub moment changes, and provided a measure of the control power available from the flaps. Hub load changes were substantial, especially considering the very stiff control system of the test stand that limited the moment control effectiveness of the flap.
8. Rotor smoothing was evaluated through steady-state inputs to a single flap. Results indicated that it may be feasible to use flaps for in-flight blade tracking.
9. Rotor performance as measured by rotor L/D was affected by 2/rev flap inputs at $\mu = 0.3$. L/D increased at 90 degrees and decreased at 270 degree phase, demonstrating the potential of the active flaps to improve performance. A 1-percent increase in L/D versus baseline was deemed too small to reach definitive conclusions.

14.0 ADDITIONAL INFORMATION

Additional information relevant to the test preparation and conduct is provided in references 43 and 44. Of particular interest are the Test Events of Note (Section 4) and the detailed Daily Test Log (Appendix B) in reference 44.

Reference 45 details the experimental data acquired from the SMART test in support of the DARPA HQP program to enable correlations/comparisons with pretest predictions. Data collected from the Boeing-SMART rotor test were examined and formatted to meet requirements as stated by DARPA for the HQP Phase Ib code validation effort. All the pertinent experimental data channels were reviewed to ensure HQP requirements were met and that the quality and repeatability of the data was adequate. One representative test point for each of the five flight conditions was selected from multiple repeats for submission to DARPA. Overall, it was determined that each individual selected test point is representative of the desired state of the rotor and is apt for HQP Phase Ib code validation.

15.0 REFERENCES

1. Straub, F. K.; Anand, V. R; Birchette, T. S; and Lau, B. H.: Wind Tunnel Test of the SMART Active Flap Rotor. AHS Annual Forum, Grapevine, TX, May 2009.
2. JanakiRam, R. D.; Straub, F. K.; Kitaplioglu, C.; and Sim, B. W.: Blade-Vortex Interaction Noise Characteristics of a Full-Scale Active Flap Rotor. AHS Annual Forum, Grapevine, TX, May 2009.
3. Sim, B. W.; JanakiRam, R. D.; Barbely, N. L.; and Solis, E.: Reduced In-Plane, Low Frequency Noise of an Active Flap Rotor. AHS Annual Forum, Grapevine, TX, May 2009.
4. Hall, S. R.; Anand, V. R.; Straub, F. K.; and Lau, B. H.: Active Flap Control of the SMART Rotor for Vibration Reduction. AHS Annual Forum, Grapevine, TX, May 2009.
5. Anand, V. R. and Straub, F. K.: SMART Rotor Wind Tunnel Test Data Report. Boeing Mesa, FTTN-2008-037, Nov. 2008; Rev. A, Jan. 2010.
6. Straub, F. K. and Anand, V. R.: 2x-Frame Actuator Flexure Fatigue Test Report. Boeing Mesa, FTTN-2008-025, June 2008.
7. Anand, V. R. and Straub, F. K.: SMART Rotor Closed Loop Control Methodologies and Piezoelectric Stack Testing. Boeing Mesa, FTTN-2010-003, Jan, 2010.
8. NFAC Staff, National Full-Scale Aerodynamics Complex: Operations Manual, Part IV, Test Planning Guide, Sept. 1989.
9. Silverthorn, L. J.: Desktop Procedure for Conducting Whirl Tower and Wind Tunnel Tests. Boeing Mesa, FTTN-97-007, Rev. A, May 2006.
10. Anand, V. R. and Lauzon, D. M.: MDX Explorer Aeroelasticity and Mechanical Stability Report, Report No. 900RR000028, Sept. 1994.
11. Hong, R.: MDX Full Scale Rotor Whirl Tower Test Plan, Report No. 11-90-078.
12. Anand, V. R. and Lauzon, D. M.: MDX Main Rotor Whirl Tower Test, Report No. 900RR100022.
13. Jacklin, S.; Lau, B.; and McNulty, M.: MDHC Advanced Rotor Technology (MDART) Test in the NASA Ames 40- by 80-Foot Wind Tunnel Test Plan, Rev. C, Jan. 29, 1992.
14. McNulty, M.: MDART Test in the NASA Ames 40- x 80-foot Wind Tunnel—Software Plan, RTTN-91-006, Rev. B, Jan. 1992.
15. Nothaft, M.: MDART Instrumentation Test Plan, Jan. 1987.
16. Stemple, A: MDART NASA Ames 40- x 80-foot Wind Tunnel Test System Safety Analysis. Boeing Mesa, FTTN-92-029, Jan. 1992.
17. McNulty, M.; Jacklin, S.; and Lau, B. H.: A Full-Scale Test of the McDonnell Douglas Advanced Bearingless Rotor in the NASA Ames 40- by 80-Ft Wind Tunnel. AHS 49th Annual Forum, St. Louis, MO, May 1993.
18. Nguyen, K.; McNulty, M.; Anand, V.; and Lauzon, D.: Aeroelastic Stability of the McDonnell Douglas Advanced Bearingless Rotor. AHS 49th Annual Forum, St. Louis, MO, May 1993; also NASA TM 108831, June 1994.
19. Smith, R. and Engelhardt, K.: MDART Wind Tunnel Test Rotor Performance Report. Boeing Mesa, FTTN-93-013, Aug. 1993.

20. Jacklin, S. A.; Lau, B. H.; Nguyen, K. Q.; Smith, R. L.; and McNulty, M. J.: Full-Scale Wind Tunnel Test of the McDonnell Douglas Five-Bladed Advanced Bearingless Rotor: Performance, Stability, Loads, Control Power, Vibration and HHC Data. AHS Aeromechanics Specialists' Conference, San Francisco, CA, Jan. 1994; also NASA TM 112094.
21. Nguyen, K.; Lauzon, D.; and Anand, V.: Computation of Loads on the McDonnell Douglas Advanced Bearingless Rotor. AHS 50th Annual Forum, Washington, D.C., May 1994; also NASA TM 111887.
22. Nguyen, K. and Lau, B. H.: Dynamics of the McDonnell Douglas Large Scale Dynamic Rig and Dynamic Calibration of the Rotor Balance, NASA TM 108855, Oct. 1994.
23. Straub, F. K.: SMART Rotor Tunnel Test Plan. Boeing Mesa, FTTN-2008-002, Feb. 2008.
24. Straub, F. K. and Anand, V. R.: SMART Rotor Extended Wind Tunnel Test Plan Draft and Closed Loop Control Methodologies Report. Boeing Mesa, FTTN-2008-10, Feb. 2008.
25. Anand, V. R. and Straub, F. K.: SMART Rotor Wind Tunnel Test Software Plan. Boeing Mesa, FTTN-2008-003, Jan. 2008; Rev. A, Jan. 2010.
26. Yates, E. and Nothaft, M.: SMART Rotor Wind Tunnel Test Instrumentation Plan. Boeing Mesa, FTTN-2008-005, Jan. 2008.
27. Straub, F. K.: SMART Rotor Wind Tunnel Test System Safety Analysis. Boeing Mesa, FTTN-2008-006, Jan. 2008; Rev. A, Mar. 2008.
28. Birchette. T. S. and Straub, F. K.: SMART Rotor Wind Tunnel Test Operation and Inspection Procedures. Boeing Mesa, FTTN-2008-007, Jan. 2008; Rev. A, Jan. 2010.
29. Birchette. T. S.: SMART Rotor Wind Tunnel Test Rigging Plan. Boeing Mesa, FTTN-2008-008, Jan. 2008.
30. Anand, V. R. and Birchette, T. S.: SMART Rotor Wind Tunnel Test Calibration Report. Boeing Mesa, FTTN-2008-024, June 2008.
31. Straub, F. K. and Hassan, A. A.: Aeromechanic Considerations in the Design of a Rotor with Smart Material Actuated Trailing Edge Flaps. AHS 52nd Annual Forum, Washington D.C., June 1996.
32. Straub, F. K. and Charles, B. D.: Comprehensive Modeling of Rotors with Trailing Edge Flaps. AHS 55th Annual Forum, Montreal, May 1999; JAHS vol. 46, no. 3, July 2001.
33. Hall, S. R.; Tzianetopoulou, T.; Straub, F. K.; and Ngo, H.: Design and Testing of a Double X-Frame Piezoelectric Actuator. SPIE Conference on Smart Structures and Materials, Newport Beach, CA, Mar. 2000.
34. Straub, F. K.; Kennedy, D. K.; Stemple, A. D.; Anand, V.; and Birchette, T.S.: Development and Whirl Tower Test of the SMART Active Flap Rotor. SPIE Conference on Smart Materials and Structures, San Diego, CA, July 2004.
35. Straub, F. K. and Kennedy, D. K.: Design, Development, Fabrication and Testing of an Active Flap Rotor System. AHS 61st Annual Forum, Grapevine, TX, June 2005.
36. Straub, F. K. and Anand, V. R.: Whirl Tower Test and Analysis of the SMART Active Flap Rotor. AHS 63rd Annual Forum, Virginia Beach, VA, 2007.
37. Stemple, A.: Smart Rotor Design Analysis Report. Boeing Mesa, STN 02-030, June 2002.

38. Hitchcock, E.: SMART Rotor Design Analysis Report. Boeing Mesa, STN 02-030a, Oct. 2007.
39. Hitchcock, E.: SMART Rotor Design Analysis Report Addendum. Boeing Mesa, STN 02-030a-Addendum, Feb. 2008.
40. Straub, F. K. and Anand, V. R.: SMART Rotor Dynamic Analysis Report. Boeing Mesa, FTTN-2007-025, Oct. 2007.
41. Straub, F. K. and Tadghighi, H.: SMART and MDART Rotor Geometry and Properties. Boeing Mesa, FTTN-2007-015, July 2007.
42. Straub, F. K.; Birchette, T. S.; Jones, M. D.; and Hamilton, B.: SMART Rotor Assessment of Flexbeam Stiffness. Boeing Mesa, FTTN-2010-002, Jan. 2010.
43. Johnson, J.; Goulding II, P.; and Sacco, J.: DARPA/NASA/Army/Boeing SMART Rotor Test in the NFAC 40- by 80-Foot Wind Tunnel—Test Plan, NFAC Report, Rev. 4, July 2009.
44. Johnson, J.; Goulding II, P.; and Sacco, J.: DARPA/NASA/Army/Boeing SMART Rotor Test in the NFAC 40- by 80-Foot Wind Tunnel—Post-Test Report, NFAC Report, Rev. 1, July 2009.
45. Lau, B. H.; Obriecht, N.; Gasow, T.; Hagerty, B.; and Cheng, K. C.: Boeing-SMART Test Report for DARPA Helicopter Quieting Program, NASA TM-2010-216404, Aug. 26, 2009.

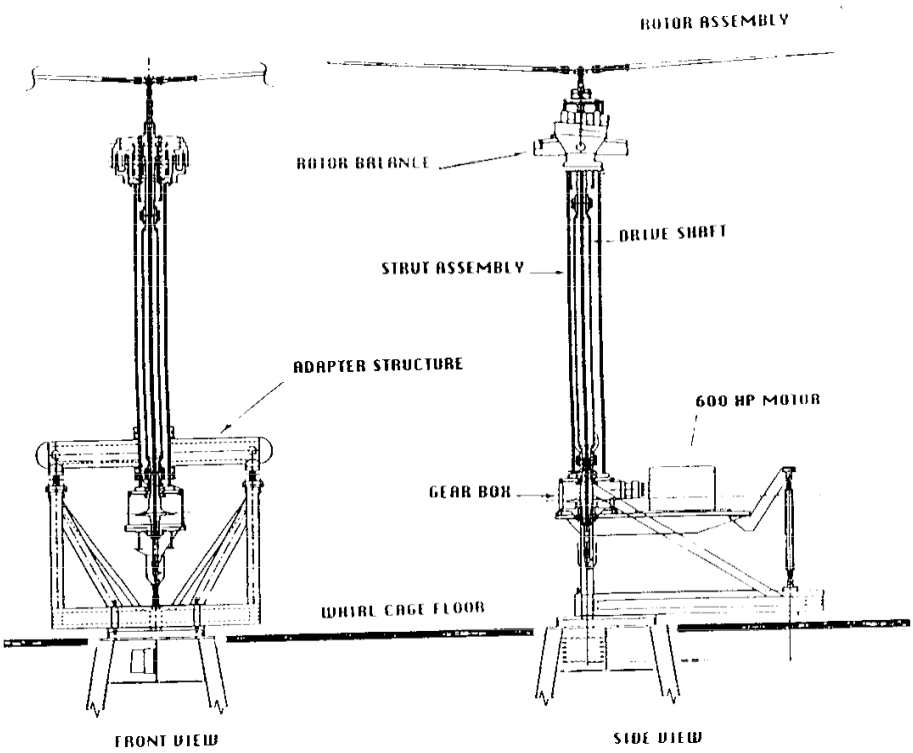

Figure 1a: Test stand, rotor, elevator setup (for LHX test).

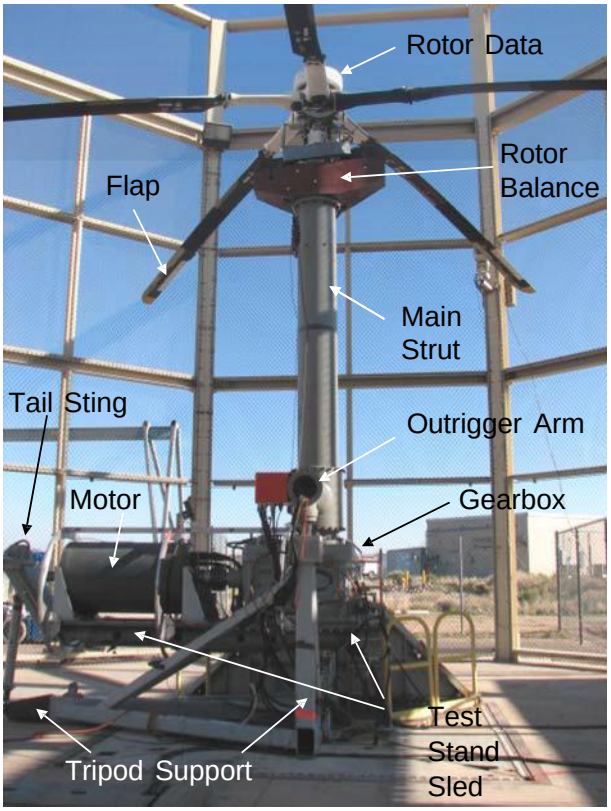

Figure 1b: System integration test at whirl tower showing LRTS test stand and SMART rotor setup (2008).

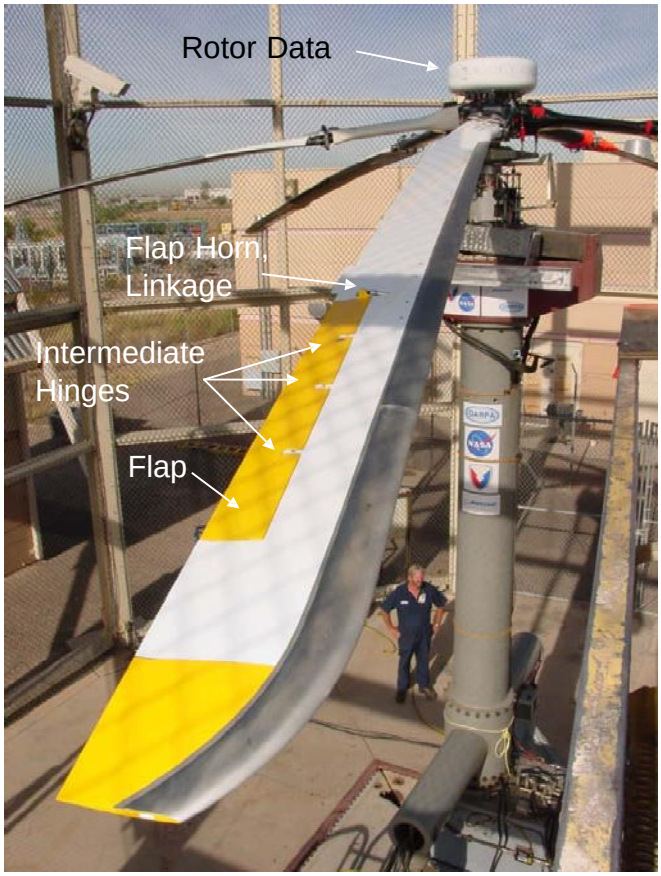

Figure 1c: SMART rotor at whirl tower (2003).

Figure 1d: MDART rotor in NFAC 40- by 80-foot wind tunnel (looking downstream (1992)).

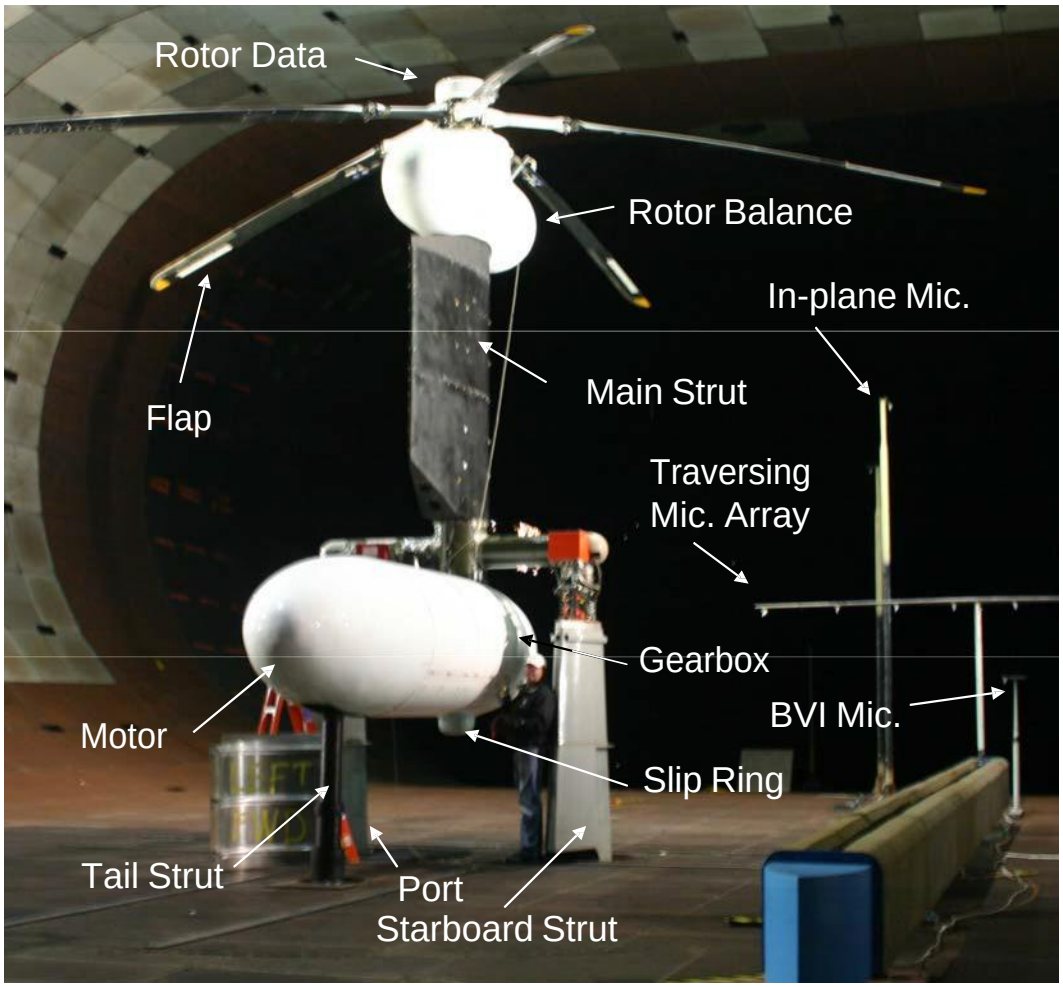

Figure 1e: SMART rotor in the NFAC 40- by 80-foot wind tunnel (looking upstream).

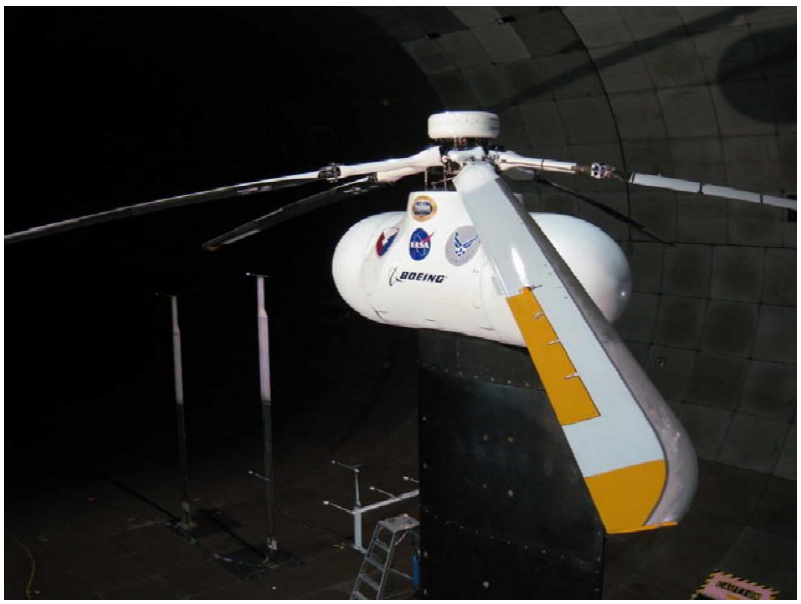

Figure 1f: Close-up view of the SMART rotor, blade, and flap in the tunnel.

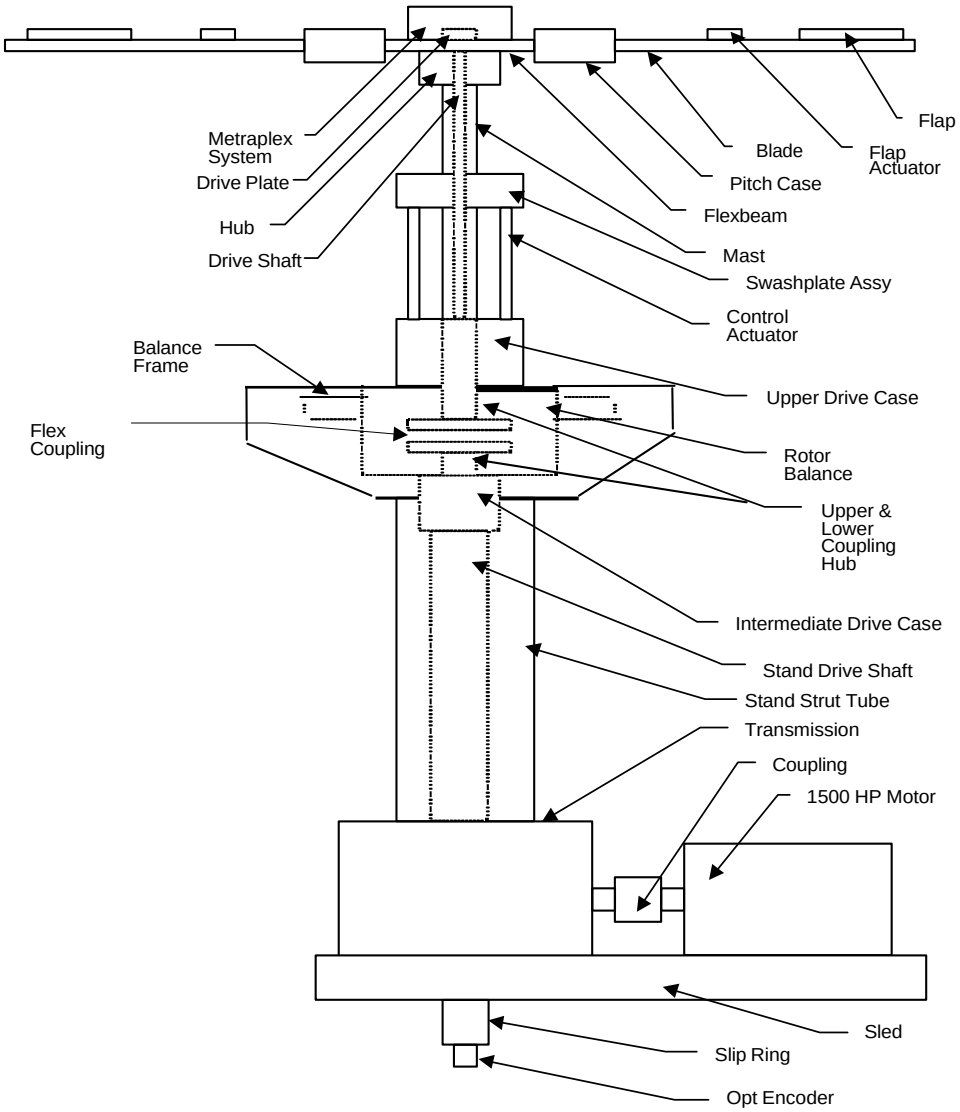

Figure 2a: Schematic of SMART rotor and test stand components.

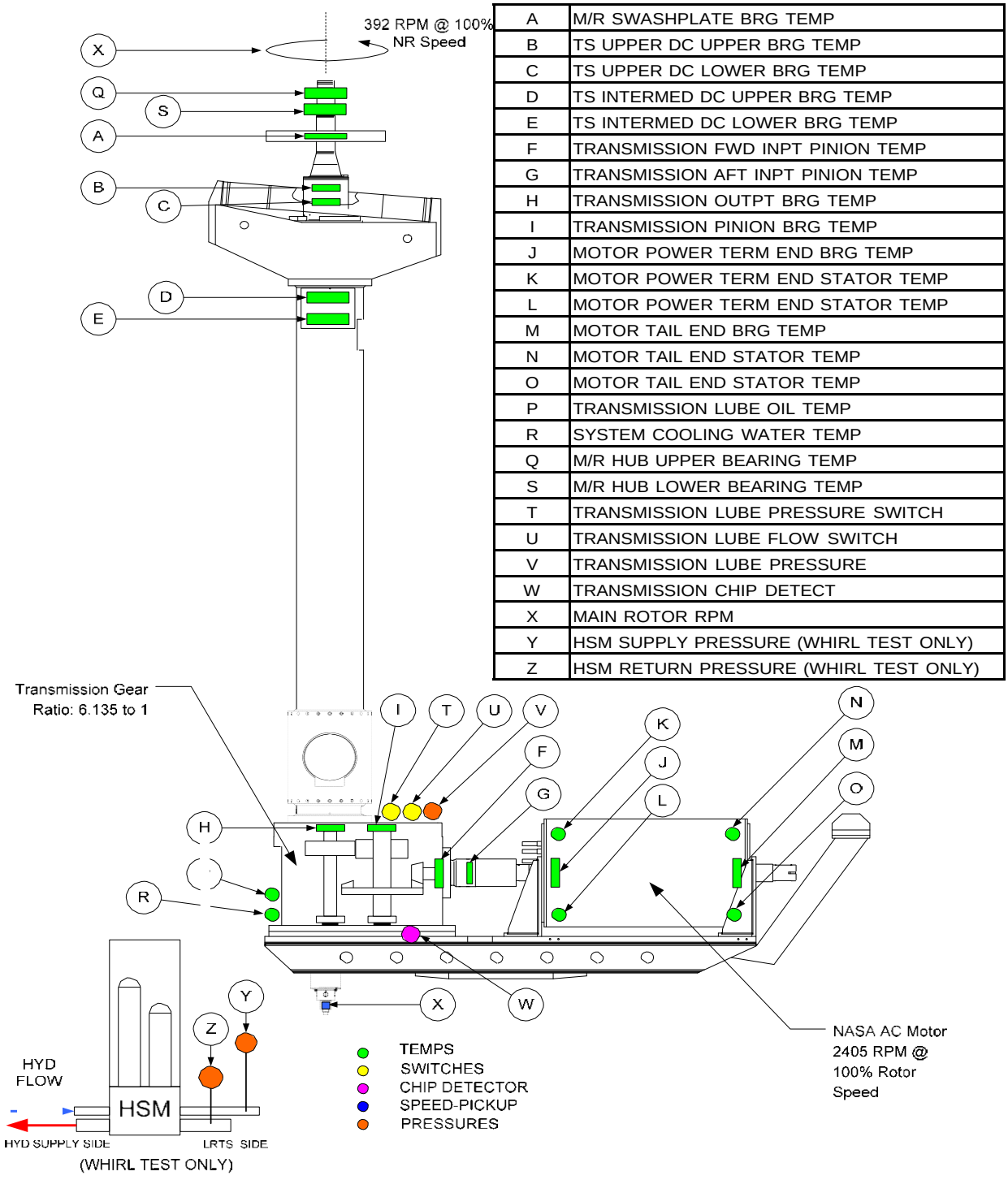

A	M/R SWASHPLATE BRG TEMP
B	TS UPPER DC UPPER BRG TEMP
C	TS UPPER DC LOWER BRG TEMP
D	TS INTERMED DC UPPER BRG TEMP
E	TS INTERMED DC LOWER BRG TEMP
F	TRANSMISSION FWD INPT PINION TEMP
G	TRANSMISSION AFT INPT PINION TEMP
H	TRANSMISSION OUTPT BRG TEMP
I	TRANSMISSION PINION BRG TEMP
J	MOTOR POWER TERM END BRG TEMP
K	MOTOR POWER TERM END STATOR TEMP
L	MOTOR POWER TERM END STATOR TEMP
M	MOTOR TAIL END BRG TEMP
N	MOTOR TAIL END STATOR TEMP
O	MOTOR TAIL END STATOR TEMP
P	TRANSMISSION LUBE OIL TEMP
R	SYSTEM COOLING WATER TEMP
Q	M/R HUB UPPER BEARING TEMP
S	M/R HUB LOWER BEARING TEMP
T	TRANSMISSION LUBE PRESSURE SWITCH
U	TRANSMISSION LUBE FLOW SWITCH
V	TRANSMISSION LUBE PRESSURE
W	TRANSMISSION CHIP DETECT
X	MAIN ROTOR RPM
Y	HSM SUPPLY PRESSURE (WHIRL TEST ONLY)
Z	HSM RETURN PRESSURE (WHIRL TEST ONLY)

Figure 2b: Health monitoring system parameters.

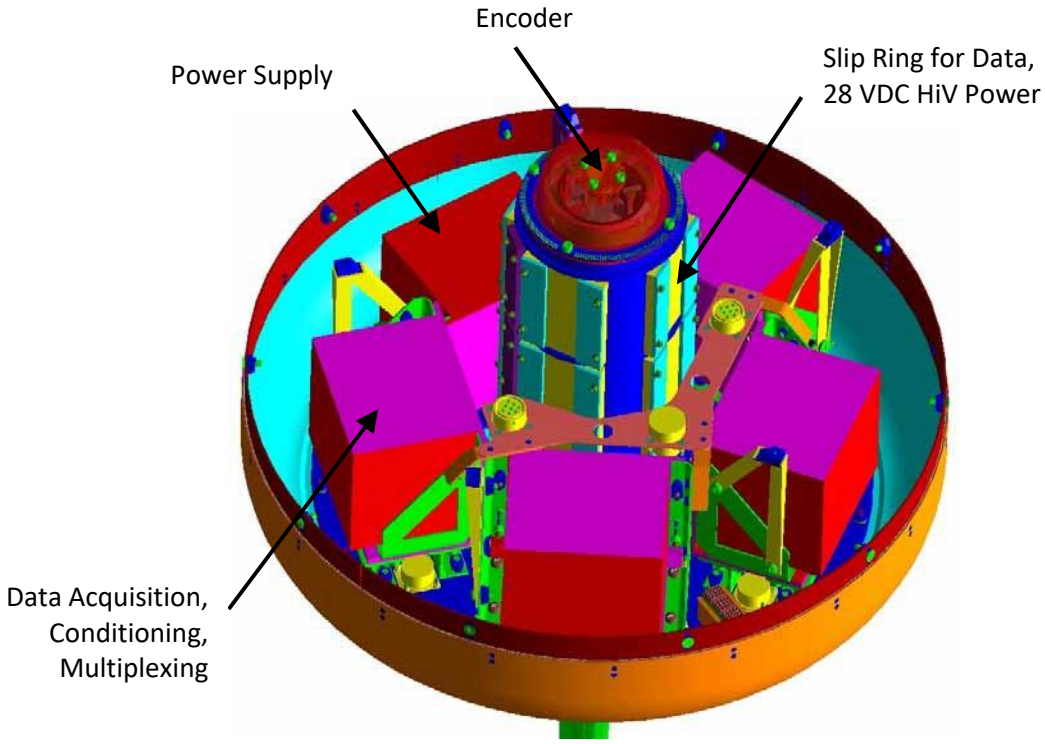

Figure 3: Hub-mounted data/power transfer system (note: in wind tunnel the slip ring and encoder are mounted below the transmission).

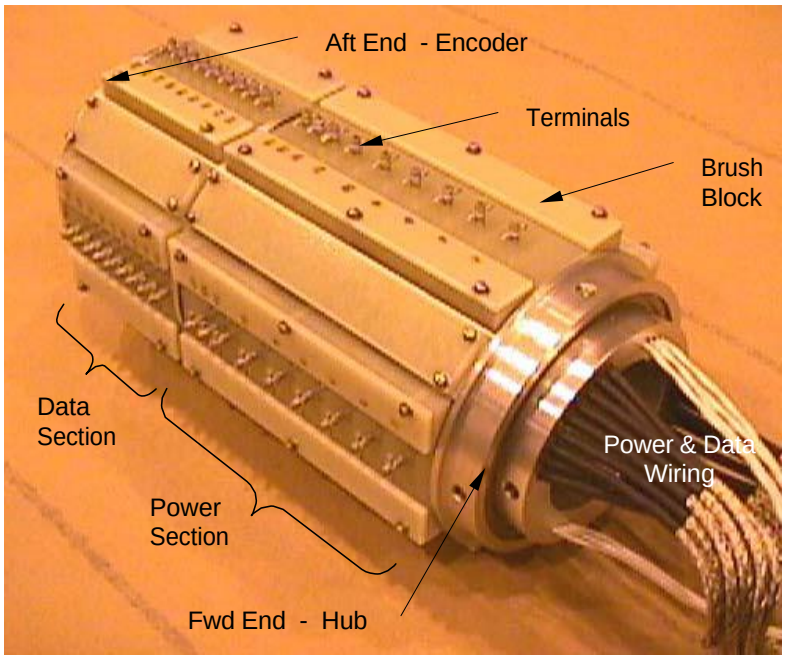

Figure 4: Slip ring for data (14 ch) and power (28V—4 ch, 1500V—8 ch).

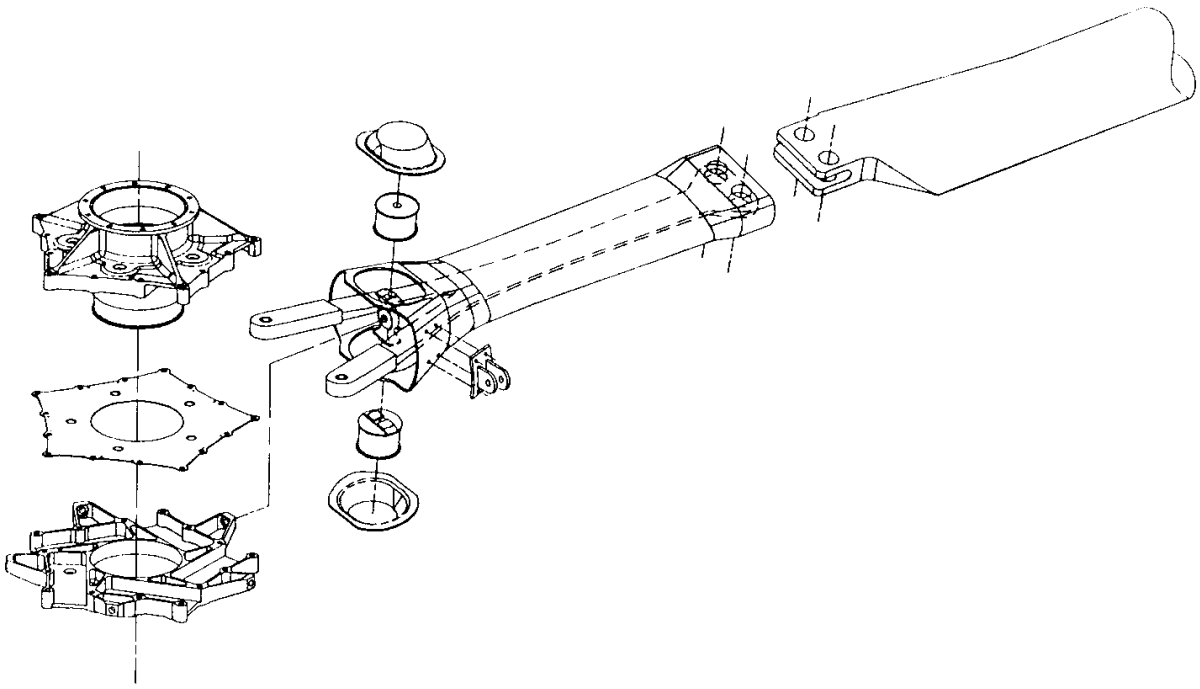

Figure 5: MD900 hub and blade root attachment structure.

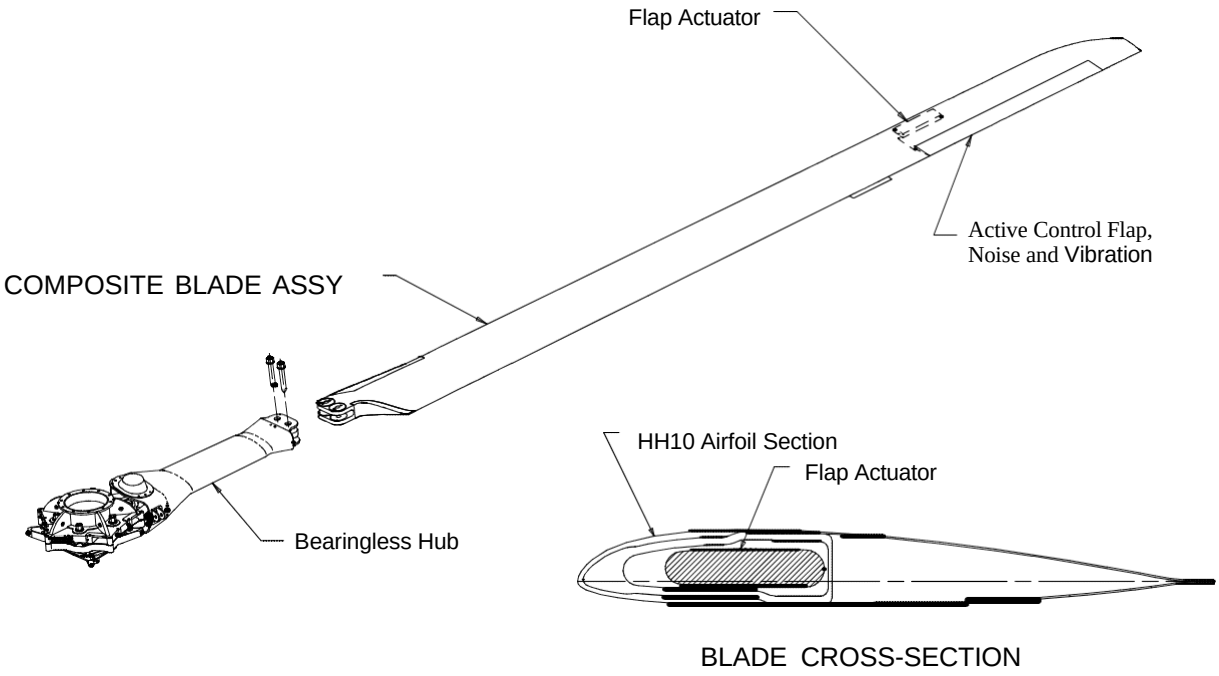

Figure 6: SMART rotor blade, trailing-edge flap, and actuator installation.

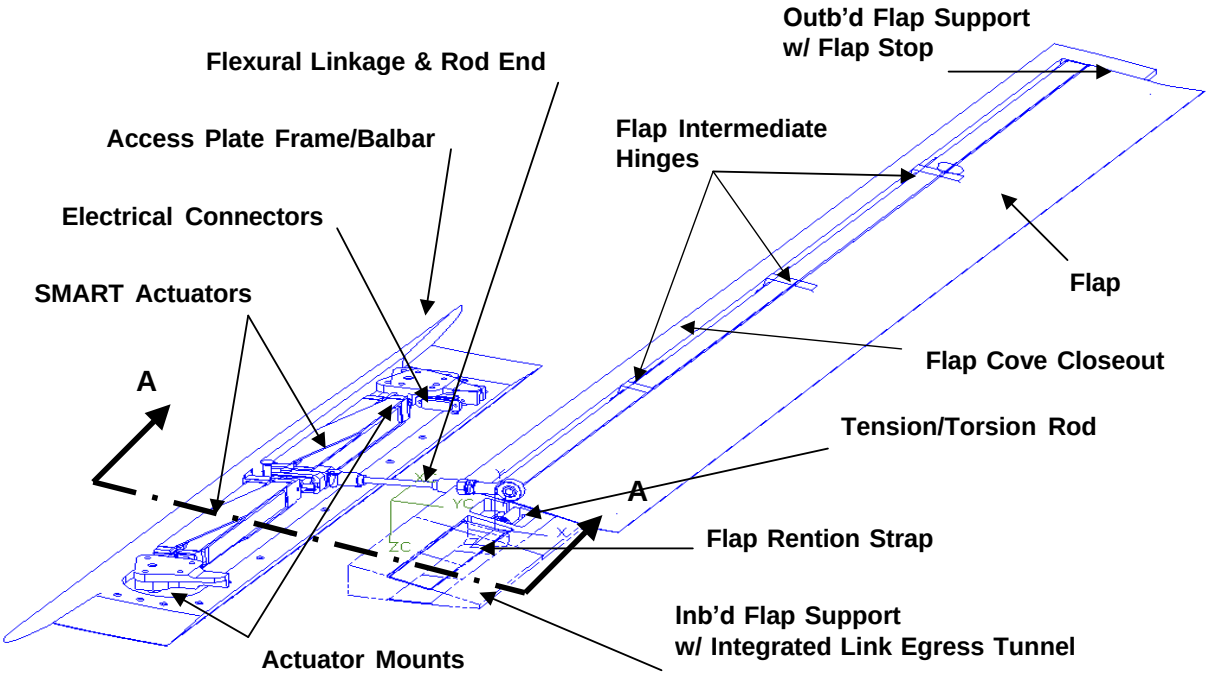

Figure 7a: Active flap components.

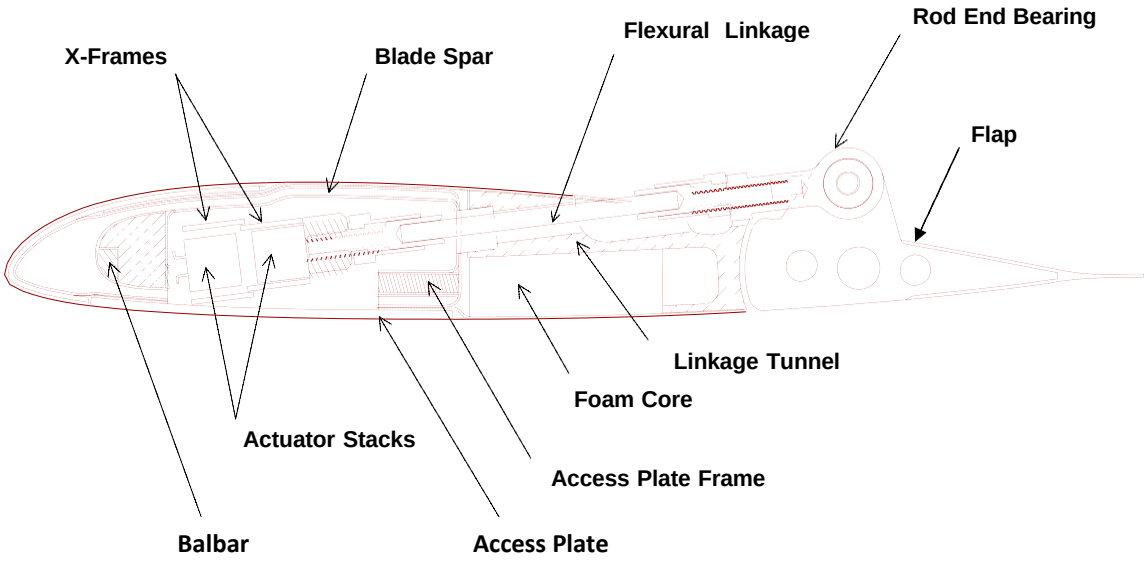

Figure 7b: Active flap rotor blade cross section.

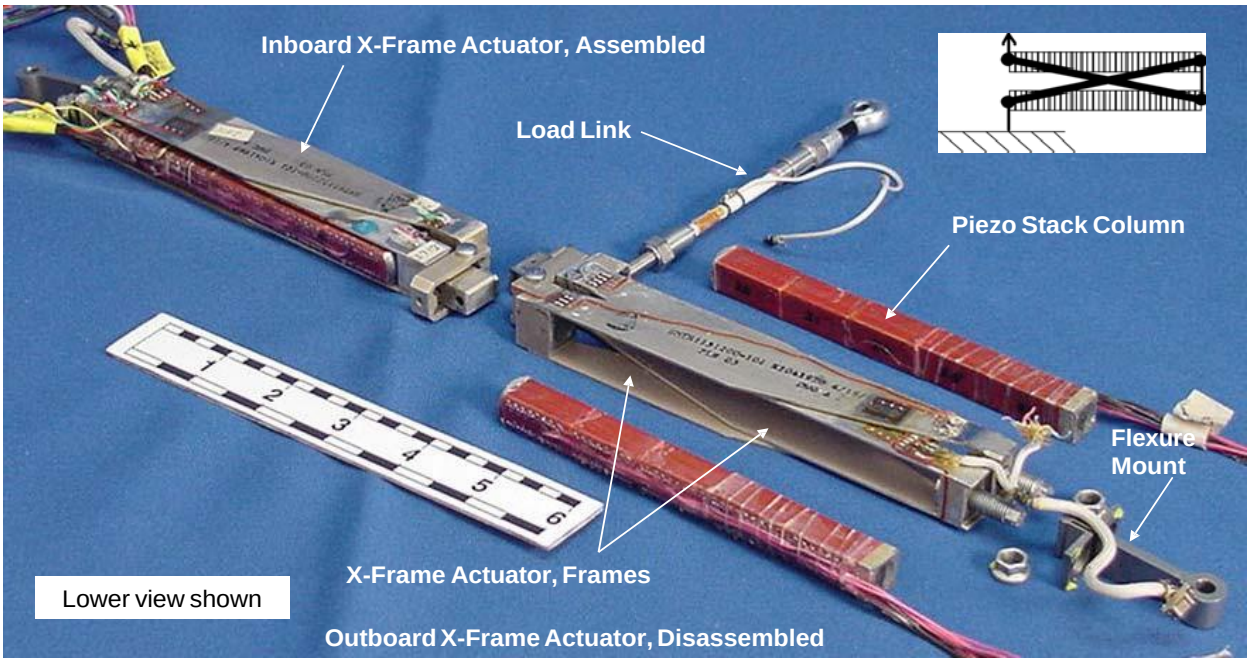

Figure 8: 2X-frame actuator, including piezoelectric stack columns.

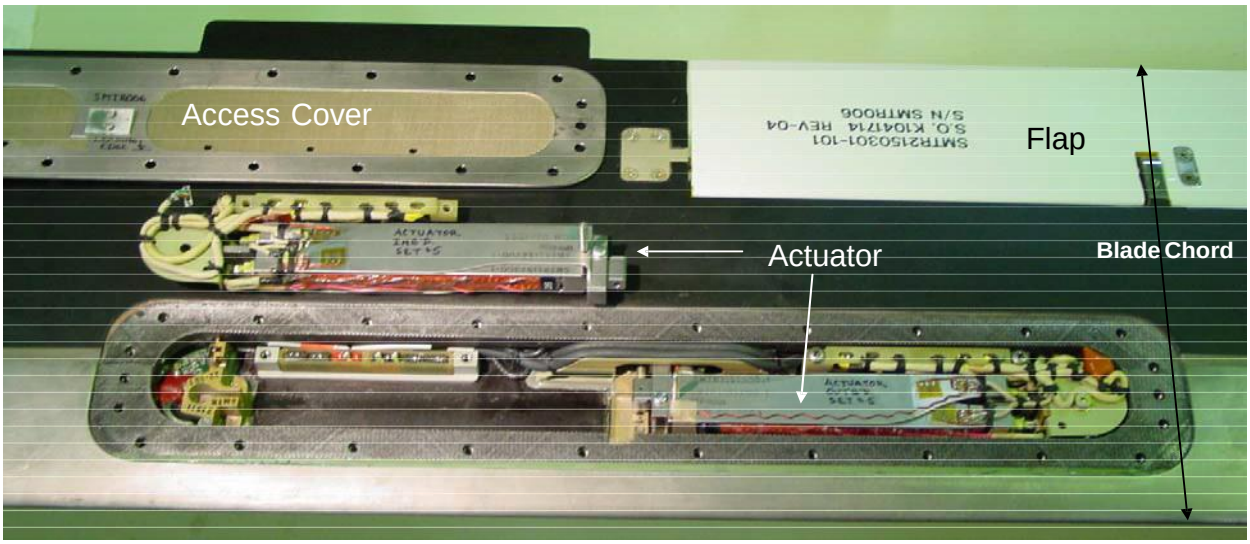

Figure 9: Blade, flap, and actuator close-up.

Blade Planform Information	Strain Gauge Locations Blade Sta		
	Flap	Chord	Torsion
Snubber Sta 10	33.25	33.25	25.5
Blade Pins Sta 41	42.75	42.75	51
Flap Sta 150–186	70	70	71
Interm. Hinge 159,168,177	87		
Tip Sta 203.1	120	120	130
Chord is 10 in. (5 in. at tip)	164	164	165
Taper starts at Sta 188.9	180		

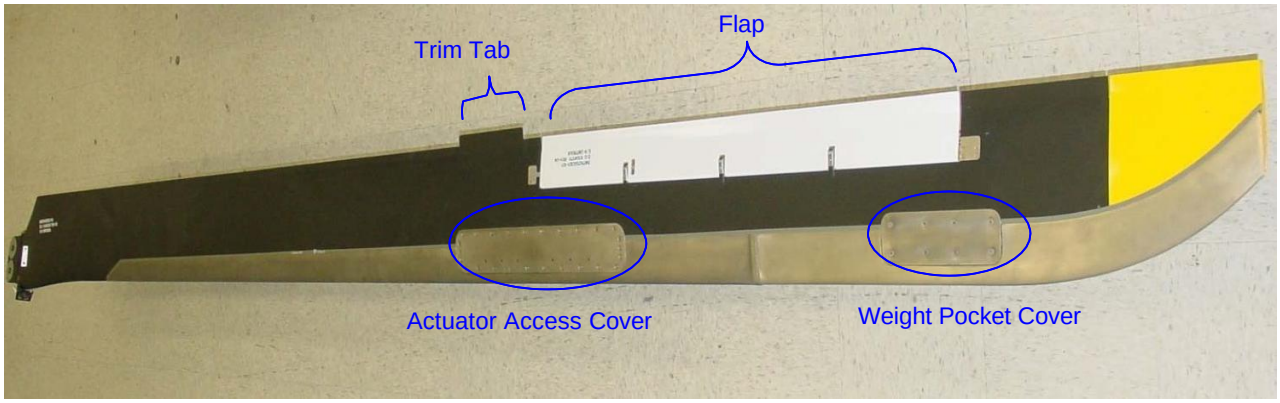

Figure 10: SMART rotor blade (bottom view).

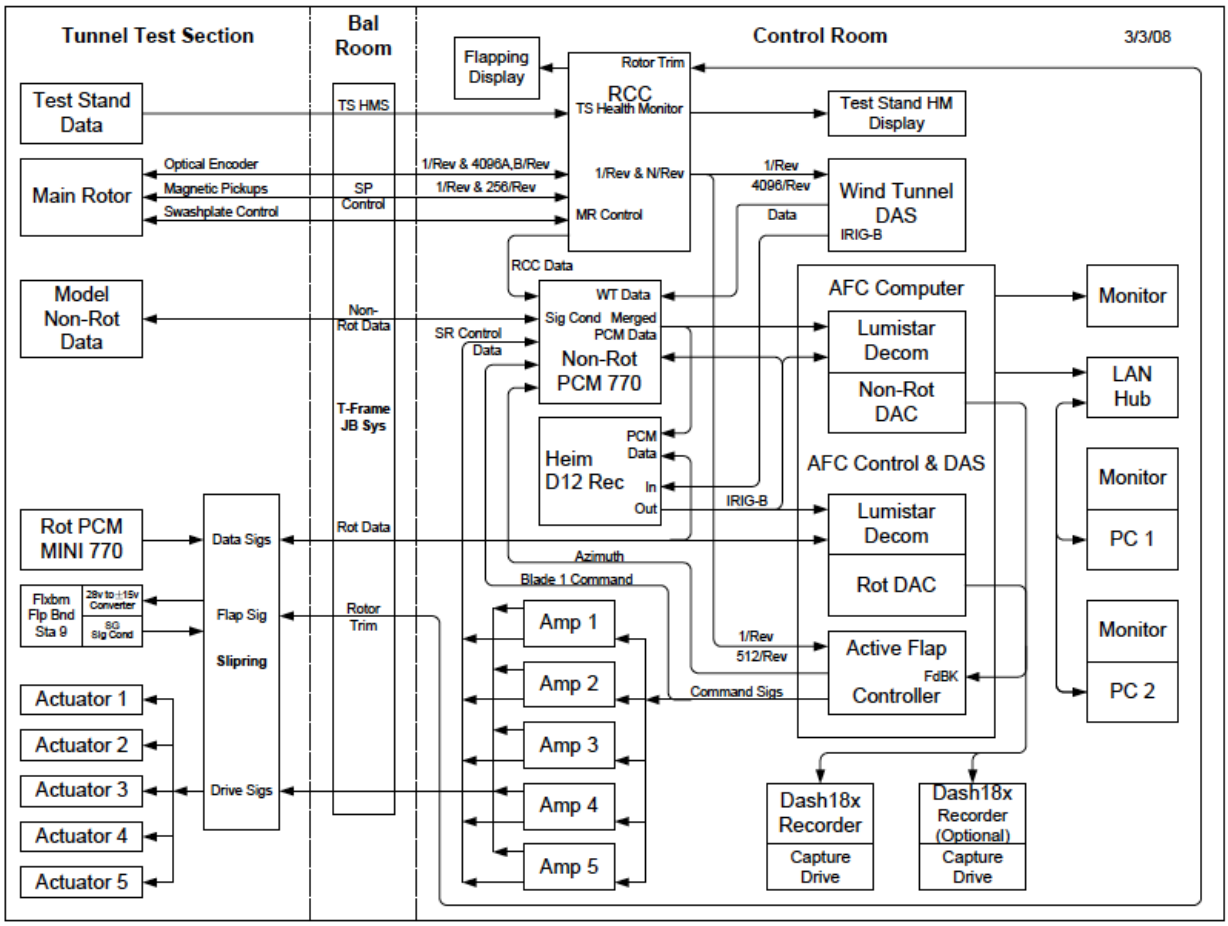

Figure 11: SMART rotor data/control system.

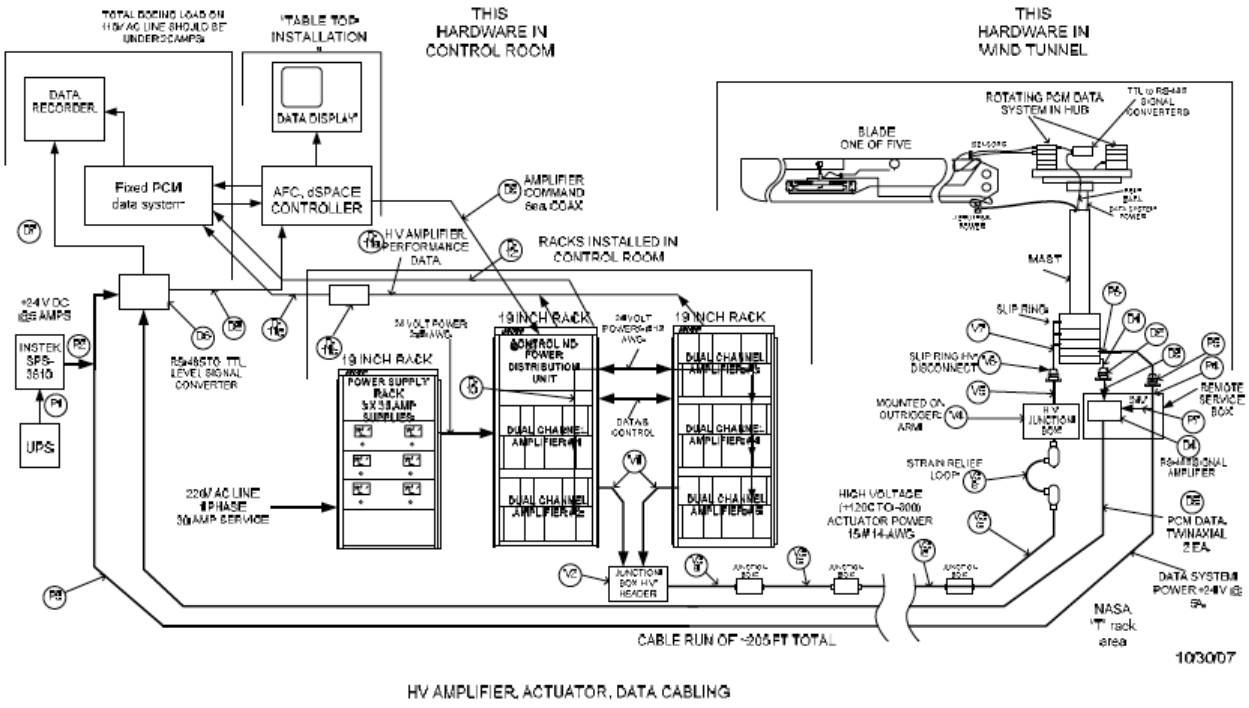

Figure 12: Data acquisition and active flap control system.

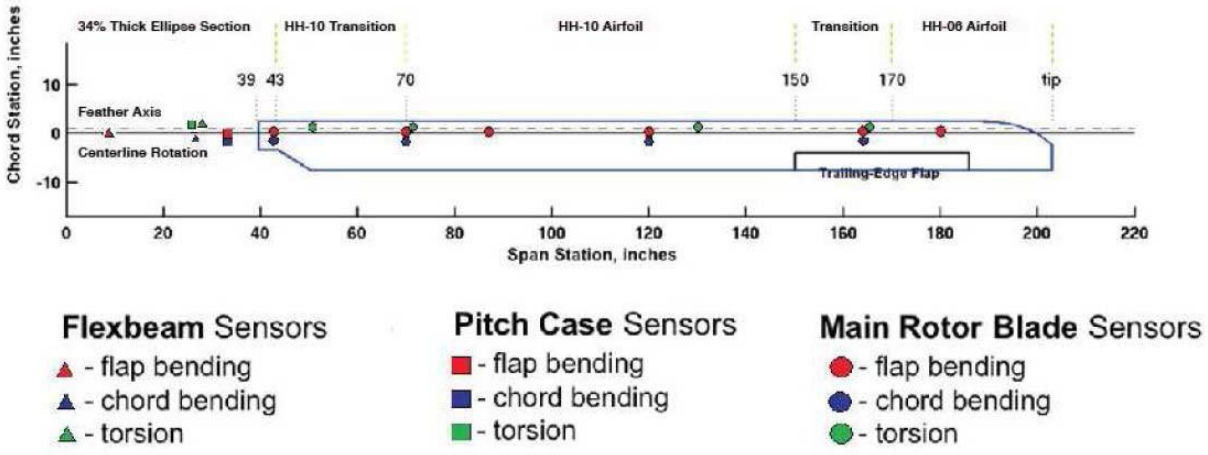

Figure 13: Blade planform, airfoil distribution, and position of strain gauges on flexbeam, pitchcase, and blade of arm 1.

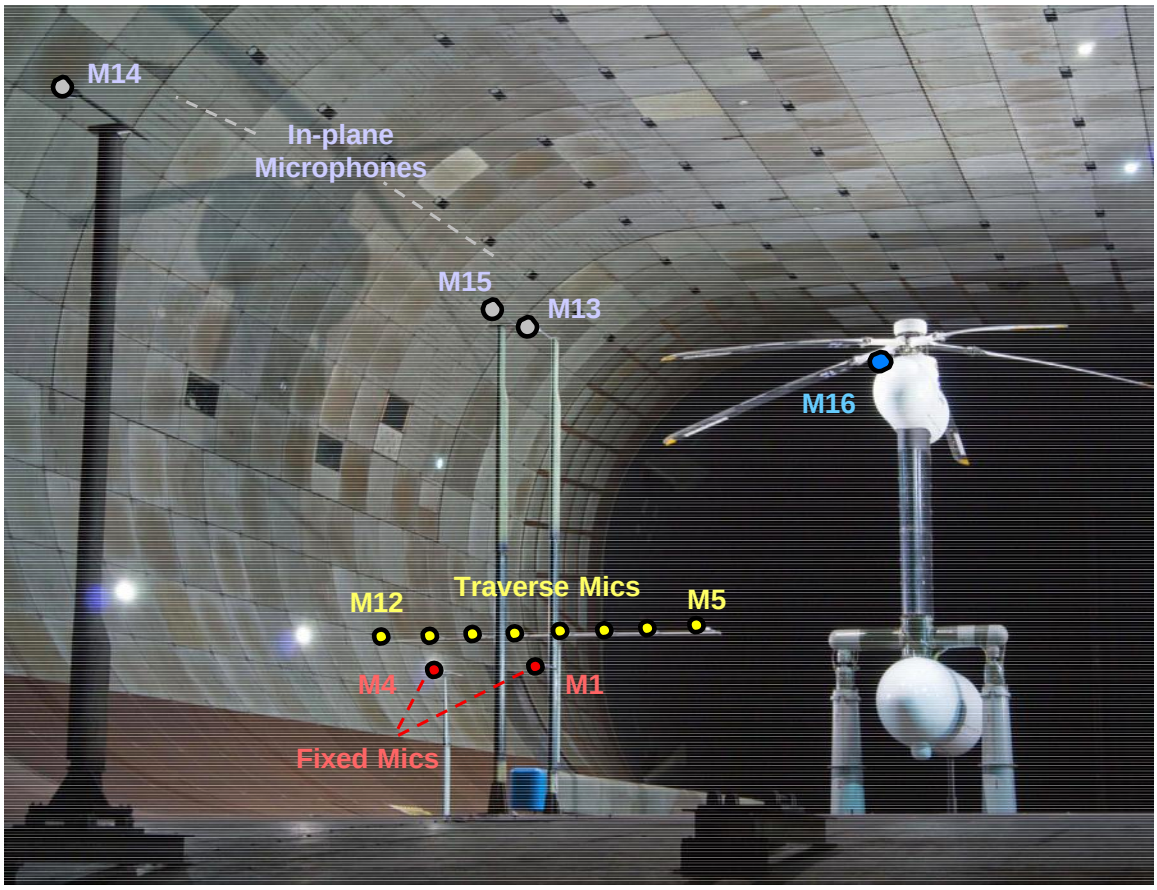

Figure 14a: SMART rotor in 40- by 80-foot anechoic test section and microphone configuration (looking downstream).

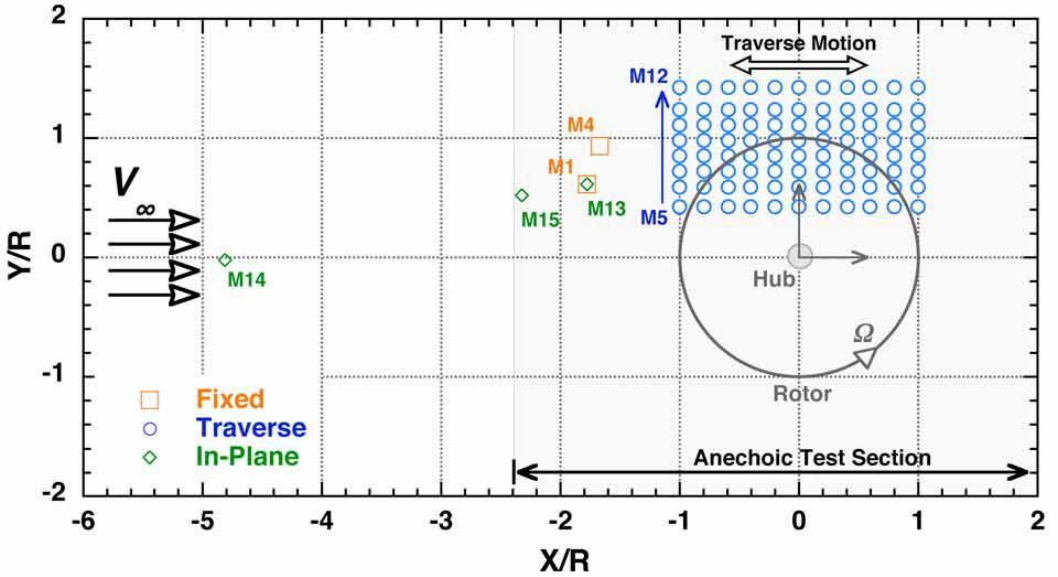

Figure 14b: SMART rotor disk and microphone layout for acoustic test setup (top view).

Run	Tare	Vel, kt	RPM	alfsu, deg min	alfsu, deg max	alfsu, deg delta	col,deg
6	Weight, hub	0	0	–15	10	2.5	10
8	Rotation, hub	0	392	–15	10	2.5	10
9	Aero, hub	20	392	–10	10	2.5	10
		40	392	–10	10	2.5	10
		60	392	–15	10	2.5	10
	HQP	83	392	–15	10	2.5	4,10,15
		100	392	–15	5	2.5	10
	HQP	123	392	–15	5	2.5	10
		160	392	–15	0	2.5	4,10,15
11	Weight, blades	0	0	–15	10	2.5	10
45	Weight, blades	0	0	–15	10	2.5	10

Figure 15: Tare Conditions. Configuration “hub” is with blades off (i.e., includes hub, PCM, flexbeam, pitchcase, spacers, and blade bolts).

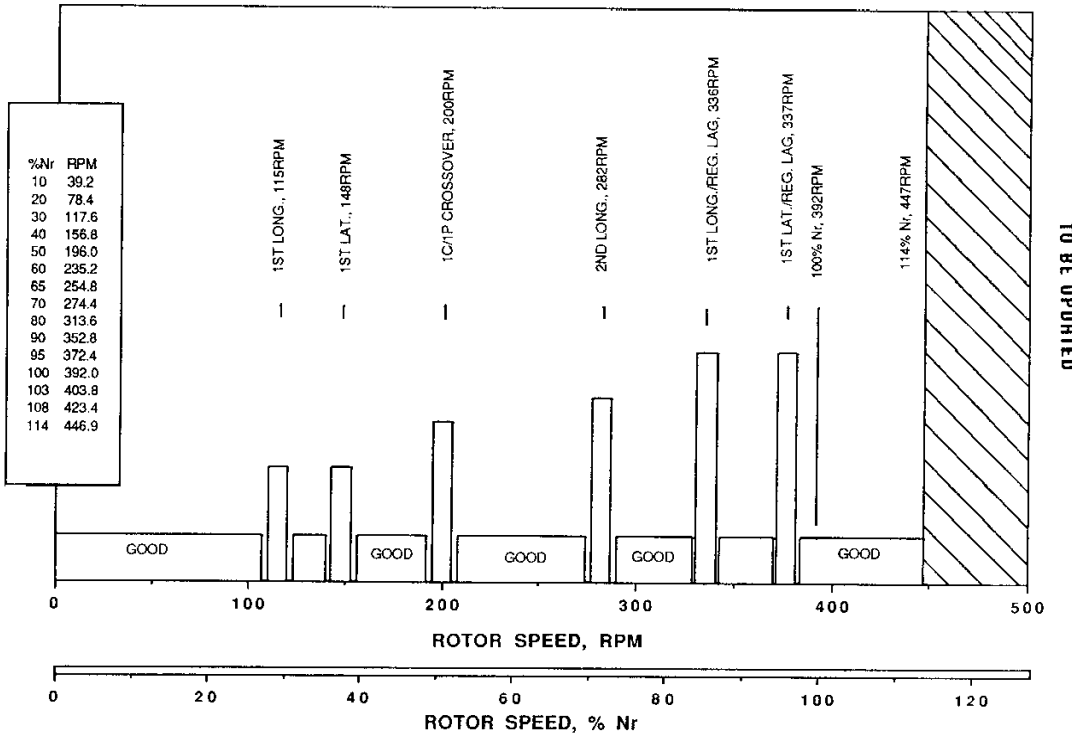

Figure 16: MDART full-scale rotor whirl tower test frequency run chart.

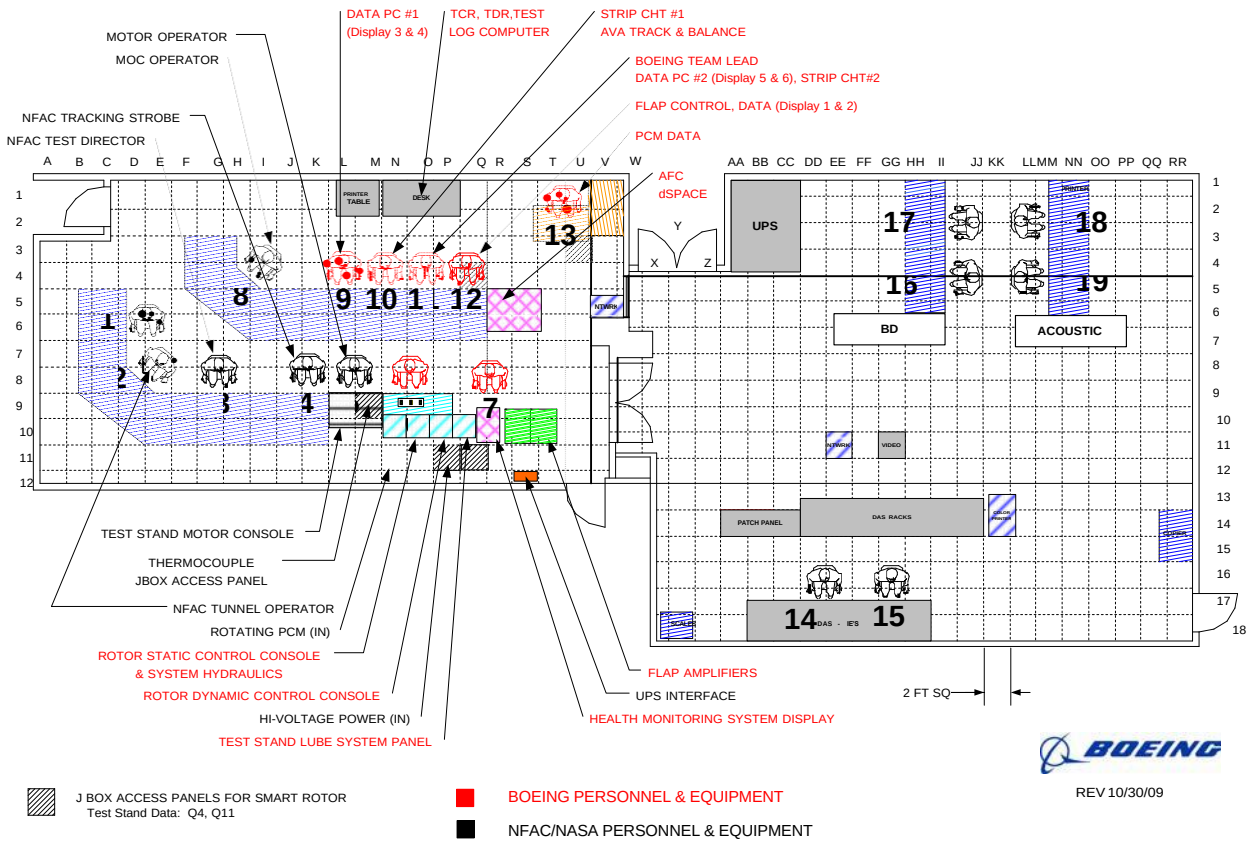

Figure 17: Control room layout and station assignments in wind tunnel.

Case No.	Tunnel Speed, kt	Shaft Axis Thrust, C_T/s	Shaft Angle	Adv Tip Mach No.	Flap Schedule
1	123	0.080	–9.1 (fwd)	0.805	Theta ($flap_k$) = 2.0*sin (5*psi_k + 90)
2	123	0.080	–9.1 (fwd)	0.805	Theta ($flap_k$) = 2.0*sin (3*psi_k + 60)
3	155	0.070	–9.1 (fwd)	0.852	Theta ($flap_k$) = 1.0*sin (5*psi_k + 180)
4	83	0.075	+1.49 (aft)	0.746	Theta ($flap_k$) = 2.0*sin (2*psi_k + 240) + 1.0*sin (5*psi_k + 330)

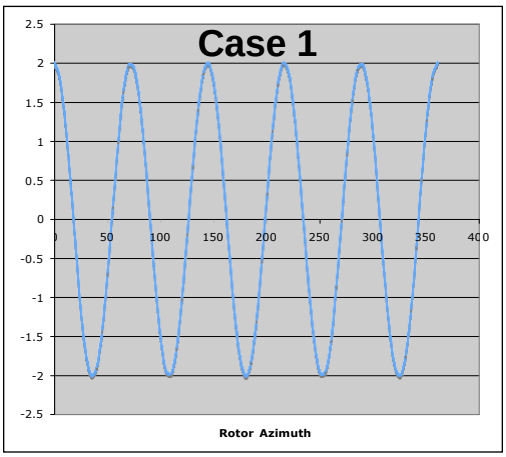

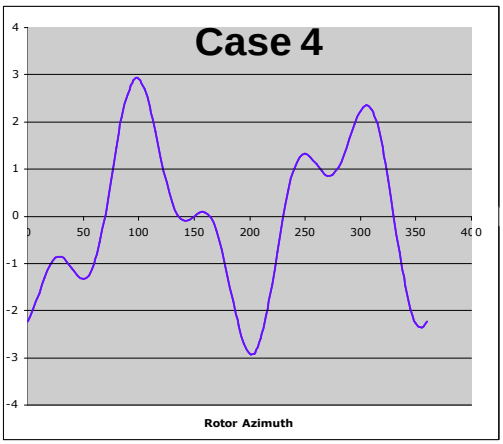

1. Density, temperature, and speed of sound are sea-level-standard conditions.
2. The rotor should be trimmed to zero hub pitch and roll moment, or to zero 1/rev tip out-of-plane deflection.
3. The deflected flap schedule is defined relative to the undeflected flap position. Positive flap deflection is flap down relative to the airfoil chord line.
4. The units are degrees and k equals blade number (1, 2, 3, 4, 5).
5. All five blades have identical flap schedules, and the blade response should be periodic with the rotor rotation rate.
6. For Case 1, the flap is fully deflected down 2 degrees as the kth blade passes over the tail.

Figure 18: Test points and conditions for validation database.

Appendix A—SMART Rotor Test Runs, Wind Tunnel and Whirl Tower

Smart Rotor Test Runs -- Wind Tunnel										
Run	Run	Date	Objective	Objective, Comments	Active	Data		Run Time, hr: min		
BA	NFAC				Control	Record	Proce	Rotor	Amplifier	Tunnel
	--	21-Feb	attempted transmission run	aborted due to MG set problem		FltTape				Drive
1	--	2/22	initial transmission run	checkout motor control		or AFC	0			
--	--	2/26	amplifier test, using RC loads	hand recorded data						
--	--	2/28-3/1	Motor run, etc.	preliminary runs		48448	0			
2	--	3/3	hydraulic accumulator test	5Gal = 1800psi; 10Gal = 270psi						
3	--	3/4	hub run, balance, up to 110%NR	exercise mixed and direct controls		48408	1			
4	--	3/10	hydraulic accumulator test	5Gal = 1000psi; 10Gal = 270psi						
5	--	3/10	rotor balance and static mast check loads	hand recorded data						
6	--	3/13	hub weight tare (doors open)	checkout alpha control		48409	1			
7	--	3/13	rotation tare, aborted at motor start (doors open)	due to incomplete 80x to 40x conversion						
8	6	3/14	rotation tare (doors open)	w acoustic traverse		48410	1			
9	6	3/14	aero tare	set, test overspeed at 107%, 420Rpm		48410,11	1			?
10	--	3/18	rotor check loading	hand recorded data						
11	11,12	3/19	blade weight tare, rotor track and balance, stability	controls sweep, accumulator test		48412	1	2:24		
12	--	3/20	rotor track and balance, stability up to 105%NR	track with strobe		48413	1	0:31		
13	16	3/24	rotor track and balance, controls sweep	track with strobe		48414	1	1:42		
14	21	3/26	forward flight checkout - 41, 62 knots	limited by fbm torsion, tunnel/motor interlock off test		48415	1	2:09		?
15	22	3/26	Forward flight checkout, 82, 103, 124 knots	fbm torsion loads		48416	1	2:45		?
16	--	3/27	actuator and amplifier checkout	non-rotating		AFC	1			
17	24	3/28	Open loop checkout, hover, 42, 62kt	Sine mode only (not synched to azimuth)		48417	1	2:14		?
				freq sweeps in hover						
18	--	3/29	rotor check loading			48418	1			
19	--	4/1	closed loop control checkout	non-rotating	(HHC)	48419	1			
20	27	4/2	open, closed loop checkout, 82, 124 kts	Alfa, CT sweep at 82kt, fan brg temp	(HHC)	48420	1	2:30		2:23
21	28	4/3	run stopped after checkout of tare reduction	implemented tare correction		48421	0	0:32		
22	29	4/3	run stopped after checkout of flap control	implemented software correction		48421	1			
23	31	4/7	open, closed loop DARPA points, 123kt	alfa, CT sweep 124kt, instrumentation problem	(HHC)	48422	1	3:06		0:25
				tunnel E-stop initiated						
24	32	4/8	open, closed loop DARPA points, 123kt		(HHC)	48423	1	1:51		1:38
25	34	4/9	open loop DARPA points, 83, 155kt	alfa, CT sweep at 154kt; pitchcase loads	(HHC)	48425	1	1:42		1:29
				tunnel E-stop, unknown reason, fly down						
26	35	4/10	open, closed loop DARPA points, 123kt; BDM	frequency, 4P phase sweeps at 124kt	(HHC)	48425	1	2:30		2:19
27	--	4/10	attempted run	tunnel not starting		y	0			
28	38,39	4/11	frequency sweep in hover	200V, 0.2-80Hz		48426	1	3:00		2:34
			freq sweep, 5,6,3,2P phase sweeps at 124kt	alfa sweep at 82kt for max BVI at 0V						
29	41	4/14	200V freq sweeps (0-80, .2-9) col,lon,lat 82kt	alfa sweep at 62,103kt for max BVI at 0V		48428	1	2:25		2:12
			250V 4P virt sp lat phase sweep at 82kt	alfa, CT sweep at 82kt						
30	42	4/15	DARPA4 at 83kt, alfa=0.89; w pos cntl	250V 4,5,6,3,2P phase sweeps.; CTC	CTC	48429	1	2:51		2:40
			DARPA2,1 at 123kt, alfa=-9.4; w pos cntl							
31	44	4/16	combined ampl, phase sweps at 82kt, alfa=2 --->	250-500V 2P90, 1.5deg 2P90 90+/-15 Mic1	CTC	(48430)	1	2:29		2:23
			traverse 0deg, 1.5deg 2P90 at 82kt, alfa=2	250-450V 3P240, 1.5deg 3P240+/-15 Mic13						
			200V freq sweep (0-80) col,lon,lat at 124kt,alfa=-9.1	150-300V 4P90, 1.5deg 4P90+/-15 Mic1						
				150-350 5P0, 1.5deg 5P0+/-15 Mic1						
32	45	4/17	closed loop vib cntl at 82kt alfa=2	200V 0-80Hz sweep col	CTC	AFC	1	2:43		2:32
				NF 5,1,1-5P; RM 5,1-5P w col; CTC						
			1.5deg 2P phase sweep; 1.5-3deg 2P300,90,105 Mic1 at 82kt, alfa=2							
33	46	4/18	closed loop vib cntl at 124kt, alfa=-9.1	175/200V 0-80Hz col,lon,lat; Mic13 transfer fctn	CTC	48431	1	2:56		2:36
				NF 1-5P, PM 1-5P, Mic1 5,1-5P						
			1.5deg 3P phase sweep, 1.5-2deg 3P230-250, Mic13 at 124kt, alfa=-9.1							
			1.5deg 5P phase sweep, 1-2deg 5P70-100, Mic13 at 124kt, alfa=-9.1							
			control power at 124kt, alfa=-9.1; lon, lat	closed loop noise cntl at 124kt, alfa=-9.1, Mic16 5, 1-5P						
			DARPA2,1 at 123kt, alfa=-9.4; w pos cntl CTC							
34	48	4/22	control power at 82kt, alfa=-5.5 and 2	200V 0.2-9Hz col, lon,lat	HHC	48432	1	2:27		2:15
				swashplate, flap virtual s/p and IBC inputs, HHC						
35	49	4/22	1.5deg 3,4,5,2P phase sweeps at 82kt alfa=2	amplitude sweeps at optimal freq. and phase, CT	CTC	48433	1	2:14		1:55
			microphone traverse, baseline and optimal open loop; 1.5deg 3P180							
36	52	4/23	1.5deg 3,4,5,2P phase sweeps at 62kt alfa=4	amplitude sweeps at optimal freq. and phase	CTC	48434	1	2:52		2:40
			microphone traverse, baseline and optimal open loop; 1.5deg 4P30							
37	53,54	4/24	control power at 124kt, alfa=-9.1	150V col, 200V lon, 175V lat 0.2-9Hz; HHC	HHC	48435	1	2:50		2:43
				swashplate, flap virtual s/p and IBC inputs;						
			inplane noise, mic13 at 124kt, -9.1deg	1.0deg 4P, 1.5deg 2P phase sweeps; CTC	CTC					
				3P+5P combined optimal open loop (SH)						
38	55	4/24	inplane noise, mic13 at 124kt, -9.1deg	amplitude sweeps at optimal freq. and phase	CTC	48436	1	2:10		1:56
				1deg 3P250 +1deg 2P phase sweep						
				1deg 3P250 +1/.75/.5deg 4P phase sweep						
			rotor smoothing, 124kt, -9.1deg	flap1 +3/-3deg, flap2 +3/-3deg, w 1deg increment						
			performance, 124kt, -9.1deg	CT/S=.04-.09, w 0deg and 0V, no retrim						
39	57	4/25	Rotor smoothing, hover	flap1 +3/-3deg, flap2 +3/-3deg, w 1deg increment	CTC	48437	1	2:59		2:43
			inplane noise, mic13 at 124kt, -9.1deg	Inplane 3P+2P, 3P+4P amplitude variations						
			Vibration closed loop control CTC2 at124kt, -9.1deg	NF 1-5P, PM 1-5P, T=10,1						
			Performance, open loop 2P phase sweep at 124kt, -	CT/S=0.075						
			traverse sweep at 103kt, -4deg	microphone traverse, baseline						

Appendix A—SMART Rotor Test Runs, Wind Tunnel and Whirl Tower (cont.)

Smart Rotor Test Runs -- Wind Tunnel										
Run	**Run**	**Date**	**Objective**	**Objective, Comments**	**Active**	**Data**		**Run Time, hr:min**		
BA	**NFAC**				**Control**	**Record**	**Proce**	**Rotor**	**Amplifier**	**Tunnel**
40	58	4/26	Vibration closed loop control HHC 62, 68kt	NF 5Pat 62kt, NF,RM,PM 5P at 68kt	HHC	48438	1	2:17		2:08
			BVI noise, mic9 at 62kt, 4deg	2P-5P combined optimal open loop (SH)						
			BVI noise, mic9 at 68kt, 1.8deg	phase, ampl. sweep, open loop						
			microphone traverse, baseline and optimal open loop; 1.5deg 3P180							
41	59,61	4/26	Vibration closed loop control at 82kt, 2deg HHC	NF, RM,3F, NF,RM,PM	HHC	48439	1	2:28		2:17
			BVI open loop optimal control at 82kt, 2deg	2P-5P combined optimal open loop (SH)						
			performance, 82kt, 2deg	CT/S=.04-.10, w 0deg and 0V, no retrim						
			Rotor smoothing 82kt, 2deg	flap1 +3/-3deg, w 1deg increment						
			DARPA4 at 83kt, HHC vs CTC	HHC, CTC						
42	63	4/28	Rotor dynamics in hover	frequency sweeps col,lon,lat at 2deg collective	CTC	48440	1	2:14		2:01
			Vibration closed loop control CTC3 at 124kt	NF 10P, T=5,1; NF 1-5,10P, T=10,5						
			Inplane open loop optimal control at 124kt	2P-5P combined optimal open loop (SH)						
			Performance, open loop 2P phase sweep at 124kt	CT/S=0.090						
			DARPA3 at 155kt	0deg data						
43	64	4/28	BVI noise, Mic1 closed loop control at 62kt, 4deg	Mic1 4P, 2-5P, RMS, 10-50N	HHC	48441	1	2:23		2:06
			BVI noise, Mic1 closed loop control at 82kt, 2deg	Mic1 4P, 2-5P, RMS, 10-50N						
			BVI noise, Mic13 closed loop control, 124kt, -9.1deg	Mic13 4P, 2-5P, RMS,1-6N						
			Vibration closed loop control at 124kt	NF 5,1-5P, RM 5,1-5P						
			Actuator baseline performance	200-400V 1Hz; 75V, 0-200Hz col,lin						
44	--	4/29	Actuator baseline performance, amplifier check	200-400V 1Hz; 75V, 0-200Hz		AFC	1			
45	--	4/29	blade weight tare (repeat of 3/19)	w hydraulics on		48449	1			
46	--	4/29	Amplifier check, power sharing	400 +/-600V, 6,12,18P		AFC	1			
47	--	4/29	Checkloads, blade, balance			48449	1			
				Total			39	65.2	hrs	45.9
Smart Rotor Test Runs -- Whirl Tower										
1		11/26	initial motor/transmission run	**Whirl Tower 2007**						
2		12/6	accumulator test							
3		1/24	initial hub run	**Whirl Tower 2008**		48442				
4		1/25	hub run, exercise controls			48443				
5		2/1	rotor track and balance, stability testing, controls sweep, up to 107%NR			48444		1:16		
6		2/1	rotor track and balance			48444		0:35		
7		2/5	track and balance, open loop flap control			48445		1:22		
8		2/6	track and balance, open loop flap control, frequency sweeps			48446		1:08		
9		2/7	track and balance, open loop flap control, frequency sweeps			48447		0:46		
				Total				5.1	hrs	
Notes										
HHC - higher harmonic control, position control of 0-5P; (HHC) - checkout, results not reliable.										
CTC - continuous time HHC, position control of 0-6p.										
AFC - data not recorder on tape; only PC-based data available.										
Pre and post test checkout test runs are: 2,4,5,10,16,18,19, 44,45,46,47.										
Runs 9-13: Boeing and NFAC point numbers not correlated.										
Run 15: started using auto setup to generate ASAP labels..										
Run 20+: Microphone cal/gain data entered for correct Boeing point numbers, correct starting Run 20.										
Run 28: FA1CmdVoltage is now up; actually is command for flap 2.										
Run 31: lost IRIG time, lost Heim recorder, apparent loss of some rot. instrumentation during Pt 127, ok after RPCM reboot.										
	MUX tape damaged, continued w/o Heim recorder, AFC time code may not be usable; fixed October 2008.									
	Tape 48430 could no longer be read in 2009. Data acquired from tape in 2008 with gaps filled is used.									
Runs 31,32,33: NFAC 11sec off; add +11-2s; provide 14s of time slice; fixed October 2008.										
Run 32: was not recorded on tape.										
Run 39: CTC controller unstable after Pt 56.										
Flight test tape 48427 does not exist.										

Appendix B—SMART Rotor 40x80 Test – Tare Data Curve Fits, 2008

1.1 SUMMARY

This document lists the various tare data curve fits used during the test of the SMART Rotor at the NFAC 40x80 wind tunnel in March–April, 2008.

1.2 BACKGROUND

The basic procedure for using tare data is described in the Software Plan. The tare data was extracted from the following test runs.

Test #	Description
6	Weight tare with hub only, shaft angle varied
8	Rotation tare with hub only, shaft angle varied
9	Aero tare with hub only, shaft angle and tunnel speed varied
11	Weight tare with hub and blades, shaft angle varied

The statistical data from the above tests were provided to NFAC for deriving the tare curve fits. The resulting polynomial curve fits for the weight and rotation tares were taken from results provided by Benton Lau. The polynomial coefficients for the aero tare were taken from results provided by Randy Peterson.

In the post-run data processing, no tare allowances up to and including test 6. Hub weight tare data allowance is made for test 8, while hub weight and shaft rotation tare allowances are made for test 9. Starting with test 11 (the first blades-on run), all of the tare curve fits are used.

It was also assumed that zeros would be taken for the balance loads and torque so that the various tare polynomial curve fits would not have a constant term in them.

1.3 HUB WEIGHT TARE

The hub weight tare polynomials are of the following form.

$$Correction = c_2 \alpha_{su}^2 + c_1 \alpha_{su}$$

As noted above, there is no constant term independent of the shaft angle as a result of the fact that zeros are taken for the balance loads and torque.

Quantity	*c2*	*c1*
Axial	0	1.65593844E+01
Side	0	0
Normal	1.50628879E-01	6.11545805E-03
Roll	0	0
Pitch	0	3.47832811E+02
Torque	0	0

1.4 SHAFT ROTATION TARE

The polynomial form is the same as that used above for the hub weight tare.

Quantity	c_2	c_1
Axial	0	1.51569176E+01
Side	0	0
Normal	1.96238481E-01	8.03048333E-01
Roll	0	0
Pitch	0	3.49176260E+02
Torque	0	0

1.5 BLADE WEIGHT TARE

The polynomial form here is also of the same form as for the hub weight tare.

Quantity	c_2	c_1
Axial	0	2.07534609E+01
Side	0	0
Normal	1.95654729E-01	-9.16578705E-02
Roll	0	0
Pitch	0	4.12665804E+02
Torque	0	0

1.6 AERO TARE

Due to the nature of the data, the aero tares were calculated in two tunnel speed ranges, one set for tunnel dynamic pressure up to 40 lb/ft^2 and a different set for tunnel dynamic pressure above this range. The compound polynomial that was fitted to the tare data is of the following form.

$$Correction = \left(c_0 + c_1\alpha_{su} + c_2\alpha_{su}^{\ 2}\right) + \left(d_1 q + d_2 q^2\right)$$

The coefficients for dynamic pressure less than 40 lb/ft^2 are given below.

Quantity	c0	c1	c2	d1	d2
Axial	4.41635E+01	3.5469E-01	-9.6949E-03	5.3657E+00	-6.87172E-02
Side	-2.60047E+01	-5.3582E-01	1.73582E-02	1.85598E+00	-4.32008E-02
Normal	-3.32883E+01	4.05031E+00	-1.50037E-01	-1.59653E+00	3.87342E-02
Roll	9.12508E+01	-3.75755E+01	1.12821E+00	-3.53552E+01	6.87260E-01
Pitch	2.93151E+02	1.64353E+01	-3.96708E-01	1.71517E+02	-7.36995E-01
Torque	1.40081E+03	-3.64107E+00	-7.98055E-02	2.45818E+01	-1.12240E-01

The coefficients for dynamic pressure greater than 40 lb/ft^2 are shown in the following table.

Quantity	c0	c1	c2	d1	d2
Axial	-9.21234E+02	-1.22059E+00	-5.54287E-02	3.32231E+01	-2.23995E-01
Side	5.39620E+02	-1.29505E+00	-4.94794E-02	-1.74372E+01	1.28125E-01
Normal	3.04635E+03	1.44131E+01	-3.01163E-01	-9.66043E+01	7.21733E-01
Roll	3.51931E+03	-1.19794E+02	-1.30131E-01	-1.31035E+02	9.48338E-01
Pitch	4.27314E+03	3.49026E+01	-3.56435E+00	3.04429E+01	7.91147E-01
Torque	-4.21734E+03	-1.65780E+01	-5.23099E-01	2.01120E+02	-1.40240E+00

In all of the above curve fits, the uncorrected shaft angle is in degrees and the uncorrected tunnel dynamic pressure is in lb/ft^2.

Appendix C—Checklist

SMART Rotor Pre-Run Checklist, V3.1					
Test No. Boeing, NFAC					
Date					
Time					
Inspections:					
Rotor head assy					
Rotor blade/flap assy					
Control system					
Hydraulics					
Motor/test stand					
Model/Instrumentation Changes:					
Test stand/model					
Instrumentation/software					
Flap actuator control/software					
Control Room/Data Computer:					
Deg F					
% RH					
Hydraulic cart on, verify pressure					
Motor cooling water (chiller) on					
Amplifier on, two fans on					
Instrumentation up & recording					
Strip charts: up & recording					
Rotor control mode normal					
Unlock controls					
Set rotor controls to ten collective, zero cyclic					
Take pre-run zero, Rcal					
Switch amplifier relays on, set Vbias to 400					
Set rotor controls to zero collective, zero cyclic					
Take pre-run zero					
Set controls to collective required for start up					
Scavenge pump on					
Mister on (30–45 drops/min)					
Health monitor up & recording					
SMART Rotor Post-Run Checklist					
Normal Shutdown Procedure:					
Set controls to collective required for shutdown, zero cyclic					
Command rotor speed to zero					
Set controls to zero collective, zero cyclic					
Take post-test zero					
Set controls to ten collective, zero cyclic					
Switch amplifier relays off, set Vbias to 0					
Take post-test zero, Rcal					
Control Room Shutdown:					
Lock rotor controls					
Mister off					
Scavenge pump off					
Amplifiers off; stop fans 10 min later					
Instrumentation, HMS, strip charts off					
Engineering & HMS data saved and archived					

Appendix D—Baseline and Performance Test Conditions

SMART Rotor Test Runs: Summary of Specific Conditions Baseline cases with no flap inputs, i.e. 0V. Swashplate controls checkout baseline performance, alfa, CT sweeps alfa sweep for max BVI. Performance with flap inputs (runs 38–42); also listed in sheet "Flap."

Boeing Values		DESCRIPTION	Vkts [mu]	Alfa (deg)	Rotor RPM [Mtip]	Col (deg) [CT/s]
Run	Points					
14	13-19	controls, +/-1 deg fwd; +/-1 deg rt	0.10	-10.0	0.623	7.0
14	20	baseline performance	0.10	-5.0	0.623	0.075
14	21-24	baseline performance	0.15	-3.7	0.623	0.060, 0.075 0.080, 0.090
14	25-31	controls, +/-1 deg fwd; +/-1 deg rt	0.15	-10.0	0.623	0.075
14	31-36	baseline performance	0.15	-10.0	0.623	0.040, 0.060, 0.075 0.080, 0.090
14	36.01-37	baseline performance	0.15	0.0, 2.4	0.623	0.075
15	11-17	controls, +/-1 deg fwd; +/-1 deg rt	0.15	-10.0	0.623	0.075
15	18	baseline performance	0.15	-3.7	0.623	0.075
15	47-52	baseline performance	0.20	-10.0	0.623	0.040, 0.060, 0.075, 0.080
15	19-23	baseline performance	0.20	-5.5	0.623	0.040, 0.060, 0.075, 0.080, 0.090
15	24,25	baseline performance	0.20	0.0, 1.6	0.623	0.075
15	29	baseline performance	0.24	-7.3	0.623	0.075
15	29.03-29.05	baseline performance	0.25	-15.0, -12.5, -5.0	0.623	0.040
15	42-44	baseline performance	0.25	-10.0	0.623	0.040, 0.060, 0.075
15	29.01-31	baseline performance	0.25	-7.3	0.623	0.040, 0.060, 0.065
15	35,36	baseline performance	0.30	-9.1	0.623	0.04, 0.045
20	32-37	baseline performance	0.20	-10.0	0.623	0.040, 0.060, 0.075, 0.080, 0.090, 0.100
20	26-27.03	baseline performance	0.20	-5.5	0.623	0.040, 0.060, 0.075, 0.080, 0.090
20	49-54	baseline performance	0.20	2.5, 5.0, 7.5	0.623	0.06, 0.075
20	55-69	baseline performance	0.30	-9.1	0.623	0.040, 0.060, 0.075, 0.080, 0.090
23	26-28	baseline performance	0.30	-15.0	0.623	0.040, 0.060, 0.070
23	21-25	baseline performance	0.30	-9.1	0.623	0.040, 0.060, 0.075, 0.080, 0.090
23	29-34	baseline performance	0.30	-5.0	0.623	0.040, 0.060, 0.075, 0.080, 0.090, 0.100
25	30-32	baseline performance	0.375	-12.0	0.623	0.040, 0.060, 0.070
25	33-35	baseline performance	0.375	-10.0	0.623	0.040, 0.060, 0.070
25	36	baseline performance	0.375	-5.0	0.623	0.040
28	85.01-98	alfa sweep for max BVI	0.20	-5.5, -2.5, 0, 1.5, 2, 2.3, 2.5, 2.7, 3, 3.5, 4, 4.5, 5,	0.623	0.075
29	23-30	alfa sweep for max BVI	0.15	0, 1, 2, 3, 4, 5, 6, 7	0.623	0.075
29	34-37.02	alfa sweep for max BVI	0.25	-3.9, -2, -1, 0, 1, 2.5	0.623	0.075
29	40-44	baseline performance	0.20	2.0	0.623	0.050, 0.060, 0.075, 0.080, 0.090
38	71-88	performance w flap 0V and 0deg	0.30	-9.1	0.623	0.040, 0.060, 0.075, 0.080, 0.090
39	69-84	performance w flap 1.5deg 2P	0.30	-9.1	0.623	0.075
41	33-46	performance w flap 0V and 0deg	0.20	2.0	0.623	0.040, 0.060, 0.075, 0.080, 0.090, 0.100
42	48-62	performance w flap 1.5deg 2P	0.30	-9.1	0.623	0.090
42	69,70,76	performance w flap 0V and 0deg	0.375	-12.0	0.623	0.040
42	71-75	performance w flap 0V and 0deg	0.375	-9.3	0.623	0.040, 0.060, 0.070

Appendix D—Active Flap Test Conditions (cont.)

SMART Rotor Test Runs: Summary of Specific Conditions Cases with flap inputs, open and closed loop.

Run	Boeing Values Points	Condition	Speed	Type	Variables		
17	8.02-23	COLL=4,ALF=-10,VKTS=0	0	actuator check rot stea	0Vbias; 0V; V1,V2,V3,V4,V5=200; V=200, 300, 400, 0, -200, -300, -400, 0		
17	86-101	COLL=4,ALF=-10,MU=0,150V,0-200Hz,120sec	0	freq sweep	0V; 150V, 0-200Hz; 200V, 0-80Hz; 0.2-5Hz, 2, 3, 4, 5, 6, 10P, sine		
20	7-15.01	COLL=4,ALF=-10,VKTS=0,df=200V1P	0	actuator check 2	0Vbias; 0V; 200V, 1-6P, harmonic, cyclic; 0V		
20	44-46.02	CT/S=0.075,ALF=1.49,MU=0.2,df=200V2P	0	actuator check rot	0V; 200,300,400V at 2P and 5P		
20	69,70,70.01	CT/S=0.08,ALF=-9.1,MU=0.3,df=0V	0.3	actuator check rot	0,200,300V at 3P60		
23	3-8	Act check,Nr=0,COLL=10,ALF=0,Vbias=400	0	actuator check 1	0Vbias; 0V; 200,300,400V, 1Hz; 0V		
23	11-18	COLL=4,ALF=-10,VKTS=0,df=200V1P	0	actuator check 2	0V; 200V, 1-6P, harmonic, cyclic; 0V		
23	36-39	CT/S=0.08,ALF=-9.4,VKTS=123,df=0V	0.3	DARPA2, OL	0V; 200, 300, 400V 3P60		
24	3-8	Act check,Nr=0,COLL=10,ALF=0,Vbias=400	0	actuator check 1	0Vbias; 0V; 200,300,400V, 1Hz; 0V		
24	11-18	COLL=4,ALF=-10,VKTS=0,df=200V1P	0	actuator check 2	0V; 200V, 1-6P, harmonic, cyclic; 0V		
24	22-25	CT/S=0.08,ALF=-9.1,VKTS=123,df=200V5P90	0.3	DARPA1, OL	0V; 200,300,400V 5P90		
24	33-43	CT/S=0.08,ALF=-9.1,VKTS=123,df=350V3P60	0.3	DARPA2, OL	0V; 350V 3P60		
24	64-68	Act check,Nr=0,COLL=10,ALF=0,400V1Hz	0	actuator check 3	0V; 400, 100V 1Hz; 0Vbias; zero		
25	3-8	Act check,Nr=0,COLL=10,ALF=0,Vbias=400	0	actuator check 1	0Vbias; 0V; 200,300,400V, 1Hz; 0V		
25	11-18	COLL=4,ALF=-10,VKTS=0,df=200V1P	0	actuator check 2	0V; 200V, 1-6P, harmonic, cyclic; 0V		
25	22-25	0.075,1.49,83,df=200V 2P240 +100V 5P330	0.2	DARPA4, OL	0V; 200V 2P240 +100V 5P330; 250V.. ; 300V..		
25	136-140	Act check,Nr=0,COLL=10,ALF=0,400V1Hz	0	actuator check 3	0V; 400, 100V 1Hz; 0Vbias; zero		
26	3-8	Act check,Nr=0,COLL=10,ALF=0,Vbias=400	0	actuator check 1	0Vbias; 0V; 200,300,400V, 1Hz; 0V		
26	11,12,17,18	COLL=4,ALF=-10,VKTS=0,df=200V1P	0	actuator check 2	0V; 200V, 1,6P, harmonic, cyclic; 0V		
26	38-41	CT/S=0.08,ALF=-9.1,VKTS=123,df=300V5P90	0.3	DARPA1, OL	0V; 300, 350, 400V, 5P90		
26	49-60	CT/S=0.08,ALF=-9.1,VKTS=123,df=300V3P60	0.3	DARPA2, OL	0V; 300,350,400V 3P60; 0V		
26	61-85	0.075,-9.1,0.3,df200V0-80,60s, col, lin	0.3	freq sweep	0V; (200V, 0-80 lin, 1-80, 0.2-5Hz, 2,3,4,5,6,10P log), col, lon, lat	SRH - data given to	
26	86.01-98.01	CT/S=0.075,ALF=-9.1,MU=0.3,df=250V4P	0.3	phase sweep	250V 4P; 0V		
26	143-147	Post-run check, COLL=10, Vbias=0	0	actuator check 3	0V, 0Vbias,zero		
28	3-9	Act check,Nr=0,COLL=10,ALF=0,Vbias=400	0	actuator check 1	0Vbias; 0V; 200,300,400V, 1Hz; 400V 5P; 0V		
28	12-16	COLL=4,-10,0,df=200V.2-80,5*40s, col,log	0	freq sweep	0V; (200V, 0.2-80Hz log), col, lon, lat, col		
28	17-19	COLL=4,ALF=-10,VKTS=0,df=200V5P	0	actuator check 2	200V, 5,6P, harmonic, cyclic; 0V		
28	23-30	0.075,-9.1,0.3,df=200V0-80,5*40s,col,lin	0.3	freq sweep	0V; (200V, 0-80 lin, 0.2-9 log, 5P lin), col, lon, lat; 0V		
28	30-84	CT/S=0.075,ALF=-9.1,MU=0.3,df=250V5P	0.3	phase sweep	0V; 250V, 5P, 6P, 3P, 2P; 0V		
28	108-112	Act check,Nr=0,COLL=10,ALF=0,400V1Hz	0	actuator check 3	0V; 400, 100V 1Hz; 0Vbias; zero		
29	3-9	Act check,Nr=0,COLL=10,ALF=0,Vbias=400	0	actuator check 1	0Vbias; 0V; 200,300,400V, 1Hz; 0V		RPCM problem, fast shut down?
29	12-19	COLL=4,ALF=-10,VKTS=0,df=200V1P	0	actuator check 2	0V; 200V, 1-6P, harmonic, cyclic; 0V		
29	44-51	0.075,2,0.2,df=200V0-80,3*40s,col,lin	0.2	freq sweep	0V; (200V, 0-80 lin, 0.2-9 log), col, lon, lat; 0V		
29	51-64.01	0.075,2,0.2,df=250V4P,virt sp lat	0.2	phase sweep	0V; 250V 4P virt sp lat		
29	123-127	Post-run check, COLL=10, Vbias=0	0	actuator check 3	0V, 0Vbias; zero		
30	3-7	Act check,Nr=0,COLL=10,ALF=0,Vbias=400	0	actuator check 1	0Vbias; 0V; 200,300,400V, 1Hz	CTC	using 1-6P fpr position control
30	8-13	COLL=10,ALF=0,MU=0,df=0deg 0-6P	0	actuator check 1b	0deg; DARPA1-4; 0V	CTC	for start up, overcome integrator limits by hand
30	16-22	COLL=4,-10,0,df=0deg 0-6P,	0	actuator check 2b	0V; 0deg; DARPA1-4; 0V	CTC	
30	26-34	0.075,0.89,83,df=2d2P240+1d5P330+0d0-6P	0.2	DARPA4, CTC	0V; 0, 1, 1.5, 2d2P240+1d5P330; 0V; also alfa=0.29, 1.49	CTC	200k limit hit
30	35-102	CT/S=0.075,ALF=2,MU=0.2,df=250V4P	0.2	phase sweep	0V; 250V 4P, 5P, 6P, 3P, 2P; 0V		
30	104-109	CT/S=0.08,-9.4,123,df=2deg 3P60 +0d0-6P	0.3	DARPA2, CTC	0V, 0, 1, 2deg 3P60; 0V	CTC	200k limit hit
30	109-114	CT/S=0.08,-9.4,123,df=2deg 5P90 +0d0-6P	0.3	DARPA1, CTC	0V; 0, 1, 2deg 5P90	CTC	390k limit hit
30	119-123	Act check,Nr=0,COLL=10,ALF=0,400V1Hz	0	actuator check 3	0V; 400, 100V 1Hz; 0Vbias; zero		
31	3-11	Act check,Nr=0,COLL=10,ALF=0,Vbias=400	0	actuator check 1,1b	0Vbias; 0V; 200,300,400V, 1Hz; 0d, 1d1P, 2d1P90; 0V	CTC	
31	14-19	COLL=4,-10,0,df=0deg 0-6P,	0	actuator check 2b	0V; 0d, 1d1P, 2d1P, 2d1P90; 0V	CTC	start up controlled by software
31	23-32	CT/S=0.075,ALF=2,MU=0.2,df=250V 2P90	0.2	phase sweep + ampl	0V; 250-500V 2P90; 1.5d 2P90, +/-15	CTC	Heim recorder failed
31	51-59	CT/S=0.075,ALF=2,MU=0.2,df=250V 3P240	0.2	phase sweep + ampl	250-450V 3P240; 1.5d 3P240, +/-15	CTC	
31	60-68	CT/S=0.075,ALF=2,MU=0.2,df=250V 4P90	0.2	phase sweep + ampl	150-300V 4P90; 1.5d 4P90, +/-15	CTC	
31	78-86	CT/S=0.075,ALF=2,MU=0.2,df=250V 5P0	0.2	phase sweep + ampl	150-350V 5P0; 1.5d 5P0, +/-15	CTC	
31	96-108	CT/S=0.075,2,0.2,df=0deg 0-6P,Trav1	0.2	trav sweep	0deg	CTC	
31	109-122	CT/S=0.075,2,0.2,df=1.5deg 2P90,Trav13	0.2	trav sweep	1.5deg 2P90; (0V)	CTC	Heim recorder failed
31	124-130	CT/S=0.075,ALF=-9.1,MU=0.3,df=0V,40s	0.3	freq sweep	0V; (200V, 0-80Hz, lin), col, lon, lat		RPCM problem, ok after reboot

Appendix D—Active Flap Test Conditions (cont.)

31	135-139	Post-run check, COLL=10, Vbias=0	0	actuator check 3	0V, 0Vbias; zero		
32	3-9	Act check,Nr=0,COLL=10,ALF=0,Vbias=400	0	actuator check 1	0Vbias; 0V; 200,300,400V, 1Hz; 0V	CTC	
32	12-17	COLL=4,ALF-10,MU0,df=0deg0-6P	0	actuator check 2b	0V; 0d, 1d1P, 2d1P; 0V	CTC	
32	21-22	CT/S=0.075,ALF=2,MU=0.2,df=200V0-80	0.2	freq sweep	0V; 200V, 0-80Hz, lin, col	CTC	
32	23.01-32	CT/S=0.075,ALF=2,MU=0.2,df=NF5P	0.2	vib control	NF 5, 1, 1-5P; RM 5, 1, 1-5P; 0V	CTC	
32	32-46	CT/S=0.075,ALF=2,MU=0.2,df=1.5deg2P	0.2	phase sweep	0V; 1.5deg 2P; 0V	CTC	
32	46-81	CT/S=0.075,ALF=2,MU=0.2,df=1.5deg2P300	0.2	phase sweep + ampl	0V; 1.5-3deg, 2P300, 90, 105; 0V	CTC	
32	126-127.01	Post-run zero, COLL=10,Vbias=0	0	actuator check 3	0V, 0Vbias; zero		
33	3-8	Act check,Nr=0,COLL=10,ALF=0,Vbias=400	0	actuator check 1	0Vbias; 0V; 200,300,400V, 1Hz; 0V	CTC	
33	11-14	COLL=4,ALF-10,MU0,df=0deg0-6P	0	actuator check 2b	0V; 0d, 1d1P, 2d1P	CTC	
33	17-22	0.075,-9.1,0.3,df=175V0-80,3*40s,col,lin	0.3	freq sweep	0Vbias; 0V; (175V col, 200V, lon, lat), 0-80Hz, lin	CTC	
33	22-26	CT/S=0.075,ALF=-9.1,MU=0.3,df=NF1-5P	0.3	vib control	0V; NF 1-5P, PM 1-5P	CTC	
33	27-30	CT/S=0.075,ALF=-9.1,MU=0.3,df=Mic15P	0.3	noise control	Mic1 5, 1-5P; 0V	CTC	
33	30-44	CT/S=0.075,ALF=-9.1,MU=0.3,df=1.5deg3P	0.3	phase sweep	0V; 1.5deg 3P; 0deg	CTC	
33	44-52	CT/S=0.075,ALF=-9.1,MU=0.3,df1.5deg3P240	0.3	phase sweep + ampl	0d; 1.5-2deg, 3P240, 230, 250; 0deg	CTC	
33	52-66	CT/S=0.075,ALF=-9.1,MU=0.3,df=1.5deg5P	0.3	phase sweep	0d; 1.5 deg 5P; 0deg	CTC	
33	66-74	CT/S=0.075,ALF=-9.1,MU=0.3,df=1.5deg5P90	0.3	phase sweep + ampl	0d; 1-2deg, 5P80, 100, 70; 0V	CTC	
33	74-84	CT/S=0.075,ALF=-9.1,MU=0.3,df=0V	0.3	control power SP	0; (1, 2, 0, -1, -2) lon; 0; (1, 0, -1, -1) lat; all at 0V		
33	102-105	CT/S=0.075,ALF=-9.1,MU=0.3,df=Mic165P	0.3	noise control	Mic16 5, 1-5P; 0V	CTC	
33	106-112	0.08,-9.4,123,df=2deg 3P60 +0d0-6P	0.3	DARPA2, CTC	0V, 0, 1, 2deg 3P60; 0d	CTC	
33	112-116.01	0.08,-9.4,123,df=2deg 5P90 +0d0-6P	0.3	DARPA1, CTC	0d; 0, 1, 2deg 5P90; 0d; 0V	CTC	
33	124,125	Post-run check, COLL=10	0	actuator check 3	0V, 0Vbias		
34	3-8	Act check,Nr=0,COLL=10,ALF=0,Vbias=400	0	actuator check 1	0Vbias; 0V; 200,300,400V, 1Hz; 0V	HHC	using 1-5P for position control
34	11-14	COLL=4,ALF-10,MU0,df=0deg0-6P	0	actuator check 2b	0V; 0d, 1d1P, 2d1P	HHC	w/o Kalman filter
34	17-21	0.075,-5.5,0.2,200V0.2-9,3*40s,col,log	0.2	freq sweep	0V; (200V, 0.2-9Hz, log), col, lon, lat	HHC	up to pt 48 some df jumps at 1sec intervals
34	21-32	CT/S=0.075+1deg,ALF=-5.5,MU=0.2,df=0V	0.2	control power SP	0; (1,-1) col; 0; (1, 2, -1, -2) lon; 0;(1, -1) lat; 0; all at 0V		from pt 50 Relax=0.5 helps to eliminate jumps
34	32-39	CT/S=0.075,ALF=-5.5,MU=0.2,df=250Vcol	0.2	control power VSP	0V; (250, -250V) col, lon, lat; 0deg	HHC	
34	39-60	CT/S=0.075,ALF=-5.5,MU=0.2,df=1deg0P	0.2	control power IBC	0d; (1,2,3,-1,-2,-3) col; 0d; (1,2,-1,-2,-3) lon; 0d; (1,2,3,-1,-2,-3) lat; 0d; 0V	HHC	
34	72-83	CT/S=0.075+1deg,ALF=2,MU=0.2,df=0V	0.2	control power SP	0; (1,-1) col; 0; (1, 2, -1, -2) lon; 0;(1, -1) lat; 0; all at 0V		
34	83-90	CT/S=0.075,ALF=2,MU=0.2,df=250Vcol	0.2	control power VSP	0V; (250, -250V) col, lon, lat; 0deg	HHC	
34	90-111	CT/S=0.075,ALF=2,MU=0.2,df=1deg0P	0.2	control power IBC	0d; (1,2,3,-1,-2,-3) col; 0d; (1,2,3,-1,-2,-3) lon; 0d; (1,2,3,-1,-2,-3) lat; 0d; 0V	HHC	
34	118-120	Post-run check, COLL=10, Vbias=0	0	actuator check 3	0V, 0Vbias; zero		
35	3-8	Act check,Nr=0,COLL=10,ALF=0,Vbias=400	0	actuator check 1	0Vbias; 0V; 200,300,400V, 1Hz; 0V	CTC	point 7 w 400V has Vcmd=300V limit
35	11-15	COLL=4,ALF-10,MU0,df=0deg0-6P	0	actuator check 2b	0V; 0d, 1d1P	CTC	
35	17-72	CT/S=0.075,ALF=2,MU=0.2,df=1.5deg3P	0.2	phase sweep	0V; 0d; 1.5d 3, 4, 5, 2P ; 0d; ASA pos at max BVI (-40)	CTC	before this ASA pos always Upstream,U=-200
35	72-81	CT/S=0.075,ALF=2,MU=0.2,df=1.5deg3P180	0.2	phase sweep + ampl	0d; 1-2.5deg, 3P180; 1,5deg (4P30, 5P300, 2P300)	CTC	
35	82-82.29	0.075,2,0.2,df=1.5deg3P180,Tr=-200	0.2	trav sweep	1.5deg 3P180; 0deg	CTC	
35	94-96	Post-run check, COLL=10, Vbias=0	0	actuator check 3	0V, 0Vbias; zero		
36	3-8	Act check,Nr=0,COLL=10,ALF=0,Vbias=400	0	actuator check 1	0Vbias; 0V; 200,300,400V, 1Hz; 0V	CTC	
36	11-13	COLL=4,ALF-10,MU0,df=0deg0-6P	0	actuator check 2b	0V; 0d, 1d1P	CTC	
36	16,98-111.06,10	0.075,4,0.15,df=0deg,Tr=-200	0.15	trav sweep	(0V); 0deg	CTC	
36	18.01-71	CT/S=0.075,ALF4,MU=0.15,df=1.5deg3P	0.15	phase sweep	0d; 1.5deg 3, 4, 5, 2P; 0d; ASA pos at max BVI (-120)	CTC	
36	71-81.01	CT/S=0.075,ALF4,MU=0.15,df=1.5deg2P180	0.15	phase sweep + ampl	0d; 1-2deg 4P30; 1.5deg 2P180, 3P150, 180, 4P60, 5P300	CTC	
36	82-124	0.075,4,0.15,df=1.5deg4P30,Tr=-120	0.15	trav sweep	1.5deg 4P30; 0deg	CTC	
36	134-138	Post-run check, COLL=10, Vbias=0	0	actuator check 3	0V, 0Vbias; zero		
37	3-8	Act check,Nr=0,COLL=10,ALF=0,Vbias=400	0	actuator check 1	0Vbias; 0V; 200,300,400V, 1Hz; 0V	HHC	
37	11-13	COLL=4,ALF-10,MU0,df=0deg0-6P	0	actuator check 2b	0V; 0d, 1d1P	HHC	
37	17-21	0.075,-9.1,0.3,150V0.2-9,3*40s,col,log	0.3	freq sweep	0V; (150V col, 200V lon, 150V lat), 0.2-9Hz, log; 0V	HHC	
37	21-32	CT/S=0.075+1deg,ALF=-9.1,MU=0.3,df=0V	0.3	control power SP	0; (1,-1) col; 0; (1, 2, -1) lon; 0;(1, -1) lat; 0; all at 0V		
37	32-39	CT/S=0.075,ALF=-9.1,MU=0.3,df=250Vcol	0.3	control power VSP	0V; (250, -250V) col, lon, lat; 0deg	HHC	
37	39-60	CT/S=0.075,ALF=-9.1,MU=0.3,df=1deg0P	0.3	control power IBC	0d; (1,2,3,-1,-2,-3) col; 0d; (1,2,-1,-2,-3) lon; 0d; (1,2,3,-1,-2,-3) lat; 0d; 0V	HHC	
37	60.1-64	0.075,-9.1,0.3,df=.7deg3P258 +.8deg5P68	0.3	noise control OL_opt	0d; .7d3P258+.8d5P68; 0d	CTC	
37	64-92	CT/S=0.075,ALF=-9.1,MU=0.3,df=1deg4P	0.3	phase sweep	0d; 1d 4P; 1.5d 2P;	CTC	
37	92-109.01	0.075,-9.1,0.3,df=.7deg3P258 +.8deg5P68	0.3	noise control OL_opt	0d; .7d3P258+.8d5P68 ; 1.1d3P268+1d5P60; 0df; 0V	CTC	
37	114-116	Post-run check, COLL=10, Vbias=0	0	actuator check 3	0V, 0Vbias; zero		

Appendix D—Active Flap Test Conditions (cont.)

38	3-8	Act check,Nr=0,COLL=10,ALF=0,Vbias=400	0	actuator check 1	0Vbias; 0V; 200,300,400V, 1Hz; 0V	CTC	
38	11-13	COLL=4,ALF-10,MU0,df=0deg 0-6P	0	actuator check 2b	0V; 0d, 1d1P	CTC	
38	17-29	CT/S=0.075,ALF=-9.1,MU=0.3,df=1deg4P180	0.3	phase sweep + ampl	0V; 0d; 0.7-1.3d, 4P180, 170; 1-2d 2P0; 1d 3P250; 0d	CTC	Pt 24- controller instability
38	29-57	0.075,-9.1,0.3,df=1deg 3P250 + 1deg2P0	0.3	phase sweep	0d; 1d 3P250 + 1d 2P; 1d 3P250 + (1, .75, .5)d4P; 0d	CTC	
38	57-71	CT/S=0.075,ALF=-9.1,MU=0.3,df1=1deg0P	0.3	rotor smoothing	0d; (1, 2, 3, -1, -2, -3) df1; (1, 2, 3, -1, -2, -3) df2	CTC	
38	71-88	CT/S=0.075,ALF=-9.1,MU=0.3,df=0deg	0.3	performance	(CTS= .075, .040, .060, .080, .090, .075) 0deg, 0V, no retrim	CTC	
38	103-105	Post-run check, COLL=10, Vbias=0	0	actuator check 3	0V, 0Vbias; zero		
39	3-8	Act check,Nr=0,COLL=10,ALF=0,Vbias=400	0	actuator check 1	0Vbias; 0V; 200,300,400V, 1Hz; 0V	CTC	
39	11-13	COLL=4,ALF-10,MU0,df=0deg 0-6P	0	actuator check 2b	0V; 0d, 1d1P	CTC	
39	14-28	COLL=4,ALF=-10,MU=0,df=1deg0P	0	rotor smoothing	0d; df1= 1, 2, 3, -1, -2, -3; 0V; 0d; df2= 1, 2, 3, -1, -2, -3; 0d	CTC	
39	49-63	0.075,-9.1,0.3,df=1deg3P250 +1deg2P0	0.3	phase sweep + ampl	0V; 0d; (1-2)d 3P250 +(1-2)d2P0; (.5-1.5)d 3P250 +(.5-1)d4P180; 0V	CTC	Pt 58+ controller instability
39	63,64,6401	0.075,-9.1,0.3,175V,150V0-80,3*40s,col,lin	0.3	freq sweep	0V; 150V, 0-80Hz, lin, col	CTC	Pt 64 aborted
39	63,65-69	0.075,-9.1,0.3,dfNF1-5P,T=10	0.3	vib control	0V; NF1-5P, (T=10,1); PM 1-5P, (T=10,1); 0d	CTC2	
39	69-84	0.075,-9.1,0.3,df=1.5deg2P	0.3	performance	0d; 1.5d 2P phase sweep, w retrim; 0d; 0V	CTC	
39	97-110	CT/S=0.075,ALF=-4,MU=0.25,df=0degTr=-200	0.25	trav sweep	(0V); 0d	CTC	
39	117-119	Post-run check, COLL=10, Vbias=0	0	actuator check 3	0V, 0Vbias; zero		
40	3-8	Act check,Nr=0,COLL=10,ALF=0,Vbias=400	0	actuator check 1	0Vbias; 0V; 200,300,400V, 1Hz; 0V	HHC	
40	11-14	COLL=4,ALF-10,MU0,df=0deg 0-6P	0	actuator check 2b	0V; 0d, 1d1P, 2d1P	HHC	
40	18-24	0.075,4,0.15,df~.75deg 2-5P,OL_opt	0.15	noise control OL_opt	0d; 1,5d4P30; xd(2-5)Py; 0d; ASA pos at max BVI (-120)	HHC	
40	24-25	CT/S=0.075,ALF=4,MU=0.15,df=NF5P,5P	0.15	vib control	0d; NF 5P	HHC	SW error
40	32-52	0.075,1.8,0.165,df=0deg,Tr=-200	0.165	trav sweep	(0V); 0d	HHC	
40	52-79	0.075,1.8,0.165,df=1.5deg3P	0.165	phase sweep	0d; 1.5d3P; 1.5d4P; 0d; ASA pos at max BVI Mic 9 (-80)	HHC	
40	79-81	0.075,1.8,0.165,df=NF,RM,PM5P,4,5,6P	0.165	vib control	0d; NF, RM, PM 5P w 4, 5, 6P; 0V	HHC	SW error
40	81-89	0.075,1.8,0.165,df=1.5deg3P180	0.165	phase sweep + ampl	0V; 1.5-2d, 3P165-180; 1.5d 4P120-180	HHC	
40	93-108	0.075,1.8,0.165,df=1.5deg3P180,Tr=-200	0.165	trav sweep	1.5d 3P180	HHC	
40	152-154	Post-run check, COLL=10, Vbias=0	0	actuator check 3	0V, 0Vbias; zero		
41	3-8	Act check,Nr=0,COLL=10,ALF=0,Vbias=400	0	actuator check 1	0Vbias; 0V; 200,300,400V, 1Hz; 0V	HHC	
41	11-13	COLL=4,ALF-10,MU0,df=0deg 0-6P	0	actuator check 2b	0V; 0d, 1d1P	HHC	
41	15.01-27	CT/S=0.075,ALF=2,MU=0.2,df=NF5P5Pcol	0.2	vib control	0V; NF; RM; 3F; NF,RM,PM; 0V; 0d	HHC	SW error
41	27-32	0.075,2,0.2,df~.75deg 2-5P,OL_opt	0.2	noise control OL_opt	0d; 1.5d 3P180; xdeg(2-5)Py; ASA pos at max BVI Mic 9 (-80)	HHC	
41	33-46	CT/S=0.075,ALF=2,MU=0.2,df=0deg	0.2	performance	(CTS= .075, .040, .060, .080, .090, .10, .075) 0deg, 0V, no retrim	HHC	
41	47-54	CT/S=0.075,ALF=2,MU=0.2,df=1deg0P	0.2	rotor smoothing	0d; df1= 1, 2, 3, -1, -2, -3; 0d	HHC	
41	55.01-61	0.075,0.89,83,df=2d2P240+1d5P330	0.2	DARPA4, HHC,CTC	HHC vs CTC: 0d; 2d2P240+1d5P330	HHC, CTC	
41	114-116	Post-run check, COLL=10, Vbias=0	0	actuator check 3	0V, 0Vbias; zero		
42	3-8	Act check,Nr=0,COLL=10,ALF=0,Vbias=400	0	actuator check 1	0Vbias; 0V; 200,300,400V, 1Hz; 0V	CTC	
42	11-15	COLL=2,-10,0,150V.2-200,3*40s,col,log	0	freq sweep	0V; 150V, .2-200Hz, col, (log, lin); 200V, 0-80Hz, lin, col, lon, lat		w AFC data
42	16,17	COLL=4,ALF-10,MU0,df=0deg 0-6P	0	actuator check 2b	0d; 1d1P	CTC	
42	20-36	0.075,-9.1,0.3,df=NF10P,T=5	0.3	vib control	0V; NF 10P, T=5,1; NF 1-5,10P, T=10,5	CTC3	coeff for 82kt
42	39,40, [41-47]	CT/S=0.075,ALF=-9.1,MU=0.3,df1.3deg4P180	0.3	noise control OL_opt	0d; 1.3d 4P180; [xdeg(2-5)Py - kill flaps]	CTC	
42	48-62	CT/S=0.09,ALF=-9.1,MU=0.3,df=1.5deg2P	0.3	performance	0d; 1.5d 2P phase sweep, w retrim; 0d	CTC	
42	71-76	CT/S=0.07,ALF=-9.3,MU=155,df=0deg	0.375	DARPA3, CTC	0d; [1.5d 5P180 - kill flaps]	CTC	
42	92-94	Post-run check, COLL=10, Vbias=0	0	actuator check 3	0V, 0Vbias; zero		
43	3-8	Act check,Nr=0,COLL=10,ALF=0,Vbias=400	0	actuator check 1	0Vbias; 0V; 200,300,400V, 1Hz; 0V	HHC	
43	11-13	COLL=4,ALF-10,MU0,df=0deg 0-6P	0	actuator check 2b	0V; 0d, 1d1P	HHC	
43	16-23.02	0.075,4,0.15,df=Mic1,4P,RMS	0.15	noise control	0V; 250V 4P30; 0d; 1.5d 4P30; Mic1	HHC	SW error
43	36-43.01	0.075,2,0.2,df=Mic1,4P,RMS	0.2	noise control	0V; 250V 3P180; 0d; 1.5d 3P180; Mic1	HHC	SW error
43	61-68.01	0.075,-9.1,0.3,df=Mic13,4P,RMS	0.3	noise control	0V; 225V 4P180; 0d; 1.3d 4P180; Mic13	HHC	SW error
43	69-72	0.075,-9.1,0.3,df=NF5P,5Pcol,Vc=300	0.3	vib control	NF 5, 1-5P; RM 5, 1-5P	HHC	SW error
43	108	10deg,0,0,75V0-200,3*40,col,lin	0	freq sweep	75V,0-200Hz, lin, col	HHC	
43	111-113	Post-run check, COLL=10, Vbias=0	0	actuator check 3	0V, 200,300,400V; 75V 0-200Hz col, lin; 100V 1Hz; 0Vbias; zero		

Appendix D—Active Flap Test Conditions (cont.)

SMART Rotor Test Runs: Summary of Specific Conditions Cases with flap inputs, open and closed loop.

Boeing Values Run	Points	Condition	Speed	Type	Variables		
23	3-8	Act check,Nr=0,COLL=10,ALF=0,Vbias=400	0		actuator check 1 0Vbias: 0V: 200.300.400V. 1Hz: 0V		
24	3-8	Act check,Nr=0,COLL=10,ALF=0,Vbias=400	0		actuator check 1 0Vbias; 0V; 200,300,400V, 1Hz; 0V		
25	3-8	Act check,Nr=0,COLL=10,ALF=0,Vbias=400	0		actuator check 1 0Vbias; 0V; 200,300,400V, 1Hz; 0V		
26	3-8	Act check,Nr=0,COLL=10,ALF=0,Vbias=400	0		actuator check 1 0Vbias; 0V; 200,300,400V, 1Hz; 0V		
28	3-9	Act check,Nr=0,COLL=10,ALF=0,Vbias=400	0		actuator check 1 0Vbias; 0V; 200,300,400V, 1Hz; 400V 5P; 0V		
29	3-9	Act check,Nr=0,COLL=10,ALF=0,Vbias=400	0		actuator check 1 0Vbias; 0V; 200,300,400V, 1Hz; 0V		RPCM problem, fast shut down?
30	3-7	Act check,Nr=0,COLL=10,ALF=0,Vbias=400	0		actuator check 1 0Vbias; 0V; 200,300,400V, 1Hz	CTC	using 1-6P fpr position control
32	3-9	Act check,Nr=0,COLL=10,ALF=0,Vbias=400	0		actuator check 1 0Vbias; 0V; 200,300,400V, 1Hz; 0V	CTC	
33	3-8	Act check,Nr=0,COLL=10,ALF=0,Vbias=400	0		actuator check 1 0Vbias; 0V; 200,300,400V, 1Hz; 0V	CTC	
34	3-8	Act check,Nr=0,COLL=10,ALF=0,Vbias=400	0		actuator check 1 0Vbias; 0V; 200,300,400V, 1Hz; 0V	HHC	using 1-5P for position control
35	3-8	Act check,Nr=0,COLL=10,ALF=0,Vbias=400	0		actuator check 1 0Vbias; 0V; 200,300,400V, 1Hz; 0V	CTC	point 7 w 400V has Vcmd=300V limit
36	3-8	Act check,Nr=0,COLL=10,ALF=0,Vbias=400	0		actuator check 1 0Vbias; 0V; 200,300,400V, 1Hz; 0V	CTC	
37	3-8	Act check,Nr=0,COLL=10,ALF=0,Vbias=400	0		actuator check 1 0Vbias; 0V; 200,300,400V, 1Hz; 0V	HHC	
38	3-8	Act check,Nr=0,COLL=10,ALF=0,Vbias=400	0		actuator check 1 0Vbias; 0V; 200,300,400V, 1Hz; 0V	CTC	
39	3-8	Act check,Nr=0,COLL=10,ALF=0,Vbias=400	0		actuator check 1 0Vbias; 0V; 200,300,400V, 1Hz; 0V	CTC	
40	3-8	Act check,Nr=0,COLL=10,ALF=0,Vbias=400	0		actuator check 1 0Vbias; 0V; 200,300,400V, 1Hz; 0V	HHC	
41	3-8	Act check,Nr=0,COLL=10,ALF=0,Vbias=400	0		actuator check 1 0Vbias; 0V; 200,300,400V, 1Hz; 0V	HHC	
42	3-8	Act check,Nr=0,COLL=10,ALF=0,Vbias=400	0		actuator check 1 0Vbias; 0V; 200,300,400V, 1Hz; 0V	CTC	
43	3-8	Act check,Nr=0,COLL=10,ALF=0,Vbias=400	0		actuator check 1 0Vbias; 0V; 200,300,400V, 1Hz; 0V	HHC	
31	3-11	Act check,Nr=0,COLL=10,ALF=0,Vbias=400	0		actuator check 1,1b 0Vbias; 0V; 200,300,400V, 1Hz; 0d, 1d1P, 2d1P90; 0V	CTC	
30	8-13	COLL=10,ALF=0,MU=0,df=0deg 0-6P	0		actuator check 1b 0deg; DARPA1-4; 0V	CTC	for start up, overcome integrator limits by hand
20	7-15.01	COLL=4,ALF=-10,VKTS=0,df=200V1P	0		actuator check 2 0Vbias; 0V; 200V, 1-6P, harmonic, cyclic; 0V		
23	11-18	COLL=4,ALF=-10,VKTS=0,df=200V1P	0		actuator check 2 0V; 200V, 1-6P, harmonic, cyclic; 0V		
24	11-18	COLL=4,ALF=-10,VKTS=0,df=200V1P	0		actuator check 2 0V; 200V, 1-6P, harmonic, cyclic; 0V		
25	11-18	COLL=4,ALF=-10,VKTS=0,df=200V1P	0		actuator check 2 0V; 200V, 1-6P, harmonic, cyclic; 0V		
26	11,12,17,18	COLL=4,ALF=-10,VKTS=0,df=200V1P	0		actuator check 2 0V; 200V, 1,6P, harmonic, cyclic; 0V		
28	17-19	COLL=4,ALF=-10,VKTS=0,df=200V5P	0		actuator check 2 200V, 5,6P, harmonic, cyclic; 0V		
29	12-19	COLL=4,ALF=-10,VKTS=0,df=200V1P	0		actuator check 2 0V; 200V, 1-6P, harmonic, cyclic; 0V		
30	16-22	COLL=4,-10,0,df=0deg 0-6P,	0		actuator check 2b 0V; 0deg; DARPA1-4; 0V	CTC	
31	14-19	COLL=4,-10,0,df=0deg 0-6P,	0		actuator check 2b 0V; 0d, 1d1P, 2d1P, 2d1P90; 0V	CTC	start up controlled by software
32	12-17	COLL=4,ALF-10,MU0,df=0deg 0-6P	0		actuator check 2b 0V; 0d, 1d1P, 2d1P; 0V	CTC	
33	11-14	COLL=4,ALF-10,MU0,df=0deg 0-6P	0		actuator check 2b 0V; 0d, 1d1P, 2d1P	CTC	
34	11-14	COLL=4,ALF-10,MU0,df=0deg 0-6P	0		actuator check 2b 0V; 0d, 1d1P, 2d1P	HHC	w/o Kalman filter
35	11-15	COLL=4,ALF-10,MU0,df=0deg 0-6P	0		actuator check 2b 0V; 0d, 1d1P	CTC	
36	11-13	COLL=4,ALF-10,MU0,df=0deg 0-6P	0		actuator check 2b 0V; 0d, 1d1P	CTC	
37	11-13	COLL=4,ALF-10,MU0,df=0deg 0-6P	0		actuator check 2b 0V; 0d, 1d1P	HHC	
38	11-13	COLL=4,ALF-10,MU0,df=0deg 0-6P	0		actuator check 2b 0V; 0d, 1d1P	CTC	
39	11-13	COLL=4,ALF-10,MU0,df=0deg 0-6P	0		actuator check 2b 0V; 0d, 1d1P	CTC	
40	11-14	COLL=4,ALF-10,MU0,df=0deg 0-6P	0		actuator check 2b 0V; 0d, 1d1P, 2d1P	HHC	
41	11-13	COLL=4,ALF-10,MU0,df=0deg 0-6P	0		actuator check 2b 0V; 0d, 1d1P	HHC	
42	16,17	COLL=4,ALF-10,MU0,df=0deg 0-6P	0		actuator check 2b 0d; 1d1P	CTC	
43	11-13	COLL=4,ALF-10,MU0,df=0deg 0-6P	0		actuator check 2b 0V; 0d, 1d1P	HHC	
24	64-68	Actcheck,Nr=0,COLL=10,ALF=0,400V1Hz	0		actuator check 3 0V; 400, 100V 1Hz; 0Vbias; zero		
25	136-140	Actcheck,Nr=0,COLL=10,ALF=0,400V1Hz	0		actuator check 3 0V; 400, 100V 1Hz; 0Vbias; zero		
26	143-147	Post-run check, COLL=10, Vbias=0	0		actuator check 3 0V, 0Vbias,zero		
28	108-112	Actcheck,Nr=0,COLL=10,ALF=0,400V1Hz	0		actuator check 3 0V; 400, 100V 1Hz; 0Vbias; zero		
29	123-127	Post-run check, COLL=10, Vbias=0	0		actuator check 3 0V, 0Vbias; zero		
30	119-123	Actcheck,Nr=0,COLL=10,ALF=0,400V1Hz	0		actuator check 3 0V; 400, 100V 1Hz; 0Vbias; zero		
31	135-139	Post-run check, COLL=10, Vbias=0	0		actuator check 3 0V, 0Vbias; zero		
32	126-127.01	Post-run zero, COLL=10,Vbias=0	0		actuator check 3 0V, 0Vbias; zero		
33	124,125	Post-run check, COLL=10	0		actuator check 3 0V, 0Vbias		
34	118-120	Post-run check, COLL=10, Vbias=0	0		actuator check 3 0V, 0Vbias; zero		

Appendix D—Active Flap Test Conditions (cont.)

35	94-96	Post-run check, COLL=10, Vbias=0	0	actuator check 3	0V, 0Vbias; zero		
36	134-138	Post-run check, COLL=10, Vbias=0	0	actuator check 3	0V, 0Vbias; zero		
37	114-116	Post-run check, COLL=10, Vbias=0	0	actuator check 3	0V, 0Vbias; zero		
38	103-105	Post-run check, COLL=10, Vbias=0	0	actuator check 3	0V, 0Vbias; zero		
39	117-119	Post-run check, COLL=10, Vbias=0	0	actuator check 3	0V, 0Vbias; zero		
40	152-154	Post-run check, COLL=10, Vbias=0	0	actuator check 3	0V, 0Vbias; zero		
41	114-116	Post-run check, COLL=10, Vbias=0	0	actuator check 3	0V, 0Vbias; zero		
42	92-94	Post-run check, COLL=10, Vbias=0	0	actuator check 3	0V, 0Vbias; zero		
43	111-113	Post-run check, COLL=10, Vbias=0	0	actuator check 3	0V, 200,300,400V; 75V 0-200Hz col, lin; 100V 1Hz; 0Vbias; zero	20	
	44-46.02	CT/S=0.075,ALF=1.49,MU=0.2,df=200V2P	0	actuator check rot	0V; 200,300,400V at 2P and 5P		
20	69,70,70.01	CT/S=0.08,ALF=-9.1,MU=0.3,df=0V	0.3	actuator check rot	0,200,300V at 3P60		
17	8.02-23	COLL=4,ALF=-10,VKTS=0	0	actuator check rot stea	0Vbias; 0V; V1,V2,V3,V4,V5=200; V=200, 300, 400, 0, -200, -300, -400, 0		
34	39-60	CT/S=0.075,ALF=-5.5,MU=0.2,df=1deg0P	0.2	control power IBC	0d; (1,2,3,-1,-2,-3) col; 0d; (1,2,-1,-2,-3) lon; 0d; (1,2,3,-1,-2,-3) lat; 0d; 0V	HHC	
34	90-111	CT/S=0.075,ALF=2,MU=0.2,df=1deg0P	0.2	control power IBC	0d; (1,2,3,-1,-2,-3) col; 0d; (1,2,3,-1,-2,-3) lon; 0d; (1,2,3,-1,-2,-3) lat; 0d;	HHC	
37	39-60	CT/S=0.075,ALF=-9.1,MU=0.3,df=1deg0P	0.3	control power IBC	0d; (1,2,3,-1,-2,-3) col; 0d; (1,2,-1,-2,-3) lon; 0d; (1,2,3,-1,-2,-3) lat; 0d; 0V	HHC	
33	74-84	CT/S=0.075,ALF=-9.1,MU=0.3,df=0V	0.3	control power SP	0; (1, 2, 0, -1, -2) lon; 0; (1, 0, -1, -1) lat; all at 0V		
34	21-32	CT/S=0.075+1deg,ALF=-5.5,MU=0.2,df=0V	0.2	control power SP	0; (1,-1) col; 0; (1, 2, -1, -2) lon; 0;(1, -1) lat; 0; all at 0V		from pt 50 Relax=0.5 helps to eliminate jumps 34
	72-83	CT/S=0.075+1deg,ALF=2,MU=0.2,df=0V	0.2	control power SP	0; (1,-1) col; 0; (1, 2, -1, -2) lon; 0;(1, -1) lat; 0; all at 0V		
37	21-32	CT/S=0.075+1deg,ALF=-9.1,MU=0.3,df=0V	0.3	control power SP	0; (1,-1) col; 0; (1, 2, -1) lon; 0;(1, -1) lat; 0; all at 0V		
34	32-39	CT/S=0.075,ALF=-5.5,MU=0.2,df=250Vcol	0.2	control power VSP	0V; (250, -250V) col, lon, lat; 0deg	HHC	
34	83-90	CT/S=0.075,ALF=2,MU=0.2,df=250Vcol	0.2	control power VSP	0V; (250, -250V) col, lon, lat; 0deg	HHC	
37	32-39	CT/S=0.075,ALF=-9.1,MU=0.3,df=250Vcol	0.3	control power VSP	0V; (250, -250V) col, lon, lat; 0deg	HHC	
30	109-114	CT/S=0.08,-9.4,123,df=2deg 5P90 +0d0-6P	0.3	DARPA1, CTC	0V; 0, 1, 2deg 5P90	CTC	390k limit hit
33	112-116.01	0.08,-9.4,123,df=2deg 5P90 +0d0-6P	0.3	DARPA1, CTC	0d; 0, 1, 2deg 5P90; 0d; 0V	CTC	
24	22-25	CT/S=0.08,ALF=-9.1,VKTS=123,df=200V5P90	0.3	DARPA1, OL	0V; 200,300,400V 5P90		
26	38-41	CT/S=0.08,ALF=-9.1,VKTS=123,df=300V5P90	0.3	DARPA1, OL	0V; 300, 350, 400V, 5P90		
30	104-109	CT/S=0.08,-9.4,123,df=2deg 3P60 +0d0-6P	0.3	DARPA2, CTC	0V, 0, 1, 2deg 3P60; 0V	CTC	200k limit hit
33	106-112	0.08,-9.4,123,df=2deg 3P60 +0d0-6P	0.3	DARPA2, CTC	0V, 0, 1, 2deg 3P60; 0d	CTC	
23	36-39	CT/S=0.08,ALF=-9.4,VKTS=123,df=0V	0.3	DARPA2, OL	0V; 200, 300, 400V 3P60		
24	33-43	CT/S=0.08,ALF=-9.1,VKTS=123,df=350V3P60	0.3	DARPA2, OL	0V; 350V 3P60		
26	49-60	CT/S=0.08,ALF=-9.1,VKTS=123,df=300V3P60	0.3	DARPA2, OL	0V; 300,350,400V 3P60; 0V		
42	71-76	CT/S=0.07,ALF=-9.3,MU=155,df=0deg	0.375	DARPA3, CTC	0d; [1.5d 5P180 - kill flaps]	CTC	
30	26-34	0.075,0.89,83,df=2d2P240+1d5P330+0d0-6P	0.2	DARPA4, CTC	0V; 0, 1, 1.5, 2d2P240+1d5P330; 0V; also alfa=0.29, 1.49	CTC	200k limit hit
41	55.01-61	0.075,0.89,83,df=2d2P240+1d5P330	0.2	DARPA4, HHC,CTC	HHC vs CTC: 0d; 2d2P240+1d5P330	HHC, CTC	
25	22-25	0.075,1.49,83,df=200V 2P240 +100V 5P330	0.2	DARPA4, OL	0V; 200V 2P240 +100V 5P330; 250V.. ; 300V..		
17	86-101	COLL=4,ALF=-10,MU=0,150V,0-200Hz,120sec	0	freq sweep	0V; 150V, 0-200Hz; 200V, 0-80Hz; 0.2-5Hz, 2, 3, 4, 5, 6, 10P, sine		
26	61-85	0.075,-9.1,0.3,df200V0-80,60s, col, lin	0.3	freq sweep	0V; (200V, 0-80 lin, 1-80, 0.2-5Hz, 2,3,4,5,6,10P log), col, lon, lat	SRH - data given to	28
	12-16	COLL=4,-10,0,df=200V.2-80,5*40s, col,log	0	freq sweep	0V; (200V, 0.2-80Hz log), col, lon, lat, col		
28	23-30	0.075,-9.1,0.3,df=200V0-80,5*40s,col,lin	0.3	freq sweep	0V; (200V, 0-80 lin, 0.2-9 log, 5P lin), col, lon, lat; 0V	29	
	44-51	0.075,2,0.2,df=200V0-80,3*40s,col,lin	0.2	freq sweep	0V; (200V, 0-80 lin, 0.2-9 log), col, lon, lat; 0V		
31	124-130	CT/S=0.075,ALF=-9.1,MU=0.3,df=0V,40s	0.3	freq sweep	0V; (200V, 0-80Hz, lin), col, lon, lat		RPCM problem, ok after reboot 32
	21-22	CT/S=0.075,ALF=2,MU=0.2,df=200V0-80	0.2	freq sweep	0V; 200V, 0-80Hz, lin, col	CTC	
33	17-22	0.075,-9.1,0.3,df=175V0-80,3*40s,col,lin	0.3	freq sweep	0Vbias; 0V; (175V col, 200V, lon, lat), 0-80Hz, lin	CTC	
34	17-21	0.075,-5.5,0.2,200V0.2-9,3*40s,col,log	0.2	freq sweep	0V; (200V, 0.2-9Hz, log), col, lon, lat	HHC	up to pt 48 some df jumps at 1sec intervals 37
	17-21	0.075,-9.1,0.3,150V0.2-9,3*40s,col,log	0.3	freq sweep	0V; (150V col, 200V lon, 150V lat), 0.2-9Hz, log; 0V	HHC	
39	63,64,6401	0.075,-9.1,0.3,175V,150V0-80,3*40s,col,lin	0.3	freq sweep	0V; 150V, 0-80Hz, lin, col	CTC	Pt 64 aborted 42
	11-15	COLL=2,-10,0,150V.2-200,3*40s, col,log	0	freq sweep	0V; 150V, .2-200Hz, col, (log, lin); 200V, 0-80Hz, lin, col, lon, lat		w AFC data 43
	108	10deg,0,0,75V0-200,3*40,col,lin	0	freq sweep	75V,0-200Hz, lin, col	HHC	
33	27-30	CT/S=0.075,ALF=-9.1,MU=0.3,df=Mic15P	0.3	noise control	Mic1 5, 1-5P; 0V	CTC	
33	102-105	CT/S=0.075,ALF=-9.1,MU=0.3,df=Mic165P	0.3	noise control	Mic16 5, 1-5P; 0V	CTC	
43	16-23.02	0.075,4,0.15,df=Mic1,4P,RMS	0.15	noise control	0V; 250V 4P30; 0d; 1.5d 4P30; Mic1	HHC	SW error
43	36-43.01	0.075,2,0.2,df=Mic1,4P,RMS	0.2	noise control	0V; 250V 3P180; 0d; 1.5d 3P180; Mic1	HHC	SW error
43	61-68.01	0.075,-9.1,0.3,df=Mic13,4P,RMS	0.3	noise control	0V; 225V 4P180; 0d; 1.3d 4P180; Mic13	HHC	SW error
37	60.1-64	0.075,-9.1,0.3,df=.7deg3P258 +.8deg5P68	0.3	noise control OL_opt	0d; .7d3P258+.8d5P68; 0d	CTC	
37	92-109.01	0.075,-9.1,0.3,df=.7deg3P258 +.8deg5P68	0.3	noise control OL_opt	0d; .7d3P258+.8d5P68 ; 1.1d3P268+1d5P60; 0df; 0V	CTC	

Appendix D—Active Flap Test Conditions (concluded)

40	18-24	0.075,4,0.15,df~.75deg 2-5P,OL_opt	0.15	noise control OL_opt	0d; 1,5d4P30; xd(2-5)Py; 0d; ASA pos at max BVI (-120)	HHC	
41	27-32	0.075,2,0.2,df~.75deg 2-5P,OL_opt	0.2	noise control OL_opt	0d; 1.5d 3P180; xdeg(2-5)Py; ASA pos at max BVI Mic 9 (-80)	HHC	42
39,40, [41-47]	CT/S=0.075,ALF=-9.1,MU=0.3,df1.3deg4P180		0.3	noise control OL_opt	0d; 1.3d 4P180; [xdeg(2-5)Py - kill flaps]	CTC	38
71-88	CT/S=0.075,ALF=-9.1,MU=0.3,df=0deg		0.3	performance	(CTS= .075, .040, .060, .080, .090, .075) 0deg, 0V, no retrim	CTC	
39	69-84	0.075,-9.1,0.3,df=1.5deg2P	0.3	performance	0d; 1.5d 2P phase sweep, w retrim; 0d; 0V	CTC	41
	33-46	CT/S=0.075,ALF=2,MU=0.2,df=0deg	0.2	performance	(CTS= .075, .040, .060, .080, .090, .10, .075) 0deg, 0V, no retrim	HHC	
42	48-62	CT/S=0.09,ALF=-9.1,MU=0.3,df=1.5deg2P	0.3	performance	0d; 1.5d 2P phase sweep, w retrim; 0d	CTC	26
	86.01-98.01	CT/S=0.075,ALF=-9.1,MU=0.3,df=250V4P	0.3	phase sweep	250V 4P; 0V		
28	30-84	CT/S=0.075,ALF=-9.1,MU=0.3,df=250V5P	0.3	phase sweep	0V; 250V, 5P, 6P, 3P, 2P; 0V		
29	51-64.01	0.075,2,0.2,df=250V4P,virt sp lat	0.2	phase sweep	0V; 250V 4P virt sp lat		
30	35-102	CT/S=0.075,ALF=2,MU=0.2,df=250V4P	0.2	phase sweep	0V; 250V 4P, 5P, 6P, 3P, 2P; 0V		
32	32-46	CT/S=0.075,ALF=2,MU=0.2,df=1.5deg2P	0.2	phase sweep	0V; 1.5deg 2P; 0V	CTC	
33	30-44	CT/S=0.075,ALF=-9.1,MU=0.3,df=1.5deg3P	0.3	phase sweep	0V; 1.5deg 3P; 0deg	CTC	
33	52-66	CT/S=0.075,ALF=-9.1,MU=0.3,df=1.5deg5P	0.3	phase sweep	0d; 1.5 deg 5P; 0deg	CTC	
35	17-72	CT/S=0.075,ALF=2,MU=0.2,df=1.5deg3P	0.2	phase sweep	0V; 0d; 1.5d 3, 4, 5, 2P ; 0d; ASA pos at max BVI (-40)	CTC	before this ASA pos always Upstream,U=-200 36
	18.01-71	CT/S=0.075,ALF4,MU=0.15,df=1.5deg3P	0.15	phase sweep	0d; 1.5deg 3, 4, 5, 2P; 0d; ASA pos at max BVI (-120)	CTC	
37	64-92	CT/S=0.075,ALF=-9.1,MU=0.3,df=1deg4P	0.3	phase sweep	0d; 1d 4P; 1.5d 2P;	CTC	
38	29-57	0.075,-9.1,0.3,df=1deg 3P250 + 1deg2P0	0.3	phase sweep	0d; 1d 3P250 + 1d 2P; 1d 3P250 + (1, .75, .5)d4P; 0d	CTC	
40	52-79	0.075,1.8,0.165,df=1.5deg3P	0.165	phase sweep	0d; 1.5d3P; 1.5d4P; 0d; ASA pos at max BVI Mic 9 (-80)	HHC	
31	23-32	CT/S=0.075,ALF=2,MU=0.2,df=250V 2P90	0.2	phase sweep + ampl	0V; 250-500V 2P90; 1.5d 2P90, +/-15	CTC	Heim recorder failed 31
	51-59	CT/S=0.075,ALF=2,MU=0.2,df=250V 3P240	0.2	phase sweep + ampl	250-450V 3P240; 1.5d 3P240, +/-15	CTC	
31	60-68	CT/S=0.075,ALF=2,MU=0.2,df=250V 4P90	0.2	phase sweep + ampl	150-300V 4P90; 1.5d 4P90, +/-15	CTC	
31	78-86	CT/S=0.075,ALF=2,MU=0.2,df=250V5P0	0.2	phase sweep + ampl	150-350V 5P0; 1.5d 5P0, +/-15	CTC	
32	46-81	CT/S=0.075,ALF=2,MU=0.2,df=1.5deg2P300	0.2	phase sweep + ampl	0V; 1.5-3deg, 2P300, 90, 105; 0V	CTC	
33	44-52	CT/S=0.075,ALF=-9.1,MU=0.3,df1.5deg3P240	0.3	phase sweep + ampl	0d; 1.5-2deg, 3P240, 230, 250; 0deg	CTC	
33	66-74	CT/S=0.075,ALF=-9.1,MU=0.3,df=1.5deg5P90	0.3	phase sweep + ampl	0d; 1-2deg, 5P80, 100, 70; 0V	CTC	
35	72-81	CT/S=0.075,ALF=2,MU=0.2,df=1.5deg3P180	0.2	phase sweep + ampl	0d; 1-2.5deg, 3P180; 1,5deg (4P30, 5P300, 2P300)	CTC	
36	71-81.01	CT/S=0.075,ALF4,MU=0.15,df=1.5deg2P180	0.15	phase sweep + ampl	0d; 1-2deg 4P30; 1.5deg 2P180, 3P150, 180, 4P60, 5P300	CTC	
38	17-29	CT/S=0.075,ALF=-9.1,MU=0.3,df=1deg4P180	0.3	phase sweep + ampl	0V; 0d; 0.7-1.3d, 4P180, 170; 1-2d 2P0; 1d 3P250; 0d	CTC	Pt 24- controller instability 39
49-63	0.075,-9.1,0.3,df=1deg3P250 +1deg2P0		0.3	phase sweep + ampl	0V; 0d; (1-2)d 3P250 +(1-2)d2P0; (.5-1.5)d 3P250 +(.5-1)d4P180; 0V	CTC	Pt 58+ controller instability 40
81-89	0.075,1.8,0.165,df=1.5deg3P180		0.165	phase sweep + ampl	0V; 1.5-2d, 3P165-180; 1.5d 4P120-180	HHC	
38	57-71	CT/S=0.075,ALF=-9.1,MU=0.3,df1=1deg0P	0.3	rotor smoothing	0d; (1, 2, 3, -1, -2, -3) df1; (1, 2, 3, -1, -2, -3) df2	CTC	
39	14-28	COLL=4,ALF=-10,MU=0,df=1deg0P	0	rotor smoothing	0d; df1= 1, 2, 3, -1, -2, -3; 0V; 0d; df2= 1, 2, 3, -1, -2, -3; 0d	CTC	
41	47-54	CT/S=0.075,ALF=2,MU=0.2,df=1deg0P	0.2	rotor smoothing	0d; df1= 1, 2, 3, -1, -2, -3; 0d	HHC	
31	96-108	CT/S=0.075,2,0.2,df=0deg 0-6P,Trav1	0.2	trav sweep	0deg	CTC	
31	109-122	CT/S=0.075,2,0.2,df=1.5deg 2P90,Trav13	0.2	trav sweep	1.5deg 2P90; (0V)	CTC	Heim recorder failed
35	82-82.29	0.075,2,0.2,df=1.5deg3P180,Tr=-200	0.2	trav sweep	1.5deg 3P180; 0deg	CTC	
36	16,98-111.06,10	0.075,4,0.15,df=0deg,Tr=-200	0.15	trav sweep	(0V); 0deg	CTC	
36	82-124	0.075,4,0.15,df=1.5deg4P30,Tr=-120	0.15	trav sweep	1.5deg 4P30; 0deg	CTC	
39	97-110	CT/S=0.075,ALF=-4,MU=0.25,df=0degTr=-200	0.25	trav sweep	(0V); 0d	CTC	
40	32-52	0.075,1.8,0.165,df=0deg,Tr=-200	0.165	trav sweep	(0V); 0d	HHC	
40	93-108	0.075,1.8,0.165,df=1.5deg3P180,Tr=-200	0.165	trav sweep	1.5d 3P180	HHC	
32	23.01-32	CT/S=0.075,ALF=2,MU=0.2,df=NF5P	0.2	vib control	NF 5, 1, 1-5P; RM 5, 1, 1-5P; 0V	CTC	
33	22-26	CT/S=0.075,ALF=-9.1,MU=0.3,df=NF1-5P	0.3	vib control	0V; NF 1-5P, PM 1-5P	CTC	
39	63,65-69	0.075,-9.1,0.3,dfNF1-5P,T=10	0.3	vib control	0V; NF1-5P, (T=10,1); PM 1-5P, (T=10,1); 0d	CTC2	
40	24-25	CT/S=0.075,ALF=4,MU=0.15,df=NF5P,5P	0.15	vib control	0d; NF 5P	HHC	SW error 40
	79-81	0.075,1.8,0.165,df=NF,RM,PM5P,4,5,6P	0.165	vib control	0d; NF, RM, PM 5P w 4, 5, 6P; 0V	HHC	SW error
41	15.01-27	CT/S=0.075,ALF=2,MU=0.2,df=NF5P5Pcol	0.2	vib control	0V; NF; RM; 3F; NF,RM,PM; 0V; 0d	HHC	SW error
42	20-36	0.075,-9.1,0.3,df=NF10P,T=5	0.3	vib control	0V; NF 10P, T=5,1; NF 1-5,10P, T=10,5	CTC3	coeff for 82kt
43	69-72	0.075,-9.1,0.3,df=NF5P,5Pcol,Vc=300	0.3	vib control	NF 5, 1-5P; RM 5, 1-5P	HHC	SW error

Appendix E—Photographs

SMART ROTOR TEST IN THE 40- X 80-FOOT WIND TUNNEL

Feb 13–May 2, 2008

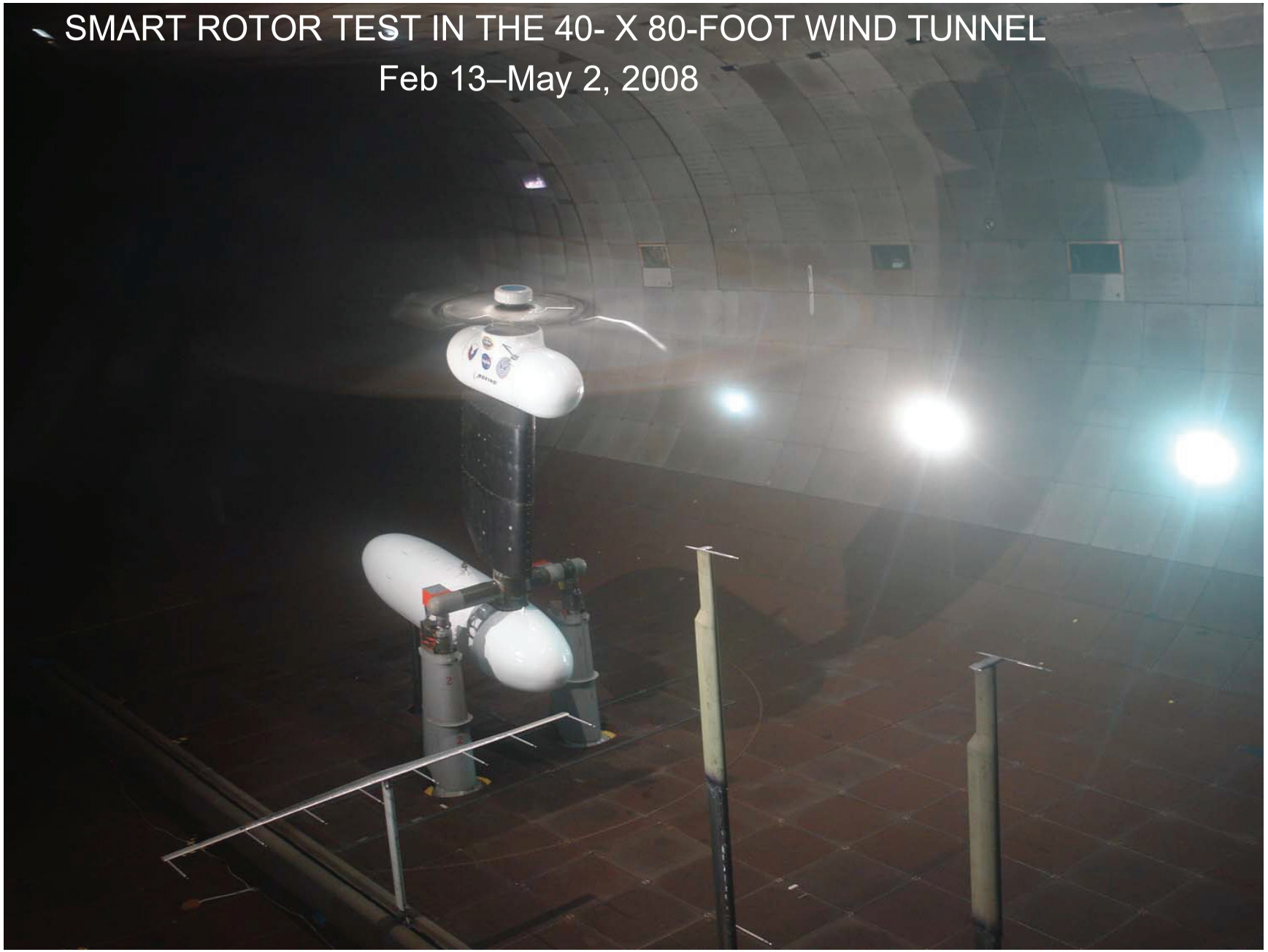

SMART ROTOR—GEOMETRY

Whirl Tower Test

Unigraphics CAD Model

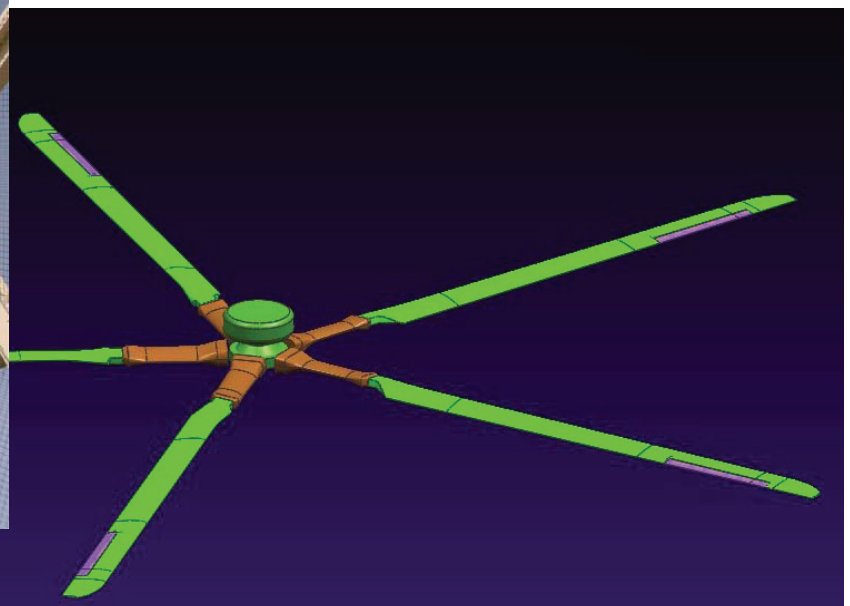

Computational Aero-Acoustics

HQP - Smart Rotor Test

BOEING

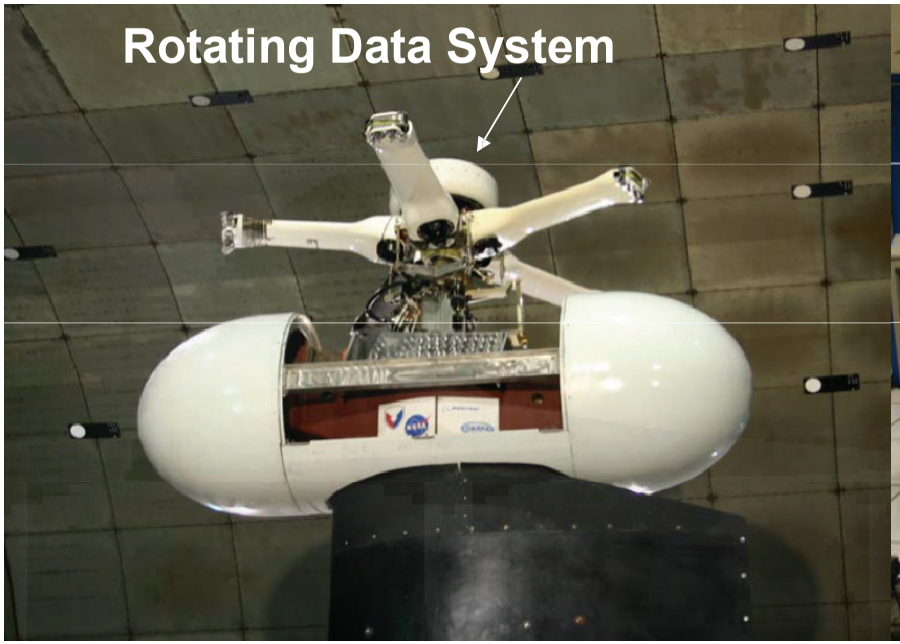
Rotating Data System

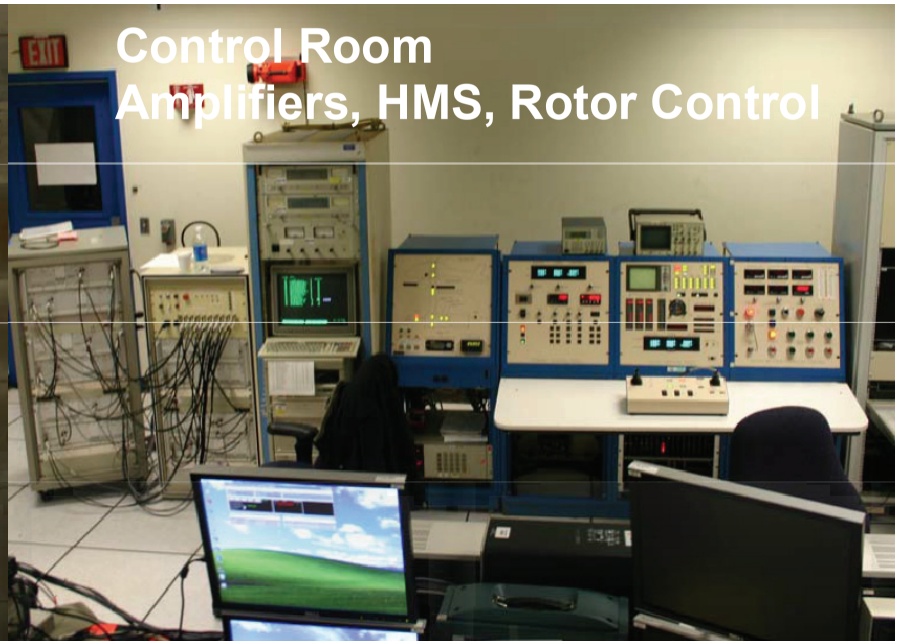
Control Room
Amplifiers, HMS, Rotor Control

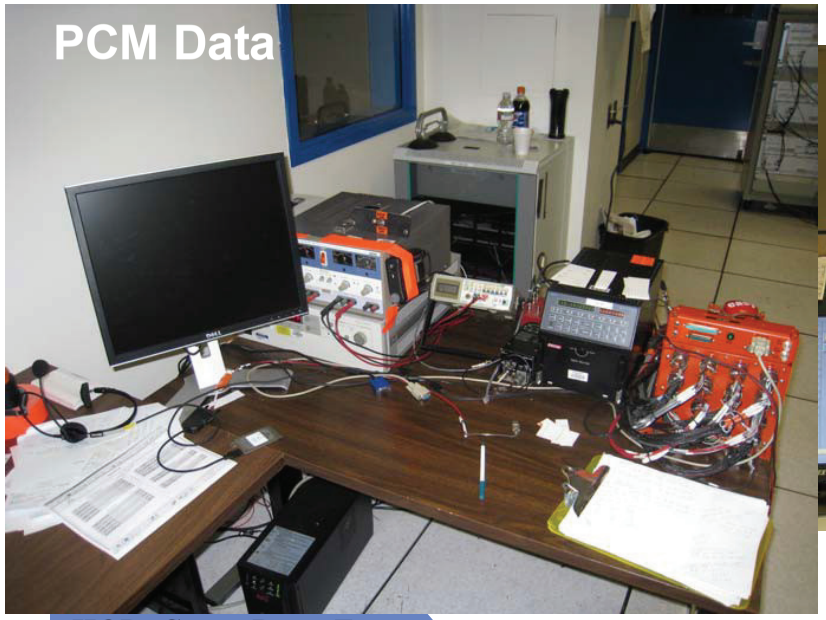
PCM Data

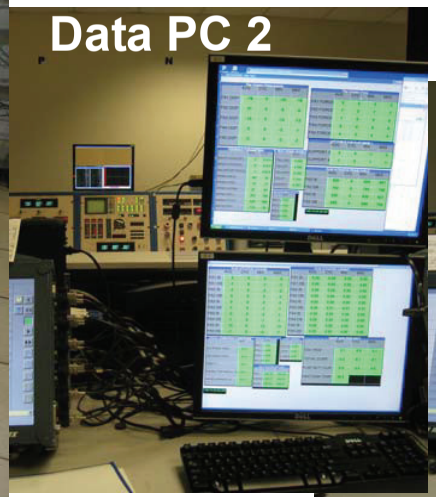
Data PC 2

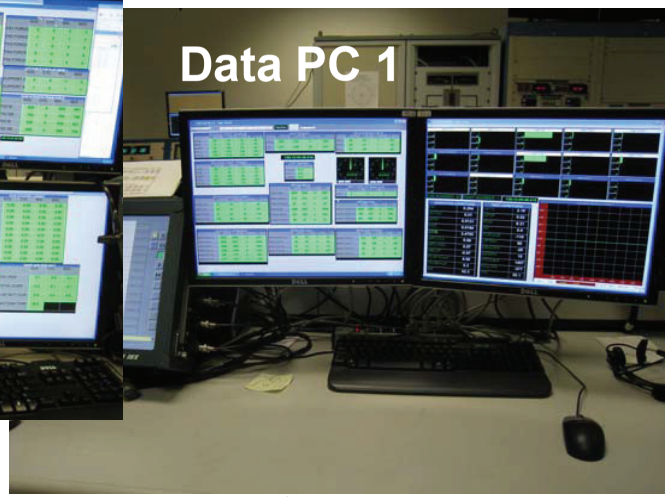
Data PC 1

BOEING

Data PC 1—Displays 3 and 4

Data PC 2—Displays 5 and 6


RCC, Motor Control, Test Conditions, Tunnel Control
AFC, Flap Control & Data Acqu., Data PC2, Data PC1

BOEING

SMART ROTOR IN THE 40- X 80-FOOT WIND TUNNEL

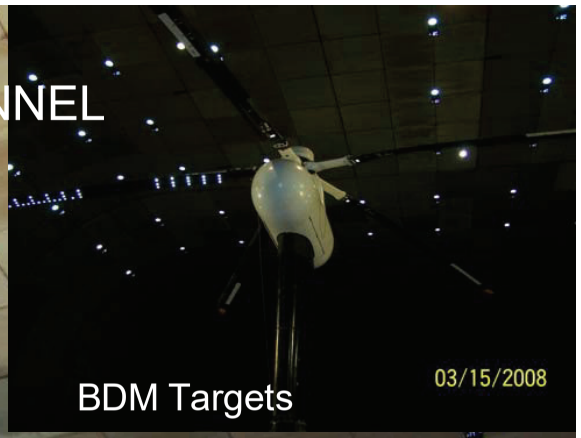

BOEING

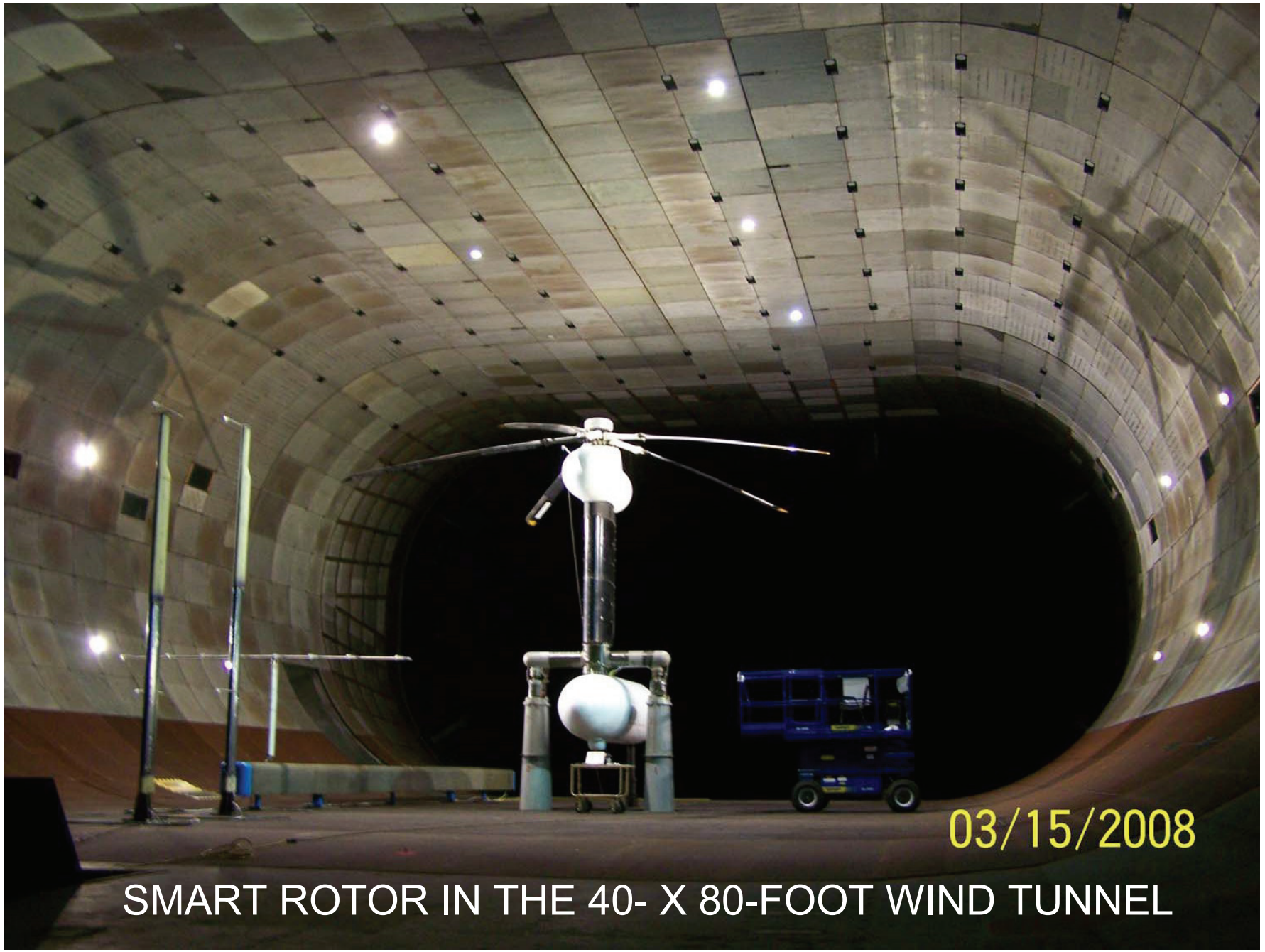

SMART ROTOR IN THE 40- X 80-FOOT WIND TUNNEL

BOEING

SMART ROTOR IN THE 40- X 80-FOOT WIND TUNNEL

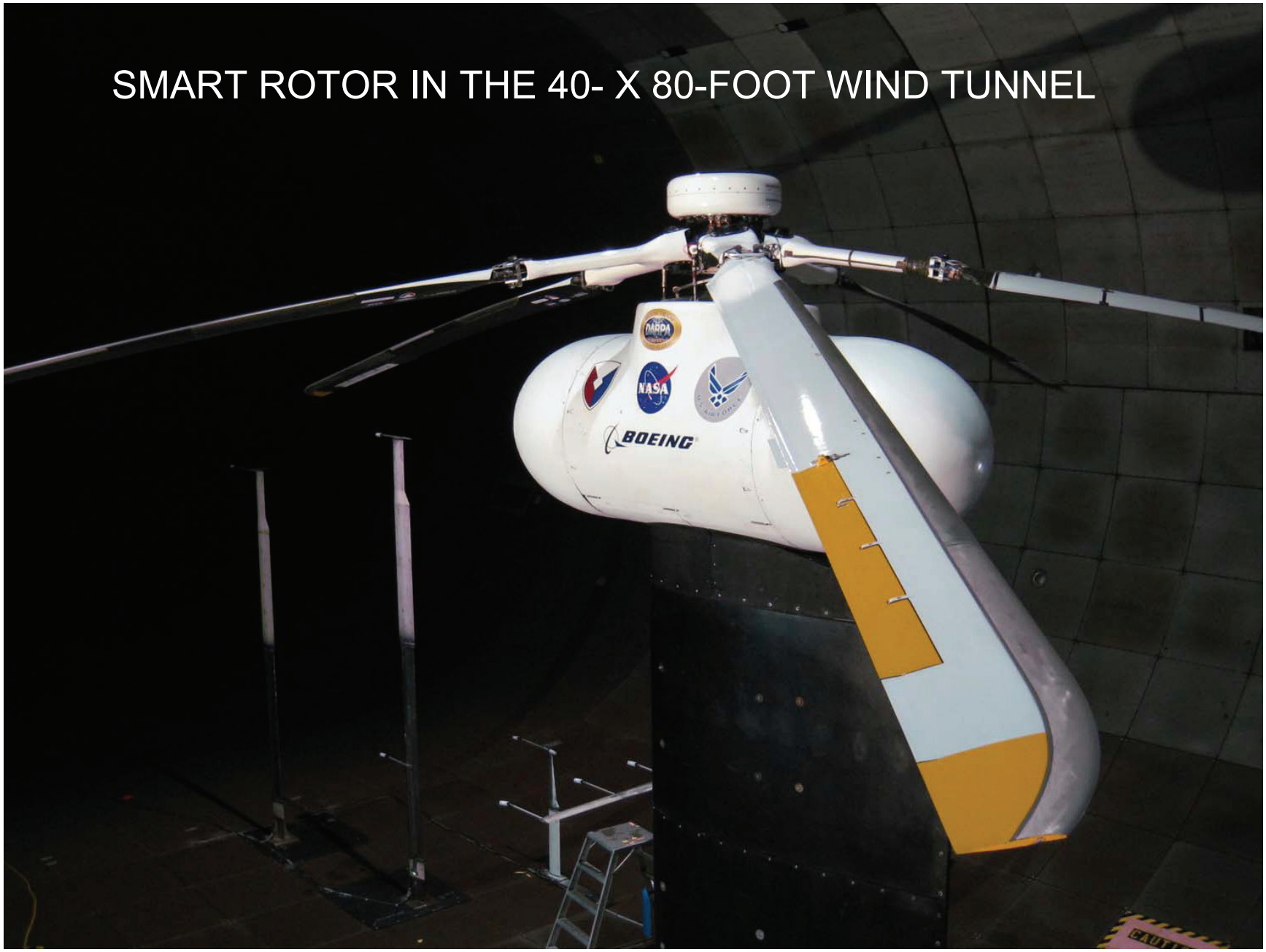

BOEING